IV Escola de Primavera de Transição e Turbulência
Universidade Federal do Rio Grande do Sul
Pontifícia Universidade Católica do Rio Grande do Sul
Porto Alegre, RS, 27 de setembro a 1º de outubro de 2004

FUNDAMENTALS OF COMPRESSIBLE TURBULENCE

R. FRIEDRICH
Fachgebiet Strömungsmechanik
TU München, Boltzmannstr. 15
85748 Garching, Germany

1. Introduction

We begin the discussion with a rough classification of compressible turbulent flows into:

I) Flows with unimportant compressibility effects due to turbulent fluctuations and
II) Flows in which such effects play a role.

Type I flows are assumed to follow Morkovin's hypothesis in it's weak form (Morkovin (1962)) which states that thermodynamic pressure and total temperature fluctuations are negligible for small turbulent Mach numbers implying negative density-temperature correlations. The hypothesis has led to the so–called strong Reynolds analogy (SRA) and is in line with the Van Driest transformation (Van Driest (1951)) which collapses velocity profiles of compressible turbulent boundary layers onto the incompressible law of the wall (Fernholz & Finley (1980), Huang & Coleman (1994)). Compressibility effects therefore manifest themselves in terms of mean density variations and can be modelled by straightforward adaptations of classical incompressible models. Besides boundary layers with zero or weak pressure gradient and freestream Mach numbers less than 5, mixing layers with convective Mach numbers less than 1 are commonly considered as examples of type I flows (Bradshaw (1977)). It is also expected (although not confirmed at present) that type II flows in which fluctuations of the thermodynamic pressure become important, are encountered at hypersonic speeds. Unfortunately, direct numerical simulation data are not yet available to clarify this issue. A closer look at DNS results for different classes of flows, however, unveils the lack of subtlety of such a classification. Coleman et al.'s (1995) DNS of supersonic fully developed flow in a channel with cooled walls e.g.

shows that, although compressibility effects due to turbulent fluctuations are unimportant, the strong Reynolds analogy in it's form for nonadiabatic flows (Gaviglio (1987), Rubesin (1990)) does not apply. A more general representation of the analogy was therefore derived by Huang et al. (1995) and shown to match the DNS data. Recent direct simulations of annular mixing layers with convective Mach numbers ranging from M_c=0.1 to 1.8 by Freund et al. (1997) indicate that pressure fluctuations are subordinate to temperature and density fluctuations (related to their mean values, respectively) only for $M_c < 0.2$. For higher values of M_c, Morkovin's hypothesis for adiabatic flows does not apply. A third example where pressure fluctuations are non-negligible, is shock isotropic turbulence interaction. Based on DNS and linear theory Mahesh et. al. (1995) found considerable deviation from Morkovin's hypothesis (in it's weak form) behind shocks, although the deviations were seen to decrease with the downstream distance. To be more specific, total temperature fluctuations are generated immediately behind the shock as a result of shock oscillation and are convected into the far field. A second important finding of their work is that upstream entropy fluctuations lead to higher amplification rates of turbulent kinetic energy and vorticity across the shock than pure vortical fluctuations. This result should be of great value in explaining the interaction between shocks and strongly cooled boundary layers.

These examples show that a conclusive classification scheme for compressible turbulent flows is difficult to find at present, especially as long as our knowledge of compressibility effects is not complete.

The paper starts from the conservation laws for ideal gases in section 1, discusses the molecular transport coefficients for high-speed flow and the coupling between vorticity and dilatation transport. In section 2 the basic equations are statistically averaged and transport equations for unknown single-point correlations like the turbulent stress, the pressure variance and the turbulent heat flux are derived. Homogeneous shear flow is discussed in detail in terms of these equations, since this flow is fundamental for the development of turbulence models. Section 3 concentrates on compressibility effects due to turbulent fluctuations as derived from direct numerical simulation. The importance of linear mechanisms is emphasized in homogeneous isotropic, respectively sheared turbulence, and assumptions in the derivation of models for explicit compressibility terms are discussed.

1.1. EQUATIONS OF MOTION

Turbulent flows of compressible polyatomic gases for which the continuum hypothesis is considered valid are governed by the following set of conservation equations:

Mass:

$$\frac{\partial \rho}{\partial t} + \frac{\partial \rho u_j}{\partial x_j} = 0, \tag{1}$$

Momentum:

$$\frac{\partial \rho u_i}{\partial t} + \frac{\partial}{\partial x_j}(\rho u_i u_j) = \frac{\partial \sigma_{ij}}{\partial x_j} = -\frac{\partial p}{\partial x_i} + \frac{\partial \tau_{ij}}{\partial x_j}, \tag{2}$$

Energy:

$$\frac{\partial \rho E}{\partial t} + \frac{\partial}{\partial x_j}(\rho E u_j) = -\frac{\partial q_j}{\partial x_j} + \frac{\partial}{\partial x_j}(u_i(\tau_{ij} - p\delta_{ij})). \tag{3}$$

Body forces are assumed small in high-speed flows. ρ, u_i, p denote the density, velocity and pressure. E is the total energy which comprises the internal energy e and the kinetic energy per unit mass:

$$E = e + \frac{1}{2} u_i u_i. \tag{4}$$

According to Fourier's law, the heat flux by conduction, q_j, is related to the temperature gradient:

$$q_j = -k \frac{\partial T}{\partial x_j}. \tag{5}$$

For Newtonian fluids the stress tensor, τ_{ij}, is proportional to the rate-of-strain tensor s_{ij}:

$$\tau_{ij} = 2\mu \left(s_{ij} - \frac{1}{3} s_{kk} \delta_{ij} \right) + \mu_v s_{kk} \delta_{ij}, \tag{6}$$

$$s_{ij} = \frac{1}{2} \left(\frac{\partial u_i}{\partial x_j} + \frac{\partial u_j}{\partial x_i} \right) \quad . \tag{7}$$

Introducing the deviatoric part of the s_{ij}-tensor, namely:

$$s_{ij}^D = s_{ij} - \frac{1}{3} s_{kk} \delta_{ij} \tag{8}$$

which describes the pure straining motion without change of volume, eq. (6) reads:

$$\tau_{ij} = 2\mu s_{ij}^D + \mu_v s_{kk} \delta_{ij}. \tag{9}$$

The set of conservation equations is not yet complete. We have to add equations of state which relate the thermodynamic variables. The assumption of a thermally perfect gas, viz:

$$p = \rho RT \tag{10}$$

allows to describe even relaxation effects in the molecular translational and rotational degrees of freedom. Eq. (10) implies a caloric equation of state of the form:

$$e = e(T) \quad . \tag{11}$$

We will use the equations

$$de = c_v(T)dT \tag{12}$$

and

$$e = c_v T \tag{13}$$

interchangeably. The latter defines the calorically perfect gas and assumes constant specific heat at constant volume. The conservation of momentum and energy is controlled by the following molecular transport coefficients:

- the shear or dynamic viscosity μ
- the bulk viscosity μ_v
- the heat conductivity k.

They all depend on temperature alone. Sutherland's formula for the shear viscosity is valid in a range of temperatures, between $200K$ and $1200K$:

$$\frac{\mu}{\mu_0} = \left(\frac{T}{T_0}\right)^{\frac{3}{2}} \frac{T_0 + S_0}{T + S_0} \tag{14}$$

The coefficients are given in table 1 for 3 gases.

Bertolotti (1997) has derived a new temperature dependence for the bulk viscosity of the form:

$$\frac{\mu_v(T)}{\mu(T)} = \left(\frac{\mu_v}{\mu}\right)_{T=293.3K} \exp\left(\frac{T - 293.3}{1940}\right) \quad , \tag{15}$$

and has demonstrated its damping effect on the instability of laminar boundary layers at M=4.5 (especially on Mack's second mode). It has to be noted, that the bulk viscosity is not a physical property of gases. It is

TABLE 1. Sutherland constants for dynamic viscosity, valid in the range $200K < T < 1200K$.

Gas	T_0(K)	S_0(K)	$10^5 \times \mu_0$ (Pa s)
N_2	273.1	106.6	1.665
O_2	273.1	138.8	1.921
CO_2	273.1	222.2	1.370

rather an approximation designed to model the effect of rotational energy relaxation[1].

The pressure p at a point in a moving fluid is defined in a mechanical way as the mean normal stress with sign reversed, i.e. $p = -\sigma_{ii}/3$ (Batchelor (1967)). The thermodynamic pressure, to which it is related, depends on two state variables, say ρ and e. The internal energy involves all molecular energies, i.e. translational and rotational e.g. If the rotational modes have relaxation times of the order of several collision intervalls and make a significant contribution to the internal energy e, then μ_v has to take care of the lag in the adjustment of the mechanical pressure to the continually changing values in ρ and e in a motion involving volume changes. The bulk viscosity is usually regarded as non-negligible in situations like the attenuation of high frequency sound waves or the structure of shock waves. Considering Bertolotti's findings (1997), it is to be expected that μ_v also plays a considerable role in high-speed compressible turbulence.

The heat conductivity is likewise affected by the state of the internal energy of the molecules and follows a similar Sutherland law (Bertolotti (1997)) obtained from a best fit to experimental data:

$$\frac{k}{k_0} = \left(\frac{T}{T_0}\right)^{3/2} \frac{T_0 + S_{k0}}{T + S_{k0}}. \tag{16}$$

The coefficients are contained in table 2.

For some situations an energy equation is needed in terms of the enthalpy h, where $h = e + p/\rho$, or of the stagnation (or total) enthalpy; $H = h + 1/2\ u_i u_i$. The balance equation for the total enthalpy is:

$$\rho \frac{DH}{Dt} = \frac{\partial p}{\partial t} - \frac{\partial q_j}{\partial x_j} + \frac{\partial}{\partial x_j}(u_i \tau_{ij}), \tag{17}$$

with the material derivative

[1]Vibrational energy relaxation cannot be treated in such an approximate way. A relaxation equation must be solved.

TABLE 2. Sutherland constants for heat conductivity, valid in the range $200K < T < 1200K$.

Gas	$T_0(K)$	$S_{k0}(K)$	$10^2 \times k_0 \left(\frac{W}{mK}\right)$
N_2	273.1	166.6	2.440
O_2	273.1	222.2	2.480
CO_2	273.1	2222.2	1.455

$$\frac{D}{Dt} = \frac{\partial}{\partial t} + u_j \frac{\partial}{\partial x_j}. \tag{18}$$

Subtracting the kinetic energy equation from (17) leads to the enthalpy equation:

$$\rho \frac{Dh}{Dt} = \frac{Dp}{Dt} - \frac{\partial q_j}{\partial x_j} + \tau_{ij} \frac{\partial u_i}{\partial x_j}. \tag{19}$$

The last term on the right-hand-side is the dissipation rate per unit volume, ϕ. Using the symbol d for the dilatation,

$$d = \frac{\partial u_j}{\partial x_j}, \tag{20}$$

we express the dissipation rate in a form which shows that it is always positive, viz:

$$\phi = \tau_{ij} \frac{\partial u_i}{\partial x_j} = \tau_{ij} s_{ij} = 2\mu s_{ij}^D s_{ij}^D + \mu_v d^2. \tag{21}$$

The bulk viscosity provides additional dissipation. From (19) a temperature equation may be derived introducing the caloric state equation in the form

$$\frac{Dh}{Dt} = c_p \frac{DT}{Dt} \tag{22}$$

appropriate for moving fluids with $c_p = c_p(T)$.

For thermally and at the same time calorically perfect gases (from now on referred to as perfect gases), the enthalpy equation (19) can also be converted into an equation for the pressure alone. Using the gas law one gets

$$h = c_p T = \frac{\gamma}{\gamma - 1} \frac{p}{\rho} \quad , \quad \gamma = c_p / c_v \quad . \tag{23}$$

and from (19) and the continuity equation:

$$\frac{Dp}{Dt} = -\gamma p \frac{\partial u_j}{\partial x_j} + (\gamma - 1)\left(\phi - \frac{\partial q_j}{\partial x_j}\right). \tag{24}$$

p is thus a measure of internal energy which is altered reversibly during compression and expansion processes and irreversibly by dissipation and heat conduction.

Finally, with the help of the Gibbs fundamental equation:

$$Tds = dh - dp/\rho \tag{25}$$

an entropy balance equation is obtained from (19):

$$\rho T \frac{Ds}{Dt} = -\frac{\partial q_j}{\partial x_j} + \phi \tag{26}$$

or in the more informative form:

$$\rho \frac{Ds}{Dt} = \frac{\partial}{\partial x_j}\left(\frac{k\frac{\partial T}{\partial x_j}}{T}\right) + \frac{1}{T}\left(\phi + \frac{k}{T}\left(\frac{\partial T}{\partial x_j}\right)^2\right) \tag{27}$$

which shows that the entropy irreversibly increases within the flow field due to friction and heat conduction. The transfer of heat across a control surface (first term on the rhs) can otherwise increase or decrease the entropy. Walls that inhibit the heat conduction across their surfaces are called adiabatic. Setting all molecular transport coefficients to zero defines isentropic flow:

$$\frac{Ds}{Dt} = 0. \tag{28}$$

1.2. TRANSPORT OF DILATATION AND VORTICITY

In high-speed non-reactive flows dilatation is a measure of compressibility, in the sense that volume changes are caused by changes in the pressure (Lele (1994)). Following Thompson (1988) we express density changes in the continuity equation (1) by changes in the pressure and the entropy. Then, introducing the speed of sound, c, for thermally and calorically perfect gases, by:

$$c^2 = \left(\frac{\partial p}{\partial \rho}\right)_s = \gamma p/\rho, \tag{29}$$

we obtain:

$$d = \frac{\partial u_j}{\partial x_j} = -\frac{1}{\gamma p}\frac{Dp}{Dt} + \frac{1}{c_p}\frac{Ds}{Dt}. \tag{30}$$

With the help of the gas law (10), the kinetic energy equation, the enthalpy and entropy equations (19), (26) one finally gets:

$$d = -\frac{1}{c^2}\left\{\frac{1}{\rho}\frac{\partial p}{\partial t} - \frac{D}{Dt}\left(\frac{1}{2}u_i u_i\right) + \frac{u_i}{\rho}\frac{\partial \tau_{ij}}{\partial x_j} - \frac{1}{\rho}(\gamma - 1)\left(\phi - \frac{\partial q_j}{\partial x_j}\right)\right\}. \tag{31}$$

The first term on the rhs of (31) represents acoustic effects. It generates compressibility when the time scale of the pressure 'oscillations' is comparable to the local acoustic time scale. The second term is of the order of the Mach number squared and states that high-speed flows are typically compressible flows. The remaining terms generally don't lead to compressibility effects. Only in extreme situations might excessive heat transfer rates cause considerable volume changes. For reactive flows, eq. (31) must be supplemented by diffusion effects, heat release and changes in the molecular weight of the gas mixture. Supersonic combustion is a situation where chemical and compressibility effects strongly interact. The modelling of correlations which involve dilatation fluctuations is then extremely complicated.

Dilatation transport:

A transport equation for d is easily derived, taking the divergence of the momentum equation (2):

$$\frac{Dd}{Dt} = -\frac{\partial u_i}{\partial x_j}\frac{\partial u_j}{\partial x_i} - \frac{1}{\rho}\frac{\partial^2 p}{\partial x_i \partial x_i} + \frac{1}{\rho^2}\frac{\partial \rho}{\partial x_i}\frac{\partial p}{\partial x_i} + \frac{\partial}{\partial x_i}\left(\frac{1}{\rho}\frac{\partial \tau_{ij}}{\partial x_j}\right). \tag{32}$$

It is useful to express the first term on the rhs by the rate-of-strain tensor and the vorticity vector ω_i, defined by:

$$\omega_i = \epsilon_{ijk}\frac{\partial u_k}{\partial x_j} = \epsilon_{ijk} r_{kj}, \tag{33}$$

where ϵ_{ijk} is the alternating unit tensor and

$$r_{ij} = \frac{1}{2}\left(\frac{\partial u_i}{\partial x_j} - \frac{\partial u_j}{\partial x_i}\right) \tag{34}$$

the rate-of-rotation tensor. The following intermediate steps

$$\begin{aligned}\frac{\partial u_i}{\partial x_j}\frac{\partial u_j}{\partial x_i} &= (s_{ij}+r_{ij})(s_{ji}+r_{ji}) \\ &= s_{ij}s_{ij} - \frac{1}{2}\omega_i\omega_i = s_{ij}^D s_{ij}^D + \frac{1}{3}d^2 - \frac{1}{2}\omega_i\omega_i \end{aligned} \tag{35}$$

lead to the final form of the dilatation transport equation:

$$\begin{aligned}\frac{Dd}{Dt} &= -s_{ij}^D s_{ij}^D - \frac{1}{3}d^2 + \frac{1}{2}\omega_i\omega_i - \frac{1}{\rho}\frac{\partial^2 p}{\partial x_i \partial x_i} \\ &\quad + \frac{1}{\rho^2}\frac{\partial \rho}{\partial x_i}\frac{\partial p}{\partial x_i} + \frac{\partial}{\partial x_i}\left(\frac{1}{\rho}\frac{\partial \tau_{ij}}{\partial x_j}\right). \end{aligned} \tag{36}$$

Obviously, pure straining motions and volume changes act in the same direction. They decrease the magnitude of d in expansion zones, whereas any vortical motions directly increase the level of d and vice versa in compression zones. The pressure field acts on d via its Laplacian and via the dot product between density and pressure gradients and, finally, d is controlled by viscous effects. For incompressible isothermal flow (36) reduces to the well-known Poisson equation for the pressure:

$$\frac{\partial u_i}{\partial x_j}\frac{\partial u_j}{\partial x_i} = -\frac{1}{\rho}\frac{\partial^2 p}{\partial x_i \partial x_i}, \tag{37}$$

which underlines the fact that p is no longer a state variable, but is completely determined by the velocity field. This change in role of the pressure also reflects the difficulties in adequately modelling correlation functions involving pressure fluctuations.

Vorticity transport:

Taking the curl of the momentum equation (2) provides the vorticity transport equation for a compressible fluid in the form:

$$\frac{D\omega_i}{Dt} = \omega_j s_{ij} - \omega_i d - \epsilon_{ijk}\left(\frac{1}{\rho^2}\frac{\partial p}{\partial x_j}\frac{\partial \rho}{\partial x_k} - \frac{\partial}{\partial x_j}\left(\frac{1}{\rho}\frac{\partial \tau_{kl}}{\partial x_l}\right)\right). \tag{38}$$

The first term on the rhs changes vorticity by stretching, contracting or tilting of vortex lines. It is this term which increases vorticity fluctuations in turbulent flows while kinetic energy is transferred from large to small scales in a cascade process, until the loss of vorticity by viscosity compensates the gain by stretching at the smallest scales. In compressible flows

two extra effects appear, namely the increase in vorticity in compression zones ($d < 0$) or a corresponding decrease in expansion zones and a change due to the baroclinic torque term (3rd term on the rhs). If pressure and density gradients are not parallel, the pressure force does not pass through the center of gravity of the fluid particle and a moment about this center exists which changes ω_i (Smits and Dussauge (1996)). The baroclinic term is zero for barotropic flows, for which the pressure is a function of density alone (isentropic flow of thermally and calorically perfect gases; e.g.). Baroclinic effects are discussed by Mahesh et al. (1995) in the context of shock/turbulence interaction. Finally, we emphasize the explicit non-linear coupling between dilatation and vorticity, which contributes to the complexity of compressible turbulent flows and is reflected in the two transport equations (36) and (38).

2. Averaged equations

2.1. DEFINITION OF AVERAGES

For compressible flows it is common practice to work with two different averages simultaneously, the Reynolds-average, denoted by a bar and the Favre- or mass-weighted average, characterized by a tilde. Density and pressure are mostly written in terms of Reynolds-averages and fluctuations, viz:

$$\begin{aligned} \rho &= \bar{\rho} + \rho' \\ p &= \bar{p} + p' \end{aligned} \tag{39}$$

whereas temperature, internal energy and velocity are split into

$$\begin{aligned} T &= \tilde{T} + T'', \\ e &= \tilde{e} + e'', \\ u_i &= \tilde{u}_i + u_i''. \end{aligned} \tag{40}$$

Mass-weighted averages are defined as

$$\bar{\rho}\tilde{T} = \overline{\rho T}, \qquad etc. \tag{41}$$

implying

$$\overline{\rho T''} = 0, \tag{42}$$

but

$$\overline{T''} \neq 0 \tag{43}$$

in general. The mean of the Reynolds-fluctuation, however, vanishes. It remains to state, how mean quantities can be obtained in the computation (DNS/LES) or the experiment. One way is by ensemble averaging over a large number of realizations:

$$\overline{\rho}^e \equiv \lim_{N\to\infty} \frac{1}{N} \sum_{n=1}^{N} \rho_n. \tag{44}$$

Another is by time-averaging over a finite time-interval τ which is large enough to cover all turbulent time scales but small with respect to the statistical unsteadiness of the flow:

$$\overline{\rho}^t = \frac{1}{\tau} \int_0^\tau \rho(t+\theta) d\theta \tag{45}$$

For stationary turbulence, τ may go to infinity, in principle. If a computed flow is homogeneous in one or two or even all three directions, spatial averaging in these directions is common. We assume that all mean values coincide in the special case of stationary and homogeneous turbulence (ergodic hypothesis), and that there is usually a way to obtain stable statistical values in general flow situations. We simply denote such statistical quantities by the overbar, $\overline{}$, or the tilde, $\widetilde{}$, and do not care anymore how they have been obtained. We further assume that the averaging procedure commutes with differentiation, is linear and preserves constants.

2.2. AVERAGED CONSERVATION EQUATIONS

The conservation equations not only contain products of ρ and u_i e.g., but also products of p and u_i or of μ and gradients of u_i etc. When averaging these products, it proves in general more convenient to use Favre variables and their fluctuations in terms resulting from convection and Reynolds-averages and -fluctuations in the remaining terms (see Huang et al. (1995)). The averaged mass, momentum and total energy equations are:

Mass:

$$\frac{\partial \overline{\rho}}{\partial t} + \frac{\partial \overline{\rho}\widetilde{u_j}}{\partial x_j} = 0, \tag{46}$$

Momentum:

$$\frac{\partial \overline{\rho}\widetilde{u_i}}{\partial t} + \frac{\partial}{\partial x_j}(\overline{\rho}\widetilde{u_i}\widetilde{u_j}) = -\frac{\partial}{\partial x_j}\overline{\rho u_i'' u_j''} - \frac{\partial \overline{p}}{\partial x_i} + \frac{\partial \overline{\tau_{ij}}}{\partial x_j}, \tag{47}$$

Energy:

$$\frac{\partial \bar{\rho}\tilde{E}}{\partial t} + \frac{\partial}{\partial x_j}(\bar{\rho}\widetilde{u_j}\widetilde{E}) =$$
$$-\frac{\partial}{\partial x_j}\overline{\rho u_j'' E''} - \frac{\partial \overline{q_j}}{\partial x_j} + \frac{\partial}{\partial x_j}\left(\overline{u_i}(\overline{\tau_{ij}} - \bar{p}\delta_{ij}) + \overline{u_i'\tau_{ij}'} - \overline{u_j' p'}\right). \quad (48)$$

Several terms in these equations need some discussion. The mean total energy, $\tilde{E}$, e.g. contains the kinetic energy of the mean motion and the turbulent kinetic energy K:

$$\tilde{E} = \tilde{e} + \frac{1}{2}\widetilde{u_i}\widetilde{u_i} + \underbrace{\frac{1}{2}\widetilde{u_i'' u_i''}}_{K}. \quad (49)$$

Consequently, a fluctuation E'' is defined as

$$E'' = e'' + \widetilde{u_i} u_i'' + \frac{1}{2} u_i'' u_i'' - K. \quad (50)$$

The energy flux term (See the 1st term on the rhs of (48)) can then be written as:

$$\overline{\rho u_j'' E''} = \overline{\rho u_j'' e''} + \widetilde{u_i}\overline{\rho u_i'' u_j''} + \frac{1}{2}\overline{\rho u_i'' u_i'' u_j''}, \quad (51)$$

i.e. as the sum of the turbulent heat flux, the work done by the Reynolds stress tensor, $\overline{\rho u_i'' u_j''}$, and the turbulent transport or diffusion.

The mean viscous stress, $\overline{\tau_{ij}}$, is

$$\overline{\tau_{ij}} = 2\overline{\mu}\overline{s_{ij}^D} + \overline{\mu_v}\ \overline{s_{kk}}\delta_{ij} + 2\overline{\mu' s_{ij}^{D'}} + \overline{\mu_v' s_{kk}'}\delta_{ij}. \quad (52)$$

It contains correlations betweeen viscosity fluctuations, $\mu' = \mu(T')$ and fluctuations of the rate-of-strain tensor:

$$s_{ij}' = \frac{1}{2}\left(\frac{\partial u_i'}{\partial x_j} + \frac{\partial u_j'}{\partial x_i}\right). \quad (53)$$

Similarly, the mean conductive heat flux is:

$$\overline{q_j} = -\bar{k}\frac{\partial \bar{T}}{\partial x_j} - \overline{k'\frac{\partial T'}{\partial x_j}}. \quad (54)$$

Consistent definitions of τ_{ij}' and q_j', in the sense that $\overline{\tau_{ij}'} = 0$ and $\overline{q_j'} = 0$, are:

$$\begin{aligned}\tau'_{ij} &= 2\mu' s^{D'}_{ij} + \mu'_v s'_{kk}\delta_{ij} \\ &\quad -2\overline{\mu' s^{D'}_{ij}} - \overline{\mu'_v s'_{kk}}\delta_{ij} \\ &\quad +2\overline{\mu} s^{D'}_{ij} + \overline{\mu_v} s'_{kk}\delta_{ij} \\ &\quad +2\mu'\overline{s^{D}_{ij}} + \mu'_v \overline{s_{kk}}\delta_{ij},\end{aligned} \tag{55}$$

$$q'_j = -k'\frac{\partial T'}{\partial x_j} + \overline{k'\frac{\partial T'}{\partial x_j}} - k'\frac{\partial \bar{T}}{\partial x_j} - \bar{k}\frac{\partial T'}{\partial x_j}. \tag{56}$$

Subtracting the transport equation for the kinetic energy of the mean motion, $\frac{1}{2}\widetilde{u_i}\widetilde{u_i}$, from the total energy balance equation (48), leads to the balance equation for the mean internal energy $\bar{\rho}\tilde{e}$:

$$\begin{aligned}&\frac{\partial \bar{\rho}\tilde{e}}{\partial t} + \frac{\partial}{\partial x_j}(\bar{\rho}\widetilde{u_j}\tilde{e}) = \\ &-\frac{\partial}{\partial x_j}\overline{\rho u''_j e''} - \frac{\partial \overline{q_j}}{\partial x_j} - \bar{p}\bar{d} - \overline{p'd'} + \overline{\tau_{ij}}\ \overline{s_{ij}} + \overline{\tau'_{ij}s'_{ij}}.\end{aligned} \tag{57}$$

In the averaged conservation equations above, the following (single-point) correlations appear that require closure:

- the turbulent (or Reynolds) stresses, $\overline{\rho u''_i u''_j} = \bar{\rho}\widetilde{u''_i u''_j}$
- the turbulent heat fluxes, $\overline{\rho u''_j e''} = \bar{\rho}\widetilde{u''_j e''}$
- the turbulent mass flux, $\overline{u''_i} = -\overline{\rho' u'_i}/\bar{\rho}$
- the pressure-velocity correlation, $\overline{p'u'_j}$
- the velocity triple correlation, $\overline{\rho u''_i u''_i u''_j}$
- the pressure dilatation, $\overline{p'd'} = \overline{p'\frac{\partial u'_j}{\partial x_j}}$
- the turbulent dissipation rate, $\bar{\rho}\epsilon = \overline{\tau'_{ij}s'_{ij}}$
- the transport by viscous stresses, $\overline{\tau'_{ij}u'_i}$
- viscosity rate-of-strain correlations. e.g. $\overline{\mu' s'_{ij}}$
- and the heat conductivity temperature gradient correlation, $\overline{k'\partial T'/\partial x_j}$

The turbulent heat flux and the pressure velocity correlation can be combined for perfect gases to:

$$\begin{aligned}&\overline{\rho u''_j e''} + \overline{p'u'_j} = \overline{\rho u''_j(e'' + p'/\rho)} = \\ &\overline{\rho c_p u''_j T''} + R\widetilde{T}\overline{\rho' u''_j} = \overline{\rho c_p u''_j T''} - \bar{p}\overline{u''_j}.\end{aligned} \tag{58}$$

Note that $\overline{p'u'_j} = \overline{p'u''_j}$ and $\bar{p} = \bar{\rho}R\tilde{T}$. The turbulent mass flux $\overline{u''_i}$ describes the difference between Reynolds and Favre-averaged velocities

$$\overline{u_i} - \widetilde{u}_i = \overline{u''_i} = -\overline{\rho' u'_i}/\bar{\rho} = -\overline{\rho u'_i}/\bar{\rho}, \tag{59}$$

and is one of the explicit compressibility terms.

We follow Huang et al. (1995) and split the turbulent dissipation rate into a total number of five terms. From the definition of τ'_{ij} in eq. (55) we first get:

$$\bar{\rho}\epsilon = \overline{\tau'_{ij} s'_{ij}} = \bar{\rho}(\epsilon_1 + \epsilon_2 + \epsilon_3), \tag{60}$$

where

$$\bar{\rho}\epsilon_1 = 2\bar{\mu}\overline{s^{D'}_{ij}\, s^{D'}_{ij}} + \bar{\mu}_v \overline{s'_{kk} s'_{jj}} \tag{61}$$

$$\bar{\rho}\epsilon_2 = 2\overline{\mu' s^{D'}_{ij}\, s^{D'}_{ij}} + \overline{\mu'_v s'_{kk} s'_{jj}} \tag{62}$$

$$\bar{\rho}\epsilon_3 = 2\overline{\mu' s^{D'}_{ij}} \cdot \overline{s^{D}_{ij}} + \overline{\mu'_v s'_{kk}} \cdot \overline{s_{jj}}. \tag{63}$$

The quantity $\bar{\rho}\epsilon_1$ is the most important one among these and can be expressed as the sum of a solenoidal (ϵ_s), a dilatational (ϵ_d) and an inhomogeneous term (ϵ_I):

$$\bar{\rho}\epsilon_1 = \bar{\rho}(\epsilon_s + \epsilon_d + \epsilon_I) \tag{64}$$

with

$$\bar{\rho}\epsilon_s = \bar{\mu}\overline{\omega'_i \omega'_i}, \tag{65}$$

$$\bar{\rho}\epsilon_d = \left(\frac{4}{3}\bar{\mu} + \overline{\mu_v}\right)\overline{s'_{kk} s'_{jj}}, \tag{66}$$

$$\bar{\rho}\epsilon_I = 2\bar{\mu}\left(\frac{\partial^2}{\partial x_i \partial x_j}\overline{u'_i u'_j} - 2\frac{\partial}{\partial x_i}\overline{u'_i s'_{jj}}\right). \tag{67}$$

$\bar{\rho}\epsilon_s$ has the same form as in incompressible turbulence and is usually obtained from a transport equation. The compressible or dilatational dissipation rate, $\bar{\rho}\epsilon_d$, is an explicit compressibility term for which several algebraic models have been proposed in the past. The inhomogeneous term vanishes for homogeneous turbulence. The turbulent dissipation rate $\bar{\rho}\epsilon$ not only appears in the internal energy balance equation, but also in the turbulence kinetic energy equation which will be derived next.

2.3. TURBULENT STRESS TRANSPORT EQUATIONS

The steps needed in order to derive a transport equation for the turbulent (or Reynolds) stress follow from the time-derivative of

$$\overline{\rho u_i u_j} = \bar{\rho}\widetilde{u_i}\widetilde{u_j} + \overline{\rho u_i'' u_j''}, \tag{68}$$

viz:

$$\begin{aligned}\frac{\partial}{\partial t}\overline{\rho u_i'' u_j''} &= \overline{\frac{\partial}{\partial t}(\rho u_j)u_i + \frac{\partial}{\partial t}(\rho u_i)u_j - \frac{\partial \rho}{\partial t}u_i u_j} \\ &\quad - \left(\frac{\partial}{\partial t}(\bar{\rho}\widetilde{u_j})\widetilde{u_i} + \frac{\partial}{\partial t}\left(\bar{\rho}\widetilde{u_i}\right)\widetilde{u_j} - \frac{\partial \bar{\rho}}{\partial t}\widetilde{u_i}\widetilde{u_j}\right).\end{aligned} \tag{69}$$

Substituting from equations (1), (2), (46) and (47) and rearranging we obtain the turbulent stress transport equation:

$$\begin{aligned}&\frac{\partial}{\partial t}(\bar{\rho}\widetilde{u_i'' u_j''}) + \frac{\partial}{\partial x_k}(\widetilde{u_k}\bar{\rho}\widetilde{u_i'' u_j''}) = \\ &\bar{\rho}P_{ij} + \bar{\rho}\Pi_{ij}^{D} + \bar{\rho}\Pi_{ij}^{DL} + M_{ij} - \bar{\rho}\epsilon_{ij} - \frac{\partial}{\partial x_k}(\bar{\rho}D_{ijk}^{T}) + \frac{\partial}{\partial x_k}D_{ijk}^{V}\end{aligned} \tag{70}$$

in which $\bar{\rho}P_{ij}$ represents the production rate tensor, $\bar{\rho}\Pi_{ij}^{D}$ the deviatoric part of the pressure-strain rate tensor; $\bar{\rho}\Pi_{ij}^{DL}$ the pressure-dilatation term (which appears as a consequence of subtracting this term out of the pressure-strain term), M_{ij} the mass flux variation, $\bar{\rho}e_{ij}$ the turbulent dissipation rate tensor and $\bar{\rho}D_{ijk}^{T}$, D_{ijk}^{V}, the turbulent, respectively viscous diffusion terms. These terms are defined by:

$$P_{ij} = -\widetilde{u_i'' u_k''}\frac{\partial \widetilde{u_j}}{\partial x_k} - \widetilde{u_j'' u_k''}\frac{\partial \widetilde{u_i}}{\partial x_k}, \tag{71}$$

$$\bar{\rho}\Pi_{ij}^{D} = \overline{p'\left(\frac{\partial {u_i}'}{\partial x_j} + \frac{\partial {u_j}'}{\partial x_i}\right)} - \frac{2}{3}\overline{p'd'}\delta_{ij} \quad , \tag{72}$$

$$\rho\Pi_{ij}^{DL} = \frac{2}{3}\overline{p'd'}\delta_{ij}, \tag{73}$$

$$M_{ij} = \overline{u_i''}\left(\frac{\partial \overline{\tau_{jk}}}{\partial x_k} - \frac{\partial \bar{p}}{\partial x_j}\right) + \overline{u_j''}\left(\frac{\partial \overline{\tau_{ik}}}{\partial x_k} - \frac{\partial \bar{p}}{\partial x_i}\right), \tag{74}$$

$$\bar{\rho}\epsilon_{ij} = \overline{\tau_{ik}'\frac{\partial u_j'}{\partial x_k}} + \overline{\tau_{jk}'\frac{\partial u_i'}{\partial x_k}}, \tag{75}$$

$$\bar{\rho} D^T_{ijk} = -(\overline{\rho u_i'' u_j'' u_k''} + \overline{p'(u_i' \delta_{jk} + u_j' \delta_{ik})}), \tag{76}$$

$$D^V_{ijk} = \overline{\tau_{ik}' u_j'} + \overline{\tau_{jk}' u_i'}. \tag{77}$$

With the help of the fluctuating viscous stress tensor according to eq. (55) the dissipation rate tensor, $\bar{\rho}\epsilon_{ij}$, can be expressed in the form:

$$\begin{aligned}
\bar{\rho}\epsilon_{ij} &= \bar{\mu}\left(2\overline{\frac{\partial u_i'}{\partial x_k}\frac{\partial u_j'}{\partial x_k}} + \overline{\frac{\partial u_i'}{\partial x_k}\frac{\partial u_k'}{\partial x_j}} + \overline{\frac{\partial u_j'}{\partial x_k}\frac{\partial u_k'}{\partial x_i}}\right) \\
&\quad +2\left(\bar{\mu}_v - \frac{2}{3}\bar{\mu}\right)\overline{s_{ij}' s_{kk}'} \\
&\quad +\overline{\mu'\left(2\frac{\partial u_i'}{\partial x_k}\frac{\partial u_j'}{\partial x_k} + \frac{\partial u_i'}{\partial x_k}\frac{\partial u_k'}{\partial x_j} + \frac{\partial u_j'}{\partial x_k}\frac{\partial u_k'}{\partial x_i}\right)} \\
&\quad +2\overline{\left(\mu_v' - \frac{2}{3}\mu'\right)s_{ij}' s_{kk}'} + 2\left(\overline{\mu'\frac{\partial u_i'}{\partial x_k}}\,\overline{s_{jk}} + \overline{\mu'\frac{\partial u_j'}{\partial x_k}}\,\overline{s_{ik}}\right) \\
&\quad +2\overline{(\mu_v' - \frac{2}{3}\mu')s_{ij}'}\,\overline{s_{kk}}.
\end{aligned} \tag{78}$$

It can be verified that the trace of this tensor is twice the dissipation rate, $\bar{\rho}\epsilon$, defined in (60), i.e.

$$\bar{\rho}\epsilon = \frac{1}{2}\bar{\rho}\epsilon_{jj}. \tag{79}$$

For later reference, we split the dominant part of the dissipation rate tensor (namely the first line of eq. (78) which does not involve correlations with viscosity fluctuations) into solenoidal, dilatational and inhomogeneous parts, in analogy to eq. (64). We get:

$$\begin{aligned}
\bar{\rho}\epsilon^1_{ij} &= \bar{\mu}\left(2\overline{\frac{\partial u_i'}{\partial x_k}\frac{\partial u_j'}{\partial x_k}} + \overline{\frac{\partial u_i'}{\partial x_k}\frac{\partial u_k'}{\partial x_j}} + \overline{\frac{\partial u_j'}{\partial x_k}\frac{\partial u_k'}{\partial x_i}}\right) + 2\left(\overline{\mu_v} - \frac{2}{3}\bar{\mu}\right)\overline{s_{ij}' s_{kk}'} \\
&= \bar{\rho}(\epsilon^s_{ij} + \epsilon^d_{ij} + \epsilon^I_{ij})
\end{aligned} \tag{80}$$

where

$$\bar{\rho}\epsilon^s_{ij} = 2\bar{\mu}(2\overline{r_{ik}' r_{jk}'} + \overline{s_{ik}' r_{jk}'} + \overline{s_{jk}' r_{ik}'}), \tag{81}$$

$$\bar{\rho}\epsilon^d_{ij} = 2\left(\overline{\mu_v} + \frac{4}{3}\bar{\mu}\right)\overline{s_{ij}' s_{kk}'}, \tag{82}$$

$$\bar{\rho}\epsilon^I_{ij} = 2\bar{\mu}\left(\frac{\partial^2}{\partial x_j \partial x_k}\overline{u_i' u_k'} + \frac{\partial^2}{\partial x_i \partial x_k}\overline{u_j' u_k'} - \frac{\partial}{\partial x_i}\overline{u_j' s_{kk}'} - \frac{\partial}{\partial x_j}\overline{u_i' s_{kk}'} - 2\frac{\partial}{\partial x_k}\overline{u_k' s_{ij}'}\right). \quad (83)$$

Note that contracting the solenoidal part leads to

$$\bar{\rho}\epsilon^s_{jj} = 4\bar{\mu}\overline{r_{ij}' r_{ij}'} = 2\bar{\mu}\overline{\omega_i'\omega_i'} \quad (84)$$

which is twice $\bar{\rho}\epsilon_s$.

The balance equation for the turbulent kinetic energy, $\bar{\rho}K = \bar{\rho}\,\widetilde{u_i'' u_i''}/2$, is the trace of eq. (70) multiplied by $\frac{1}{2}$:

$$\begin{aligned}\frac{\partial}{\partial t}(\bar{\rho}K) &+ \frac{\partial}{\partial x_j}(\widetilde{u_j}\bar{\rho}K) = -\bar{\rho}\widetilde{u_i'' u_j''}\frac{\partial \widetilde{u}_i}{\partial x_j} + \overline{p' d'} \\ &+ \overline{u_i''}\left(\frac{\partial \overline{\tau_{ij}}}{\partial x_j} - \frac{\partial \bar{p}}{\partial x_i}\right) - \overline{\tau_{ij}' s_{ij}'} \\ &- \frac{\partial}{\partial x_j}\left(\bar{\rho}\,\frac{\left(u_i''\widetilde{u_i'' u_j''}\right)}{2} + \overline{p' u_j'} + \overline{\tau_{ij}' u_i'}\right). \end{aligned} \quad (85)$$

Comparison of the K-equation with the balance equation (57) for the mean internal energy, $\rho\tilde{e}$, shows that K and $\tilde{e}$ exchange energy via the following terms:

- pressure dilatation, $\overline{p'd'}$
- turbulent dissipation rate, $\bar{\rho}\epsilon = \overline{\tau_{ik}' s_{ik}'}$
- mass flux variation, $\overline{u_i''}\left(\frac{\partial \overline{\tau_{ik}}}{\partial x_k} - \frac{\partial \bar{p}}{\partial x_i}\right)$.

In eq. (57) the mass flux variation is contained implicitely and appears, if the Favre-averaged velocity is used to express the dissipation rate by the mean velocity field and the work done by compression or expansion, viz:

$$\begin{aligned}&-\bar{p}\bar{d} + \overline{\tau_{ij}}\,\overline{s_{ij}} = \\ &-\bar{p}\left(\frac{\partial \widetilde{u_j}}{\partial x_j} + \frac{\partial \overline{u_j''}}{\partial x_j}\right) + \overline{\tau_{ij}}\left(\frac{\partial \widetilde{u}_i}{\partial x_j} + \frac{\partial \overline{u_i''}}{\partial x_j}\right) = \\ &-\bar{p}\frac{\partial \widetilde{u_j}}{\partial x_j} + \overline{\tau_{ij}}\frac{\partial \widetilde{u}_i}{\partial x_j} + \frac{\partial}{\partial x_j}\left(-\bar{p}\overline{u_j''} + \overline{\tau_{ij}}\,\overline{u_i''}\right) + \overline{u_i''}\left(\frac{\partial \bar{p}}{\partial x_i} - \frac{\partial \overline{\tau_{ij}}}{\partial x_j}\right). \end{aligned} \quad (86)$$

On the other hand, turbulent kinetic energy is extracted from the mean motion via the production term $-\bar{\rho}\widetilde{u_i''u_k''}\partial\widetilde{u}_i/\partial x_k$. The whole energy exchange in compressible turbulent flows is illustrated in an instructive diagram by Lele (1994).

The viscous diffusion term

$$D_{iij}^V/2 = \overline{\tau_{ij}' u_i'} \tag{87}$$

can be simplified by neglecting fluctuations of viscosity (see e.g. Gatski (1997)). The complete and simplified expressions are:

$$\begin{aligned}
\overline{\tau_{ij}' u_i'} &= 2\bar{\mu}\overline{s_{ij}' u_i'} + \left(\overline{\mu_v} - \frac{2}{3}\bar{\mu}\right)\overline{s_{ii}' u_j'} + 2\overline{\mu' s_{ij}^{D'} u_i'} + \overline{\mu_v' s_{ii}' u_j'} \\
&\quad + 2\overline{\mu' u_i'} \cdot \overline{s_{ij}^D} + \overline{\mu_v' u_j'} \cdot \overline{s_{ii}} \\
&\approx \bar{\mu}\left(\frac{1}{2}\frac{\partial}{\partial x_j}\overline{u_i' u_i'} + \frac{\partial}{\partial x_i}\overline{u_i' u_j'} - \frac{5}{3}\overline{s_{ii}' u_j'}\right) + \overline{\mu_v}\overline{s_{ii}' u_j'}.
\end{aligned} \tag{88}$$

Between correlations involving Favre fluctuations and those involving Reynolds fluctuations there are the following relations:

$$\widetilde{u_i'' u_j''} + \overline{u_i''} \cdot \overline{u_j''} = \overline{u_i' u_j'} + \overline{\rho' u_i' u_j'}/\bar{\rho}, \tag{89}$$

$$\widetilde{s_{ii}'' u_j''} - \overline{\rho' s_{ii}'}\,\overline{u_j''}/\bar{\rho} = \overline{s_{ii}' u_j'} + \overline{\rho' s_{ii}' u_j'}/\bar{\rho}. \tag{90}$$

2.4. TRANSPORT EQUATIONS FOR THE PRESSURE VARIANCE AND THE TURBULENT HEAT FLUX

There is a third equation in which the pressure-dilatation correlation appears as an explicit compressibility term, the pressure variance equation. We will see later (section 3.2.3) that a simplified version of this equation forms the basis for Zeman's pressure-dilatation model. Mostly algebraic models are being used to treat the turbulent heat flux. Since it is advantageous to solve a heat flux transport equation, it will be derived in this subsection.

2.4.1. *Pressure variance transport equation*

This equation is obtained via the following procedure:

$$\frac{\partial}{\partial t}\overline{p'^2} = 2\overline{p'\frac{\partial p}{\partial t}}. \tag{91}$$

We keep in mind that eq. (24) for the pressure involves the assumption of perfect gases. Then, multiplying eq. (24) by $2p'$, using Favre as well as Reynolds splitting where desirable and averaging, we get:

$$\begin{aligned}\frac{\partial}{\partial t}\overline{\rho p'^2} \quad + \quad \widetilde{u_j}\frac{\partial}{\partial x_j}\overline{\rho p'^2} &= -2\overline{p'u_j''}\frac{\partial \bar{p}}{\partial x_j} - 2\gamma\overline{\rho p'^2}\frac{\partial \widetilde{u_j}}{\partial x_j} \\ &-2\gamma\bar{p}\,\overline{p'\frac{\partial u_j''}{\partial x_j}} - (2\gamma-1)\overline{p'^2\frac{\partial u_j''}{\partial x_j}} - \frac{\partial}{\partial x_j}\overline{u_j'' p'^2} \\ &+2(\gamma-1)\left(\overline{p'\tau_{ij}'}\frac{\partial \widetilde{u_i}}{\partial x_j} + \overline{p'\frac{\partial u_i''}{\partial x_j}}\overline{\tau_{ij}} + \overline{p'\frac{\partial u_i''}{\partial x_j}\tau_{ij}'} - \overline{p'\frac{\partial q_j'}{\partial x_j}}\right). \quad (92)\end{aligned}$$

The equation is discussed by Sarkar (1992) and Lele (1994). Pressure fluctuations are produced when the mean flow has strong pressure gradients or thin compression zones like shocks. In the special case of a homogeneous turbulence field, the third term on the rhs (the pressure-dilatation term) is the dominant term. DNS data show that the pressure dilatation term is weakly positive (and oscillatory) for isotropic turbulence and predominantly negative (and again oscillatory) for homogeneous shear turbulence (Sarkar (1992)). An explanation for the different signs is given by Sarkar et al. (1991). These few comments already show the limitations of a model which is based on a direct relation between the time evolution of $\overline{\rho p'^2}$ and the pressure dilatation, since algebraic models for $\partial\overline{\rho p'^2}/\partial t$ can hardly predict the sign change.

2.4.2. *Turbulent heat flux transport equation*
We present equations for both $\bar{\rho}\widetilde{e''u_i''}$ and $\bar{\rho}\widetilde{h''u_i''}$ and note that these equations can be converted one into the other for perfect gases. The relation guiding the derivation of a transport equation for $\bar{\rho}\widetilde{e''u_i''}$ is:

$$\begin{aligned}\frac{\partial}{\partial t}\overline{\rho e''u_i''} \quad = \quad & \overline{u_i\frac{\partial}{\partial t}(\rho e) + e\frac{\partial}{\partial t}(\rho u_i) - eu_i\frac{\partial \rho}{\partial t}} \\ & - \left(\widetilde{u_i}\frac{\partial}{\partial t}(\bar{\rho}\tilde{e}) + \tilde{e}\frac{\partial}{\partial t}(\bar{\rho}\widetilde{u_i}) - \tilde{e}\widetilde{u_i}\frac{\partial \bar{\rho}}{\partial t}\right), \quad (93)\end{aligned}$$

A similar relation holds for $\partial\overline{\rho h''u_i''}/\partial t$. After combining the corresponding equations we obtain the transport equation for $\bar{\rho}\widetilde{e''u_i''}$ in the form:

$$\frac{\partial}{\partial t}\overline{\rho e''u_i''} \quad + \quad \widetilde{u_j}\frac{\partial}{\partial x_j}\overline{\rho e''u_i''} = -\overline{\rho u_i''u_j''}\frac{\partial \tilde{e}}{\partial x_j}$$

$$
\begin{aligned}
- \quad & \overline{\rho e'' u_j''} \frac{\partial \widetilde{u}_i}{\partial x_j} - (\overline{\rho e'' u_i''} + \overline{p u_i''}) \frac{\partial \widetilde{u_j}}{\partial x_j} + \overline{u_i'' \tau_{jk}} \frac{\partial \widetilde{u_j}}{\partial x_k} \\
- \quad & \frac{\partial}{\partial x_j} \overline{\rho e'' u_i'' u_j''} - \overline{p u_i'' \frac{\partial u_j''}{\partial x_j}} + \overline{u_i'' \tau_{jk} \frac{\partial u_j''}{\partial x_k}} \\
- \quad & \overline{e'' \frac{\partial p}{\partial x_i}} + \overline{e'' \frac{\partial \tau_{ij}}{\partial x_j}} - \overline{u_i'' \frac{\partial q_j}{\partial x_j}}. \qquad (94)
\end{aligned}
$$

In order to avoid the appearance of too many terms, the instantaneous pressure and the viscous stress tensor have been kept in the correlations. A turbulent heat flux is generated due to mean temperature gradients (first term on the rhs), due to mean shear and mean dilatation. In compressible homogeneous turbulence there is no turbulent heat flux because there is no mean temperature gradient (Blaisdell et al. (1991)).

The transport equation for $\overline{\rho h'' u_i''}$ reads:

$$
\begin{aligned}
& \frac{\partial}{\partial t} \overline{\rho h'' u_i''} + \widetilde{u_j} \frac{\partial}{\partial x_j} \overline{\rho h'' u_i''} = - \overline{\rho u_i'' u_j''} \frac{\partial \tilde{h}}{\partial x_j} \\
& - \overline{\rho h'' u_j''} \frac{\partial \widetilde{u}_i}{\partial x_j} - \overline{\rho h'' u_i''} \frac{\partial \widetilde{u_j}}{\partial x_j} + \overline{u_i'' \tau_{jk}} \frac{\partial \widetilde{u_j}}{\partial x_k} \\
& - \frac{\partial}{\partial x_j} \overline{\rho h'' u_i'' u_j''} + \widetilde{u_j} \overline{u_i'' \frac{\partial p}{\partial x_j}} + \overline{u_i'' u_j'' \frac{\partial p}{\partial x_j}} + \overline{u_i'' \frac{\partial p}{\partial t}} \\
& + \overline{u_i'' \tau_{jk} \frac{\partial u_j''}{\partial x_k}} - \overline{h'' \frac{\partial p}{\partial x_i}} + \overline{h'' \frac{\partial \tau_{ij}}{\partial x_j}} - \overline{u_i'' \frac{\partial q_j}{\partial x_j}}. \qquad (95)
\end{aligned}
$$

Similar production terms appear as in eq. (94). The turbulent heat fluxes and the pressure velocity correlation are related by:

$$
\overline{\rho h'' u_i''} = \overline{\rho e'' u_i''} + \overline{p u_i''} \qquad (96)
$$

which becomes for perfect gases:

$$
\overline{\rho h'' u_i''} = \frac{\gamma}{\gamma - 1} \overline{p u_i''}. \qquad (97)
$$

In this case the turbulent heat flux equations (94) and (95) can also be considered as transport equations for the pressure velocity correlation. Since $\overline{\rho e'' u_i''}$ vanishes in homogeneous turbulence, $\overline{\rho h'' u_i''}$ and $\overline{p u_i''}$ are zero as well. It is certainly wrong to conclude from this fact that in general inhomogeneous flows these terms are of minor importance. In strongly compressible flows with shocks, e.g., these terms are important and have to be modelled properly (Gatski (1997)).

2.5. TRANSPORT EQUATIONS FOR HOMOGENEOUS SHEAR FLOW

Homogeneous shear flow has been frequently used in the past to test turbulence models and to tune model constants. Direct numerical simulation has provided insight into the physics of compressible turbulent shear flow and has helped to develop pressure-dilatation and compressible dissipation rate models. It is therefore useful to discuss the characteristics of this flow. We first derive conditions under which homogeneous turbulent flows can exist.

2.5.1. *Necessary conditions for homogeneity*

Homogeneous turbulence has statistics of fluctuating quantities which are independent of space. This definition allows for non-zero mean velocity gradients. Blaisdell et al. (1991) have inspected transport equations for $\overline{u_i'' u_j''}$ (a quantity which is unusual in turbulence modelling), for $\overline{\rho'^2}$ and $\overline{p'^2}$ in order to find necessary conditions under which initially homogeneous turbulence remains homogeneous.

Starting from transport equations for u_i'' and ρ', one concentrates on terms involving velocities only. Then, from the identities

$$\frac{\partial u_i''}{\partial t} = \frac{1}{\rho}\left(\frac{\partial}{\partial t}(\rho u_i) - u_i \frac{\partial \rho}{\partial t}\right) - \frac{1}{\bar{\rho}}\left(\frac{\partial}{\partial t}(\bar{\rho}\widetilde{u}_i) - \widetilde{u}_i \frac{\partial \bar{\rho}}{\partial t}\right), \tag{98}$$

$$\frac{\partial \rho'}{\partial t} = \frac{\partial \rho}{\partial t} - \frac{\partial \bar{\rho}}{\partial t}, \tag{99}$$

one finds:

$$\frac{\partial u_i''}{\partial t} = -\widetilde{u_j}\frac{\partial u_i''}{\partial x_j} - u_j''\frac{\partial \widetilde{u}_i}{\partial x_j} - u_j''\frac{\partial u_i''}{\partial x_j} + \frac{1}{\bar{\rho}}\frac{\partial}{\partial x_j}\overline{\rho u_i'' u_j''} + \ldots, \tag{100}$$

$$\begin{aligned}\frac{\partial \rho'}{\partial t} \;=\; & -\rho'\frac{\partial \widetilde{u_j}}{\partial x_j} - \bar{\rho}\frac{\partial u_j''}{\partial x_j} - \rho'\frac{\partial u_j''}{\partial x_j} \\ & -u_j''\frac{\partial \bar{\rho}}{\partial x_j} - \widetilde{u_j}\frac{\partial \rho'}{\partial x_j} - u_j''\frac{\partial \rho'}{\partial x_j}.\end{aligned} \tag{101}$$

Averaging the combined transport of $u_j'' \partial u_i''/\partial t$ and $u_i'' \partial u_j''/\partial t$ as well as the transport of $2\rho' \partial \rho'/\partial t$ and applying homogeneity, gives rise to:

$$\frac{\partial}{\partial t}\overline{u_i'' u_j''} = -\overline{u_i'' u_k''}\frac{\partial \widetilde{u_j}}{\partial x_k} - \overline{u_j'' u_k''}\frac{\partial \widetilde{u}_i}{\partial x_k} + \overline{u_i'' u_j''\frac{\partial u_k''}{\partial x_k}} + \ldots \tag{102}$$

$$\frac{\partial}{\partial t}\overline{\rho'^2} = -2\overline{\rho'^2}\frac{\partial \widetilde{u_j}}{\partial x_j} - 2\bar{\rho}\overline{\rho'\frac{\partial u_j''}{\partial x_j}} - 2\overline{\rho' u_j''}\frac{\partial \bar{\rho}}{\partial x_j} - \overline{\rho'^2\frac{\partial u_j''}{\partial x_j}}. \tag{103}$$

Now, Blaisdell et al. (1991) argue that due to homogeneity, correlation functions can only depend on time. Since the left hand side of equations (102), (103) is solely a function of time, the same must be valid for the right hand side, especially for each of the rhs terms. Thus from (102):

$$\frac{\partial \widetilde{u_i}}{\partial x_j} = A_{ij}(t) \tag{104}$$

which corresponds to a linear mean velocity field

$$\widetilde{u_i}(\vec{x}, t) = A_{ij}(t)x_j. \tag{105}$$

The time-dependent constant of integration is not considered because it can be treated as a time-dependent body force, which is not of interest to us. Similarly, eq. (103) provides the condition

$$\bar{\rho} = \bar{\rho}(t), \tag{106}$$

since $\overline{\rho'\partial u_j''/\partial x_j}$ is generally non-zero. Restrictions on $\bar{p}$ can be derived from eq. (92). From the third term on the rhs one gets (since $\overline{p'd'}$ is non-zero):

$$\bar{p} = \bar{p}(t). \tag{107}$$

From the averaged equation of state for perfect gases:

$$\bar{p} = \bar{\rho}R\tilde{T}\,. \tag{108}$$

One finally concludes that for spatially uniform mean density and pressure the temperature must also be uniform is space, i.e. $\tilde{T} = \tilde{T}(t)$.

2.5.2. *Mean flow characteristics of homogeneous shear turbulence*
Taking equations (104), (106) and (107) into account the mean mass and momentum transport equations (46), (47) reduce to:

$$\frac{d\bar{\rho}}{dt} + \bar{\rho}A_{jj}(t) = 0, \tag{109}$$

$$\frac{\partial \widetilde{u_i}}{\partial t} + \widetilde{u_k}\frac{\partial \widetilde{u_i}}{\partial x_k} = 0. \tag{110}$$

Differentiation of (110) with respect to x_j provides a nonlinear coupled set of ordinary differential equations to be satisfied by the mean velocity gradient tensor A_{ij}:

$$\frac{dA_{ij}}{dt} + A_{ik}A_{kj} = 0. \tag{111}$$

These equations which apply to any homogeneous turbulence field further simplify in the case of homogeneous shear flow with constant shear rate in x_2-direction. We assume a mean momentum transport in x_1-direction:

$$\widetilde{u_i}(\vec{x},t) = (\widetilde{u_1}(x_2,t), 0, 0) \tag{112}$$

and obtain from (109) and (111):

$$\bar{\rho} = const, \tag{113}$$

$$A_{12}(t) = \frac{d\widetilde{u_1}}{dx_2} = S = const. \tag{114}$$

The mean internal energy balance (57) reduces to

$$\bar{\rho}\frac{d\tilde{e}}{dt} = -\overline{p'd'} + \bar{\mu}S^2 + \bar{\rho}\epsilon \tag{115}$$

if fluctuations of viscosity are neglected in the mean flow dissipation rate (2nd term on the rhs). The turbulence kinetic energy (TKE) balance takes the simple form:

$$\bar{\rho}\frac{dK}{dt} = -\bar{\rho}\widetilde{u_1''u_2''}S + \overline{p'd'} - \bar{\rho}\epsilon. \tag{116}$$

The sum of $\tilde{e}$ and K increases in time due to TKE-production and mean flow dissipation. Since $\overline{p'd'}$ is predominantly negative, $\tilde{e}$ grows in time. DNS data indicate an exponential growth of K for long times, i.e. $dK/dt \sim K$ and, since the production and $\overline{p'd'}$ terms do not balance, ϵ grows in time as well. The mean shear rate introduces directionality into the turbulence structure. Hence, the Reynolds stress tensor is homogeneous, but anisotropic:

$$\widetilde{u_i''u_j''} = \begin{pmatrix} \widetilde{u_1''^2} & \widetilde{u_1''u_2''} & 0 \\ \widetilde{u_1''u_2''} & \widetilde{u_2''^2} & 0 \\ 0 & 0 & \widetilde{u_3''^2} \end{pmatrix} \quad , \qquad \widetilde{u_1''^2} \neq \widetilde{u_2''^2} \neq \widetilde{u_3''^2} \; . \tag{117}$$

Blaisdell et. al. (1991) provide a conclusive argument that the mass flux $\overline{\rho u_i'}$ vanishes in homogeneous turbulence. This means that Reynolds

and Favre averaged velocities coincide. In the TKE dissipation rate, $\bar{\rho}\epsilon$, the inhomogeneous term vanishes. If we further exclude viscosity fluctuations, $\bar{\rho}\epsilon$ takes the simple form:

$$\bar{\rho}\epsilon = \bar{\mu}\overline{\omega_i'\omega_i'} + \left(\frac{4}{3}\bar{\mu} + \overline{\mu_v}\right)\overline{d''^2}. \tag{118}$$

2.5.3. *Turbulent stress transport in homogeneous shear flow*
Although the homogeneity condition removes several unknown terms from the full transport equations, compressible homogeneous shear turbulence is still today a flow case which is hard to predict accurately. One reason is certainly the difficulty associated with pressure strain modelling. From equations (70) - (83) we obtain the transport equations for the four Reynolds stresses:

$$\bar{\rho}\frac{d}{dt}\left(\frac{1}{2}\widetilde{u_1''^2}\right) = -\bar{\rho}\widetilde{u_1''u_2''}S + \overline{p'\frac{\partial u_1'}{\partial x_1}} - \bar{\rho}\left(\epsilon_{11}^S + \epsilon_{11}^d\right), \tag{119}$$

$$\bar{\rho}\frac{d}{dt}\left(\frac{1}{2}\widetilde{u_2''^2}\right) = \overline{p'\frac{\partial u_2'}{\partial x_2}} - \bar{\rho}\left(\epsilon_{22}^S + \epsilon_{22}^d\right), \tag{120}$$

$$\bar{\rho}\frac{d}{dt}\left(\frac{1}{2}\widetilde{u_3''^2}\right) = \overline{p'\frac{\partial u_3'}{\partial x_3}} - \bar{\rho}\left(\epsilon_{33}^S + \epsilon_{33}^d\right), \tag{121}$$

$$\bar{\rho}\frac{d}{dt}\left(\widetilde{u_1''u_2''}\right) = -\bar{\rho}\widetilde{u_2''^2}S + \overline{p'\left(\frac{\partial u_1'}{\partial x_2} + \frac{\partial u_2'}{\partial x_1}\right)} - \bar{\rho}\left(\epsilon_{12}^S + \epsilon_{12}^d\right). \tag{122}$$

Only the streamwise component and the shear stress obtain energy directly via production. The remaining components are fed by redistribution of energy. As shown by Blaisdell et al. (1991) the ordering of the normal stresses in compressible homogeneous shear turbulence is the same as in the incompressible case, i.e. the streamwise component is the most energetic, followed by the spanwise component, with the component in the shear direction being the least energetic. So far, the only explicit differences to the incompressible case are the appearance of dilatational dissipation rates $\bar{\rho}\epsilon_{ij}^d$ and the fact that the pressure strain terms sum up to a non-zero pressure-dilatation term.

2.5.4. *Compressibility parameters*
The TKE equation (116) can be used to derive two independent compressibility parameters which are needed to quantify effects of compressibility on the turbulence structure. To this end, we nondimensionalize the K-equation

choosing $1/S$ as the time scale, two different length scales l_0, λ_0 (an integral scale l_0 and a Taylor microscale λ_0), u_0 as a fluctuating velocity scale, $\bar{\rho}u_0^2$ as a characteristic pressure fluctuation and μ_0 as a reference viscosity. The index '0' refers to constant initial values of these quantities. Then the nondimensional TKE equation reads:

$$M_{go}\frac{dK^*}{dt^*} = -M_{go}\overline{\rho^* u_1''^* u_2''^*} - M_{to}\overline{p'^* d'^*} - \frac{M_{to}}{Re_{to}}\left(\frac{l_0}{\lambda_0}\right)^2 \epsilon^*, \tag{123}$$

with the:

– gradient Mach number:

$$M_{go} = Sl_0/\overline{c_0} \tag{124}$$

– turbulent Mach number:

$$M_{to} = u_0/\overline{c_0} \tag{125}$$

– turbulent Reynolds number:

$$Re_{to} = \bar{\rho} l_0 u_0/\mu_0 \tag{126}$$

as free parameters. The star $*$ indicates non-dimensional quantities. (It has this meaning only in eq. (123)).

The turbulent Reynolds number Re_{to} drops out of the list of nondimensional parameters, if a simple estimate of l_0/λ_0, as provided by Tennekes and Lumley (1972), is assumed to hold, namely

$$l_0/\lambda_0 = O\left(Re_{to}^{1/2}\right). \tag{127}$$

This is also found if u_0^3/l_0 is used to scale ϵ. Sarkar (1995) has found the gradient Mach number, M_{go}, to be the key parameter in explaining the stabilizing effect of compressibility on the TKE growth rate. We will come back to this point later. Earlier Blaisdell et al. (1991) had already used a gradient Mach number which they called shear rate Mach number and which differs from Sarkar's definition only in the specification of the integral length scale. Durbin and Zeman (1992) had introduced a distortion Mach number in their RDT analysis that can be interpreted as the mean Mach number change across an 'eddy'. The expression 'distortion Mach number' was then adopted by Jacquin et al. (1993), Cambon et al. (1993) and Simone et al. (1997) to parameterize rapidly sheared and strained compressible homogeneous turbulence. It is important to note that M_{go} and M_{to} are two independent parameters since their ratio Sl_0/u_0 can be changed via l_0, u_0.

There is some ambiguity in the definition of l_0. While Sarkar (1995) chooses

$$l_0 = \int_{-\infty}^{\infty} (u_1''(x_2)\widetilde{u_1''(x_2+r_2)})\Big|_{t=0} dr_2 \;/\; \widetilde{u_1''^2}(x_2)\Big|_{t=0}, \tag{128}$$

Blaisdell et al. (1991) define

$$l_0 = \int_{-\infty}^{\infty} (u_1''(x_2)\widetilde{u_2''(x_2+r_2)})\Big|_{t=0} dr_2 \;/\; \widetilde{u_1''u_2''}(x_2)\Big|_{t=0}. \tag{129}$$

In view of the fact that the 2-2 components of the Reynolds stress tensor, of the pressure strain tensor and of the compressibe dissipation rate tensor are the most affected by compressibility (Blaisdell et al. (1991)), a suitable alternative to the definitions (128), (129) would be:

$$l_0 = \int_{-\infty}^{\infty} (u_2''(x_2)\widetilde{u_2''(x_2+r_2)})\Big|_{t=0} dr_2 \;/\; \widetilde{u_2''^2}(x_2)\Big|_{t=0} \tag{130}$$

A supporting argument for this definition follows from the linearized inviscid equations of motion. For homogeneous shear turbulence there exists a direct link between u_2' and d' in Fourier space (Friedrich and Bertolotti (1997)). On the other hand, the linear inviscid momentum balance in x_2-direction,

$$\left(\frac{\partial}{\partial t} + \bar{u_1}\frac{\partial}{\partial x_1}\right) u_2' = -\frac{1}{\bar{\rho}}\frac{\partial p'}{\partial x_2}, \tag{131}$$

reflects the coupling between u_2- and p-fluctuations. Pressure fluctuations are found to be strongly affected by compressibility effects in plane and annular mixing layers (Vreman et al. (1996), Freund et al. (1997)). The suppression of the pressure strain rate correlation in the stress equation for the shear direction (x_2) is explained primarily by the reduction of pressure fluctuations due to compressibility. In fact, Freund et al. (1997) demonstrate a significant decrease of the correlation length of velocity fluctuations in the shear direction, which supports a definition of l_0 according to (130).

3. Compressibility effects due to turbulent fluctuations and modelling of explicit compressibility terms

Most of our present knowledge about compressibility effects due to turbulent fluctuations (intrinsic effects of compressibility) stems from direct numerical simulations and rapid distortion analysis. In this chapter we will therefore first inspect the linear equations of motion in order to gain some

insight into the physics of compressible turbulence, then summarize the most important recent findings of DNS before we discuss turbulence models derived from DNS data.

3.1. HOMOGENEOUS ISOTROPIC TURBULENCE

The statistical equations for decaying isotropic turbulence are obtained from those for homogeneous shear turbulence setting the mean shear rate equal to zero. Without loss of generality the mean velocity can be assumed zero. The mean density is constant, thus:

$$\bar{\rho} = const., \quad \tilde{u}_i = 0. \tag{132}$$

The turbulent stress tensor is isotropic, with

$$\widetilde{u_1''^2} = \widetilde{u_2''^2} = \widetilde{u_3''^2} = 2K/3. \tag{133}$$

The time evolutions of the mean internal energy, $\bar{\rho}\tilde{e}$, and of the turbulent kinetic energy, $\bar{\rho}K$, are determined by $\overline{p'd'}$ and $\bar{\rho}\epsilon$ alone, consequently:

$$\tilde{e} + K = const. \tag{134}$$

While K decays, $\tilde{e}$ increases in time, along with $\bar{p}$ and $\tilde{T}$. The decay of K entrains that of $\bar{\rho}\epsilon$ and $\overline{p'd'}$ after initial transients. Normalized density, pressure and temperature variances decay as well. Integral and Taylor microscales grow after some initial decay.

3.1.1. *Linear analysis of turbulent fluctuations*

We assume fluctuations of density, pressure and temperature to be small with respect to their mean values, and velocity fluctuations to be small compared to the mean speed of sound, $\bar{c}_0$. The latter is equivalent to assuming low turbulent Mach number, M_{to}. There are two characteristic velocities in compressible isotropic turbulence, namely $u_0 = (2K_0/3)^{1/2}$ and $\overline{c_0}$. Together with an integral length scale l_0 they define two timescales:

- the eddy-turnover time, $\tau_t = l_0/u_0$
- and the acoustic time, $\tau_a = l_0/\overline{c_0}$.

The ratio of these two time scales is the turbulent Mach number:

$$M_{to} = \tau_a/\tau_t. \tag{135}$$

Low M_{to} means that the two time scales are disparate. In this situation we may linearize the equations of motion with respect to fluctuations. From (1), (2), (24) we then obtain for decaying isotropic turbulence:

$$\frac{\partial \rho'}{\partial t} + \bar{\rho} d' = 0, \tag{136}$$

$$\frac{\partial u_i'}{\partial t} = -\frac{1}{\bar{\rho}} \frac{\partial p'}{\partial x_i} + \bar{\nu} \frac{\partial^2 u_i'}{\partial x_j \partial x_j} + (\bar{\nu}/3 + \bar{\mu}_v/\bar{\rho}) \frac{\partial d'}{\partial x_i}, \tag{137}$$

$$\frac{\partial p'}{\partial t} = -\gamma \bar{p} d' + (\gamma - 1) \bar{k} \frac{\partial^2 T'}{\partial x_j \partial x_j}. \tag{138}$$

An alternative energy equation follows from the entropy balance, viz:

$$\frac{\partial s'}{\partial t} = \frac{\bar{k}}{\bar{\rho} \bar{T}} \frac{\partial^2 T'}{\partial x_j \partial x_j}. \tag{139}$$

From this coupled set of equations we now derive wave equations for p', ρ', d' and diffusion equations for ω_i' and s'. Thereby we use the linearized perfect gas relation

$$p' = R(\rho' \bar{T} + T' \bar{\rho}) \tag{140}$$

and the linearized state relation $p' = p'(\rho', s')$ to express time-derivatives

$$\frac{\partial p'}{\partial t} = \gamma R \bar{T} \frac{\partial \rho'}{\partial t} + \frac{\bar{p}}{c_v} \frac{\partial s'}{\partial t} \tag{141}$$

or the Laplacian:

$$\frac{\partial^2 p'}{\partial x_j \partial x_j} = \gamma R \bar{T} \frac{\partial^2 \rho'}{\partial x_j \partial x_j} + \frac{\bar{p}}{c_v} \frac{\partial^2 s'}{\partial x_j \partial x_j}. \tag{142}$$

Equation (141) is valid on an acoustic time scale, τ_a, in which the time variations of $\bar{T}$ and $\bar{p}$ due to viscous effects can be neglected. (142) is straightforward due to spatial homogeneity of $\bar{T}, \bar{p}$.

Now, applying the Laplacian to eq. (136), differentiating (138), (139) with respect to time, taking the divergence of eq. (137), introducing (140) and combining these results, leads to the following wave equation for the pressure fluctuations:

$$\begin{aligned} \frac{\partial^2 p'}{\partial t^2} - \bar{c}^2 \frac{\partial^2 p'}{\partial x_j \partial x_j} &= \gamma \left(\frac{4}{3} \bar{\nu} + \bar{\mu}_v/\bar{\rho} \right) \frac{\partial^2}{\partial x_j \partial x_j} \left(\frac{\partial p'}{\partial t} \right) \\ &\quad + \left(1 - \frac{4}{3} \overline{Pr} - \frac{c_p \bar{\mu}_v}{\bar{k}} \right) \frac{\bar{p}}{\bar{c}_v} \frac{\partial^2 s'}{\partial t^2}. \end{aligned} \tag{143}$$

The first term on the rhs accounts for sound absorption at high frequencies. $\overline{Pr} = \bar{\mu} c_p / \bar{k}$ is the mean Prandtl number. Equations, similar to (143) are obtained for ρ' and d':

$$\frac{\partial^2 \rho'}{\partial t^2} - \bar{c}^2 \frac{\partial^2 \rho'}{\partial x_j \partial x_j} = \left(\frac{4}{3} \bar{\nu} + \bar{\mu}_v / \bar{\rho} \right) \frac{\partial^2}{\partial x_j \partial x_j} \left(\frac{\partial \rho'}{\partial t} \right) + \frac{\bar{p}}{c_v} \frac{\partial^2 s'}{\partial x_j \partial x_j}, \tag{144}$$

$$\begin{aligned} \frac{\partial^2 d'}{\partial t^2} - \bar{c}^2 \frac{\partial^2 d'}{\partial x_j \partial x_j} &= \left(\frac{4}{3} \bar{\nu} + \bar{\mu}_v / \bar{\rho} \right) \frac{\partial^2}{\partial x_j \partial x_j} \left(\frac{\partial d'}{\partial t} \right) \\ &\quad - (\gamma - 1) \bar{T} \frac{\partial^2}{\partial x_j \partial x_j} \left(\frac{\partial s'}{\partial t} \right). \end{aligned} \tag{145}$$

Taking the curl of eq. (137) and replacing the Laplacian of T' with the help of (140) and (142) gives rise to diffusion equations for the velocity and entropy fluctuations:

$$\frac{\partial \omega_i'}{\partial t} = \bar{\nu} \frac{\partial^2 \omega_i'}{\partial x_j \partial x_j}, \tag{146}$$

$$\frac{\partial s'}{\partial t} = \frac{\bar{\nu}}{\overline{Pr}} \left(\frac{\partial^2 s'}{\partial x_j \partial x_j} + \frac{R}{\bar{p}} \frac{\partial^2 p'}{\partial x_j \partial x_j} \right). \tag{147}$$

The conclusions we draw from these equations as long as viscosity plays a role, are:

- pressure (density and dilatation) fluctuations are coupled with entropy fluctuations. The coupling between p' and s' is via viscosity and therefore weak,
- only vorticity fluctuations develop independently,
- the wave character of p', ρ', d' and the diffusive character of ω_i', s' are obvious.

If we neglect viscosities, we note that:

- the vorticity and entropy fluctuations are frozen (this corresponds to Taylor's hypothesis used in experiments),
- the pressure and dilatation fluctuations follow a pure wave equation,
- density fluctuations are still coupled with entropy fluctuations.

Vorticity, pressure and entropy fluctuations have been called 'modes' by Kovasznay (1953) and Morkovin (1962), and are since then referred to as the vorticity mode, the acoustic mode and the entropy mode of compressible turbulence. In isotropic turbulence these three modes are decoupled.

The decoupling is a result of the missing of mean shear or of gradients of mean thermodynamic variables. It has the important consequence that compressibility effects studied in DNS depend more on the initial conditions than on the turbulent Mach number (Blaisdell et al. (1993)). Therefore DNS data of isotropic turbulence can in general not be used to validate turbulence models for the compressible dissipation rate and the pressure-dilatation correlation. We come back to the effect of initial conditions in chapter 3.1.2.

In order to demonstrate the coupling between the acoustic pressure mode and the velocity field, we apply Helmholtz's decomposition of u_i' into incompressible, $u_i^{s\prime}$, and compressible parts, $u_i^{d\prime}$:

$$u_i' = u_i^{s\prime} + u_i^{d\prime} \tag{148}$$

where

$$\frac{\partial u_i^{s\prime}}{\partial x_i} = 0, \quad \epsilon_{ijk}\frac{\partial u_k^{d\prime}}{\partial x_j} = 0. \tag{149}$$

Furthermore, we follow Simone (1995) and use the Craya-Herring formalism (Craya (1958), Cambon(1990)) to express the Fourier transform of u_i' in an orthonormal frame of reference with bases $(e_i^{(1)}, e_i^{(2)}, e_i^{(3)})$ normal and parallel to the wavevector $\vec{k}$. Defining a pair of three-dimensional Fourier transforms by

$$\hat{A}(\vec{k},t) = \frac{1}{(2\pi)^3}\int\limits_{V(\vec{x})} A(\vec{x},t)exp(-i\vec{k}\cdot\vec{x})d\vec{x}, \tag{150}$$

$$A(\vec{x},t) = \int\limits_{V(\vec{k})} \hat{A}(\vec{k},t)exp(i\vec{k}\cdot\vec{x})d\vec{k}, \tag{151}$$

(where the caret denotes the Fourier coefficient and $i^2 = -1$), the Fourier transform of the velocity fluctuation[2] reads:

$$\hat{u}_i(\vec{k},t) = \underbrace{\hat{\varphi}^{(1)}(\vec{k},t)e_i^{(1)}(\vec{k}) + \hat{\varphi}^{(2)}(\vec{k},t)e_i^{(2)}(\vec{k})}_{\hat{u}_i^s} + \underbrace{\hat{\varphi}^{(3)}(\vec{k},t)e_i^{(3)}(\vec{k})}_{\hat{u}_i^d}. \tag{152}$$

The first two terms on the rhs of (152) represent the Fourier transform of the solenoidal velocity fluctuation $u_i^{s\prime}$; the third is the compressible (or dilatational) contribution, aligned with $\vec{k}$. $\hat{u}_i^s$ lies in the plane $(\vec{e}^{(1)}, \vec{e}^{(2)})$

[2]For simplification we omit the dash in Fourier space

perpendicular to $\vec{k}$. It is possible to fix the coordinates in that plane by introducing a polar axis $\vec{n}$ (Herring (1974)) either according to symmetries of the mean flow (if any) or the statistical properties of the fluctuating field, viz:

$$\vec{e}^{(1)} = \frac{\vec{k} \times \vec{n}}{|\vec{k} \times \vec{n}|}, \quad \vec{e}^{(2)} = \vec{e}^{(3)} \times \vec{e}^{(1)}, \quad \vec{e}^{(3)} = \vec{k}/|\vec{k}|. \tag{153}$$

The Fourier transforms of vorticity and dilatation fluctuations have the form:

$$\hat{\omega}_i = \epsilon_{ijk} i k_j \hat{u}_k = ik \left(\hat{\varphi}^{(1)} e_i^{(2)} - \hat{\varphi}^{(2)} e_i^{(1)} \right), \tag{154}$$

$$\hat{d} = i k_i \hat{u}_i = ik \hat{\varphi}^{(3)}, \quad k = |\vec{k}|. \tag{155}$$

Only the incompressible modes $(\hat{\varphi}^{(1)}, \hat{\varphi}^{(2)})$ contribute to Kovasznay's vorticity mode, while the compressible mode $\hat{\varphi}^{(3)}$ alone determines the dilatation fluctuation. Fourier transforming the inviscid equations of motion (136) - (138), leads to:

$$\frac{\partial \hat{\rho}}{\partial t} + \bar{\rho} i k \hat{\varphi}^{(3)} = 0, \tag{156}$$

$$\frac{\partial \hat{u}_i}{\partial t} = -\frac{1}{\bar{\rho}} i k_i \hat{p}, \tag{157}$$

$$\frac{\partial \hat{p}}{\partial t} = -\gamma \bar{p} i k \hat{\varphi}^{(3)}, \tag{158}$$

Introducing (152) into (157) and multiplying (157) scalarly with $e_i^{(j)} (j = 1, 2, 3)$, one obtains a set of equations determining the behaviour of the incompressible and compressible modes $\hat{\varphi}^{(3)}, \hat{\varphi}^{(4)} = i\hat{p}/(\bar{\rho}\bar{c})$:

$$\frac{\partial \hat{\varphi}^{\alpha}}{\partial t} = 0, \quad \alpha = 1, 2, \tag{159}$$

$$\frac{\partial \hat{\varphi}^{(3)}}{\partial t} + \bar{c} k \hat{\varphi}^{(4)} = 0, \tag{160}$$

$$\frac{\partial \hat{\varphi}^{(4)}}{\partial t} - \bar{c} k \hat{\varphi}^{(3)} = 0. \tag{161}$$

Cambon et al. (1993) and Simone (1995) call this the purely acoustic regime of isotropic turbulence, where energy is exchanged between the dilatational velocity and the pressure at a frequency $\bar{c}k$, while the solenoidal

component $u_i^{s\prime}$ is frozen. Differentiating equations (160) and (161) with respect to time and combining them gives rise to the two wave equations in Fourier space:

$$\frac{\partial^2 \hat{\varphi}^{(3)}}{\partial t^2} + \bar{c}^2 k^2 \hat{\varphi}^{(3)} = 0, \tag{162}$$

$$\frac{\partial^2 \hat{\varphi}^{(4)}}{\partial t^2} + \bar{c}^2 k^2 \hat{\varphi}^{(4)} = 0, \tag{163}$$

which, together with eq. (159), demonstrate the independence of all modes and e.g. the fact that the pressure fluctuations have no influence on the solenoidal velocity component. The analytical solution of eqs. (162), (163) is given by Simone (1995) in the form:

$$\hat{\varphi}^{(3)}(\vec{k},t) = \hat{\varphi}^{(3)}(\vec{k}_0,0)\cos\omega t - \hat{\varphi}^{(4)}(\vec{k}_0,0)\sin\omega t, \tag{164}$$

$$\hat{\varphi}^{(4)}(\vec{k},t) = \hat{\varphi}^{(3)}(\vec{k}_0,0)\sin\omega t + \hat{\varphi}^{(4)}(\vec{k}_0,0)\cos\omega t, \tag{165}$$

with $\omega = \bar{c}k = \bar{c}_0 k_0$. k_0 is the magnitude of the wavevector at time t_0. $\vec{k}_0$ plays the same role in wavenumber space as the Lagrangian coordinate in physical space. In isotropic turbulence $\vec{k}$ is independent of time, i.e. $\vec{k} = \vec{k}_0$. Figure 1 shows the time evolution of the compressible modes $\hat{\varphi}^{(3)}$, $\hat{\varphi}^{(4)}$ for initial values between 0 and 1, corresponding to acoustical equilibrium[3], i.e. to a situation in which the kinetic energy of the dilatational velocity mode equals the potential energy of the pressure mode:

$$\frac{1}{2}\overline{u_i^{d\prime} u_i^{d\prime}} = \frac{1}{2}\overline{p'p'}/(\bar{\rho}\bar{c})^2. \tag{166}$$

A measure for acoustical equilibrium or non-equilibrium had earlier been introduced by Sarkar et al. (1991) in the form of the energy partition parameter

$$F = \gamma\bar{\rho}\bar{p}\frac{\overline{u_i^{d\prime} u_i^{d\prime}}}{\overline{p'p'}}. \tag{167}$$

One easily verifies that eq. (166) corresponds to $F = 1$. Sarkar et al. (1991) had shown, based on DNS data of isotropic turbulence that $F = 1$ even holds for high turbulent Mach numbers ($M_{to} = 0.5$) and had used the value $F = 1$ in deriving a model for the compressible dissipation rate (see section 3.1.3).

[3]A 'strong form' of acoustical equilibrium was used to specify initial conditions for fig. 1, by assuming that the energy balance occurs at each wavenumber.

3.1.2. *Importance of initial conditions*
Blaisdell et al. (1991, 1993) emphasize that initial conditions strongly influence the time evolution of correlation functions which makes it difficult to use simulations of decaying isotropic turbulence to evaluate compressible turbulence models. This difficulty is removed when a mean shear rate is introduced (See section 3.2).

The authors have performed several DNS to demonstrate the effect of initial conditions. They varied the initial rms-values of density and temperature, of turbulent Mach number and of the fraction χ of compressible kinetic energy, defined as:

$$\chi = \overline{u_i^{d'} u_i^{d'}}/(2K). \tag{168}$$

Table 3 contains the simulation parameters of six of the simulations. The number 96 appearing in the case identifications refers to the 96^3 grid

TABLE 3. Initial parameters for DNS of isotropic turbulence. Taken from Blaisdell et al. (1991).

Case	iga96	igb96	idc96	ie96	ifd96	ife96
$\rho_{rms,0}$	0.1	0.016	0	0.15	0.15	0
$T_{rms,0}$	0.1	0.016	0	0.15	0.15	0
χ_o	0.1	0.816	0	0.25	0.25	0
M_{to}	0.05	0.11	0.3	0.3	0.7	0.7
Re_{to}	90.6	360	160	160	90	91

used in these simulations. The initial spectra are the same in all cases. Cases iga96 and igb96 have been chosen to test how well ideas from linear acoustics could predict the evolution of turbulence. While the turbulent Mach numbers are low in both cases, the equilibrium parameters F_0 are very different. Case iga96 has an F_0 of 1/40, corresponding to comparatively large pressure fluctuations and case igb96 is characterized by $F_0 \approx 40$ and large dilatational velocity fluctuations. Cases idc96 and ie96 have moderate turbulent Mach numbers and differ in the initial fluctuations of density, temperature and dilatational velocity. Cases ifd96 and ife96 have been selected to show the effect of higher Mach number. The turbulent Reynolds numbers $Re_{to} = 2\bar{\rho}K/(\epsilon\bar{\mu})$ do not vary much from case to case and need therefore not be discussed.

Figure 2 shows the nondimensional variances of pressure and density fluctuations for the cases iga96 (top) and igb96 (bottom). Simulation iga96

starts with remarkable density and pressure fluctuations. Energy is transferred from pressure to dilatational velocity fluctuations in a highly oscillatory way. The transfer process reaches an acoustical equilibrium state after one eddy-turnover time. Simulation igb96 on the other hand produces pressure and density fluctuations from low levels, in close agreement with an isentropic process. These results demonstrate the existence of linear acoustic mechanisms in compressible turbulence as described in the previous subsection.

Figure 3 aims at illustrating the dependence of compressibility effects on initial conditions. It shows the time evolution of the dilatational fraction χ_ϵ of the turbulent dissipation rate:

$$\chi_\epsilon = \frac{\epsilon_d}{\epsilon} = \frac{\epsilon_d/\epsilon_s}{1+\epsilon_d/\epsilon_s}, \tag{169}$$

for the 4 remaining flow cases of table 3. The top figure contains the $M_{to} = 0.3$ cases, the bottom figure the $M_{to} = 0.7$ cases. The values of χ_ϵ differ from case to case. It is obvious that χ_ϵ not only depends on M_t, but also on the initial conditions. The behaviour of χ_ϵ is also consistent with linear analysis, since the coupling between acoustical and vortical modes is weak. Strong coupling could only be due to nonlinearities and would lead to curves which approach each other. Of course, nonlinear vortex interactions are weak for low Reynolds number turbulence. Blaisdell et al. (1991) could however show that the dependence on initial conditions persists at higher Reynolds numbers.

The authors conclude that simulations of isotropic turbulence cannot be used to validate turbulence models. Recently Ristorcelli and Blaisdell (1996) have designed consistent initial conditions for DNS. Tests for decaying isotropic turbulence show the natural development of the flow during the initial phase.

3.1.3. *Turbulence models for the compressible dissipation rate*

Model proposed by Sarkar et al. (1991):

Sarkar et al.'s model is based on ideas from linear acoustics and uses assumptions such as

$$F = 1, \quad \overline{p'd'} \approx 0. \tag{170}$$

Based on an asymptotic analysis for low turbulent Mach numbers M_t and on DNS data, the authors show that isotropic turbulence, in the state of acoustic equilibrium, is characterized by (170). F=1 is a good approx-

imation even at $M_t = 0.5$. Using the definitions (65), (66) for ϵ_s, ϵ_d and $\bar{\mu}_v = 0$, the dilatational fraction χ_ϵ of the dissipation rate reads

$$\chi_\epsilon = \frac{4\overline{d'^2}/3}{\overline{\omega_i'\omega_i'} + 4\overline{d'^2}/3} \tag{171}$$

Then defining compressible and incompressible Taylor microscales λ_d, λ_s:

$$\lambda_d^2 = \overline{u_i^{d'} u_i^{d'}}/\overline{d'^2}, \tag{172}$$

$$\lambda_s^2 = \overline{u_i^{s'} u_i^{s'}}/\overline{\omega_i'\omega_i'} \tag{173}$$

and using χ, the fraction of compressible kinetic energy, given by eq. (168), χ_ϵ takes the form:

$$\chi_\epsilon = \frac{\chi}{\chi + \frac{3}{4}\left(\frac{\lambda_d}{\lambda_s}\right)^2 (1-\chi)}, \tag{174}$$

from which ϵ_d/ϵ_s is obtained:

$$\frac{\epsilon_d}{\epsilon_s} = \frac{4\lambda_s^2 \chi}{3\lambda_d^2(1-\chi)}. \tag{175}$$

For weakly compressible turbulence

$$\lambda_d/\lambda_s = O(1) \tag{176}$$

is a permissible assumption. In compressed turbulence, as e.g. in shock-turbulence interactions, relation (176) certainly makes no sense in general. Introducing (176) into (175) leads to:

$$\frac{\epsilon_d}{\epsilon_s} = \beta_1 \chi + O(\chi^2), \tag{177}$$

where $\beta_1 = O(1)$. Now, from the definition of F

$$F = \gamma \bar{\rho} \bar{p} \frac{\overline{u_i^{d'} u_i^{d'}}}{\overline{p'p'}} = \frac{(\gamma \bar{p})^2}{\overline{p'p'}} \chi M_t^2, \tag{178}$$

the order of magnitude relation

$$\overline{p'p'} = O(\bar{\rho}^2 u_{rms}^4) = O(\bar{\rho}^2 K^2) \tag{179}$$

and $F = 1$, the authors conclude

$$\chi = O(M_t^2). \tag{180}$$

From (177) they obtain the model

$$\epsilon_d = \epsilon_s \alpha_1 M_t^2. \tag{181}$$

The model constant α_1 is specified in the following way: Decaying isotropic turbulence is governed by the transport equations:

$$\bar{\rho} c_v \frac{d\tilde{T}}{dt} = -\overline{p'd'} + \epsilon_s + \epsilon_d, \tag{182}$$

$$\bar{\rho} \frac{dK}{dt} = \overline{p'd'} - \epsilon_s - \epsilon_d, \tag{183}$$

$$\frac{d\epsilon_s}{dt} = -c_{\epsilon 2} \frac{\epsilon_s^2}{K}. \tag{184}$$

The equations for $\tilde{e}$ and K are still exact. Only the last equation is modelled. $c_{\epsilon 2}$ is set to 1.83, which is the proper value for decaying incompressible isotropic turbulence at high Reynolds number. With the help of eq. (183) and the definition $M_t^2 = 2K/(\gamma R \tilde{T})$, the equation for $\tilde{T}$ is converted into an equation for M_t^2. Setting $\overline{p'd'}$ to zero the set of equations for M_t^2, K, ϵ_s is solved for different initial conditions and different values of α_1. The best agreement between modelled and directly simulated turbulence decay was achieved for $\alpha_1 = 1$. For homogeneous shear turbulence, however, Sarkar (1992) suggested the value $\alpha_1 = 0.5$.

Zeman's model:

Zeman (1990) has formulated a model assuming the existence of shock-like structures in the flow. On the basis of a stochastic shocklet model he inferred the parametric expression

$$\frac{\epsilon_d}{\epsilon_s} = c_z f(M_t, F). \tag{185}$$

$c_z = 0.75$. The so-called shocklet dissipation function $f(M_t, F)$ is an integral functional of a pdf (m, F) of the fluctuating Mach number m. F is the kurtosis of m, i.e. $F = \overline{m^4} / \left(\overline{m^2}\right)^2$ and characterizes the departure from Gaussianity. From DNS of homogeneous turbulence, F was estimated as $F \approx 4$ and $f(M_t, F)$ approximated as

$$f(M_t) = \left[1 - exp\left(-\frac{1}{2}(\gamma+1)(M_t - M_{to})^2/\Lambda^2\right)\right] \mathcal{H}(M_t - M_{to}), \tag{186}$$

TABLE 4. Parameters of Zeman's dissipation model

	Λ	M_{to}
free shear flows	0.6	$0.1(2/(\gamma+1))^{1/2}$
boundary layers	0.66	$0.25(2/(\gamma+1))^{1/2}$

where γ is the ratio of specific heats, $\mathcal{H}(x)$ the Heaviside step function and M_{to} a threshold value, below which shocklets cannot occur. The parameters Λ, M_{to} have different values for free and wall bounded turbulence, see table 4. The function $f(M_t)$ is taken from Wilcox (1993).

Fauchet's model:

Based on a new two-point closure for weakly compressible isotropic turbulence, Fauchet (1998), Fauchet et al. (1997) derived a model for the compressible dissipation rate valid for low turbulent Mach numbers:

$$\frac{\epsilon_d}{\epsilon_s} = c_\epsilon M_t^4 ln\,(Re_L)\, Re_L^{-1} \quad , \qquad \text{for } M_t < 0.1 \tag{187}$$

M_t and Re_L are defined as follows:

$$M_t = (2K)^{1/2}/\overline{c_o} \quad , \qquad Re_L = (2K)^{1/2} L/\nu_o. \tag{188}$$

The integral scale L is computed from the energy spectrum $E(k)$:

$$L = \frac{\pi}{8K} \int_0^\infty \frac{E(k)}{k} dk \quad . \tag{189}$$

In contrast to Sarkar's model where ϵ_d/ϵ_s grows with M_t^2 and contrary to results obtained with EDQNM models by Bertoglio et al. (1998) where ϵ_d/ϵ_s is found to scale as M_t^2 (in perfect agreement with Sarkar), Fauchet's model predicts a behaviour which coincides with Ristorcelli's (1995) pseudo-sound theory. Moreover, Fauchet is able to confirm his model by LES results of forced isotropic turbulence with a subgrid-scale model of the Chollet-Lesieur type.

3.2. HOMOGENEOUS SHEAR TURBULENCE

We quickly recall the mean flow characteristics of homogeneous shear turbulence, discussed in section 2.5.2, before we turn to the linear inviscid

equations for the turbulent fluctuations. The mean density and mean shear rate are space-time constants, viz:

$$\overline{\rho} = \text{const.}, \qquad \frac{d\tilde{u_1}}{dx_2} = S = \text{const.} \tag{190}$$

The mean pressure and mean temperature are homogeneous in space, but grow in time due to dissipative effects.

3.2.1. *Linear inviscid analysis of turbulent fluctuations*
From equations (1), (2) and (24) we derive the linear inviscid equations of motion for homogeneous shear turbulence:

$$\frac{D\rho'}{Dt} + \overline{\rho} d' = 0, \tag{191}$$

$$\frac{Du_i'}{Dt} + u_2' S\delta_{i1} + \frac{1}{\overline{\rho}} \frac{\partial p'}{\partial x_i} = 0, \tag{192}$$

$$\frac{Dp'}{Dt} + \gamma \overline{p} d' = 0. \tag{193}$$

The material derivative along mean flow trajectories has the form:

$$\frac{D}{Dt} = \frac{\partial}{\partial t} + S x_2 \frac{\partial}{\partial x_1}. \tag{194}$$

Blaisdell et al. (1991, 1993) have discussed these equations in a transformed coordinate system which moves with the mean velocity. They have Fourier transformed the vorticity equations in order to show the coupling between vorticity and acoustic modes due to the presence of mean shear. It is this coupling which ensures that measures of compressibility become independent of their initial conditions. We follow Simone (1995), Simone et al. (1997) and Fourier transform equations (191) - (194) using the Craya-Herring reference frame in Fourier space with bases ($e_i^{(1)}$, $e_i^{(2)}$, $e_i^{(3)}$) normal and parallel to the wavevector $\vec{k}$. The polar vector $\vec{n}$ is chosen parallel to the direction of mean shear, i. e. the x_2-direction. The base vectors then have the form:

$$\begin{aligned} e_i^{(1)} &= (\epsilon_{i12} k_1 - \epsilon_{i23} k_3)/k' \quad , \\ e_i^{(2)} &= (k_2 k_i - k^2 n_i)/(k k') \quad , \\ e_i^{(3)} &= k_i/k \quad . \end{aligned} \tag{195}$$

ϵ_{ijk} is the alternating unit tensor and k' the magnitude of $\vec{k} \times \vec{n}$:

$$\left|\vec{k}\times\vec{n}\right| = k' = (k_1^2 + k_3^2)^{1/2}. \tag{196}$$

Figure 4 shows the Craya-Herring reference frame. The compressible velocity mode is parallel to the wavevector $\vec{k}$. The incompressible modes lie in the plane perpendicular to $\vec{k}$. This plane also contains the vorticity mode. Before transforming the linear equations we discuss the mean flow trajectories in physical and Fourier space. The material derivative in eq. (194) corresponds to a partial derivative with respect to time at fixed Lagrangian coordinate X_j:

$$\frac{D}{Dt} = \left(\frac{\partial}{\partial t}\right)_{\vec{X}} \quad . \tag{197}$$

In homogeneous shear flow Eulerian and Lagrangian coordinates are related by:

$$x_i = x_i\left(X_j, t_0, t\right) \quad , \qquad x_i\left(X_j, t_0, t\right) = F_{ij}\left(t_0, t\right) X_j \quad . \tag{198}$$

x_i is the position of a fluid particle moving with the mean flow at time t, and X_j denotes its position at time t_0, i.e. $X_j = x_j(t_0)$. The gradient displacement tensor is defined by the mean shearing motion:

$$F_{ij}(t_0, t) = \frac{\partial x_i(X_j, t_0, t)}{\partial X_j} = \delta_{ij} + St\delta_{i1}\delta_{j2} \quad . \tag{199}$$

The fluid particle coordinates are therefore:

$$x_1 = X_1 + StX_2 \quad , \qquad x_2 = X_2 \quad , \qquad x_3 = X_3 \quad . \tag{200}$$

A moving coordinate system in physical space corresponds to a time-dependent wave vector $\vec{k}(t)$. $\vec{k}(t)$ represents the position of a fluid particle in Fourier space at time t which at time t_0 had the position $\vec{K}$. (see Lesieur (1997)). The wavenumbers are obtained from:

$$k_i = F_{ji}^{-1}(t_0, t)K_j \quad . \tag{201}$$

The tensor F_{ji}^{-1} is the inverse of the transpose of F_{ij} given in eq. (199). The components of k_i are:

$$k_1 = K_1 \quad , \qquad k_2 = K_2 - K_1 St \quad , \qquad k_3 = K_3 \quad . \tag{202}$$

One easily verifies the wave conservation law (Cambon (1982)):

$$k_i x_i = K_i X_i \quad . \tag{203}$$

The Fourier transform of the material derivative, eq. (194), is denoted by the symbol $\frac{\mathcal{D}}{\mathcal{D}t}$:

$$\frac{\mathcal{D}}{\mathcal{D}t} = \frac{\partial}{\partial t} - k_1 S \frac{\partial}{\partial k_2} \quad . \tag{204}$$

The linear inviscid equations of motion finally take the spectral form:

$$\frac{\mathcal{D}\hat{\rho}}{\mathcal{D}t} + ik\overline{\rho}\hat{\varphi}^{(3)} = 0 \quad , \tag{205}$$

$$\frac{\mathcal{D}\hat{u}_i}{\mathcal{D}t} + \hat{u}_2 S\delta_{i1} + \frac{ik_i}{\overline{\rho}}\hat{p} = 0 \quad , \tag{206}$$

$$\frac{\mathcal{D}\hat{p}}{\mathcal{D}t} + ik\gamma\overline{p}\hat{\varphi}^{(3)} = 0 \quad . \tag{207}$$

The transformed velocity fluctuation, $\hat{u}_i$, consists of a solenoidal and a compressible part, as defined in eq. (152). By scalar multiplication of eq. (206) with $e_i^{(j)} (j = 1, 2, 3)$, Simone (1995) gets the mode equations. The derivation needs some care since the base vectors depend on $\vec{k}$ and only implicitly on time. Eq. (206) is equivalent to the component relations:

$$\frac{\mathcal{D}\hat{\varphi}^{(1)}}{\mathcal{D}t} + S\frac{k_3}{k}\hat{\varphi}^{(2)} - S\frac{k_2 k_3}{k k'}\hat{\varphi}^{(3)} = 0 \quad , \tag{208}$$

$$\frac{\mathcal{D}\hat{\varphi}^{(2)}}{\mathcal{D}t} - S\frac{k_1 k_2}{k^2}\hat{\varphi}^{(2)} + S\frac{k_1}{k'}\hat{\varphi}^{(3)} = 0 \quad , \tag{209}$$

$$\frac{\mathcal{D}\hat{\varphi}^{(3)}}{\mathcal{D}t} - 2S\frac{k_1 k'}{k^2}\hat{\varphi}^{(2)} + S\frac{k_1 k_2}{k^2}\hat{\varphi}^{(3)} + \overline{c}k\hat{\varphi}^{(4)} = 0 \quad . \tag{210}$$

The mode $\hat{\varphi}^{(4)}$ replaces the pressure:

$$\hat{\varphi}^{(4)} = i\frac{\hat{p}}{\overline{\rho}\ \overline{c}} \quad . \tag{211}$$

One immediately recognizes the differences to the case of isotropic turbulence. The incompressible modes $\hat{\varphi}^{(1)}$, $\hat{\varphi}^{(2)}$ are no longer frozen, but get energy from the dilatational mode $\hat{\varphi}^{(3)}$. There is even a coupling among the incompressible modes as a result of the mean shearing motion. For $S = 0$ the equations (159), (160) are recovered. The compressible velocity mode on the other hand is fed by the acoustic pressure mode $\hat{\varphi}^{(4)}$. Analytical solutions of this set of equations are not available. Simone et al. (1997), however, discuss two special solutions. The first is the *solenoidal limit*, given by $\hat{\varphi}^{(3)} = 0$. From (208) and (209) one then gets:

$$\frac{\mathcal{D}\hat{\varphi}^{(1)}}{\mathcal{D}t} + S\frac{k_3}{k}\hat{\varphi}^{(2)} = 0 \quad , \tag{212}$$

$$\frac{\mathcal{D}\hat{\varphi}^{(2)}}{\mathcal{D}t} - S\frac{k_1 k_2}{k^2}\hat{\varphi}^{(2)} = 0 \quad . \tag{213}$$

Taking the wavenumber relations (202) into account, the second equation can be directly integrated. The exact solution of (212) is then found. Simone et al. (1997) show that the modes $k\hat{\varphi}^{(2)}$ and $\hat{\varphi}^{(1)}$ are directly linked to the variables $\nabla^2 u_2$ and ω_2 which are typically used in the stability analysis of parallel incompressible shear flow (Orr–Sommerfeld equations).
The second special case is the so–called *pressure–released limit*. In this case pressure fluctuations are unable to draw energy from the dilatational velocity field. The mathematical model for this limit is obtained by removing the $\hat{\varphi}^{(4)}$ mode from the equations. The most simple way to study this case is in the form of eq. (192). One has:

$$\frac{Du_1'}{Dt} + u_2' S = 0 \quad , \qquad \frac{Du_2'}{Dt} = 0 \quad , \qquad \frac{Du_3'}{Dt} = 0 \quad , \tag{214}$$

which means that the vertical and spanwise velocity fluctuations are only advected with the mean velocity $\tilde{u_1}$. The integration along particle trajectories yields the solution:

$$\begin{aligned} u_1'(x_i,t) &= u_1'(X_i,t_0) - St\, u_2'(X_i,t_0) \quad , \\ u_2'(x_i,t) &= u_2'(X_i,t_0) \quad , \\ u_3'(x_i,t) &= u_3'(X_i,t_0) \quad . \end{aligned} \tag{215}$$

It immediately leads to the following expression for the turbulent kinetic energy, provided the turbulence field is initially isotropic:

$$\frac{K(t)}{K(0)} = 1 + \frac{(St)^2}{3} \quad . \tag{216}$$

A term linear in St does not appear because the Reynolds shear stress vanishes in isotropic turbulence. In the case where the initial turbulence field is not completely isotropic, Simone (1995) obtains:

$$\frac{K(t)}{K(0)} = 1 + \frac{\overline{u_2'(0)u_2'(0)}}{K(0)}(St)^2 - 2St\frac{\overline{u_1'(0)u_2'(0)}}{K(0)} \quad . \tag{217}$$

This is an important result of rapid-distortion theory (RDT)[4], because the pressure–released regime constitutes an upper bound to the TKE amplification. This will be shown later in comparison to DNS data.
Another aspect that can be deduced from the linear equations, concerns the special role of the velocity fluctuations in the direction of mean shear. The 2-component of the momentum equation (192) and the energy equation (193) reflect the direct coupling between u_2- and pressure fluctuations on one side and pressure and dilatation fluctuations on the other side:

$$\frac{Du_2'}{Dt} + \frac{1}{\overline{\rho}}\frac{\partial p'}{\partial x_2} = 0 \quad , \tag{218}$$

$$\frac{Dp'}{Dt} + \gamma \overline{p} d' = 0 \quad . \tag{219}$$

The Fourier transforms of these relations are:

$$\frac{\mathcal{D}\hat{u_2}}{\mathcal{D}t} + \frac{1}{\overline{\rho}} i k_2 \hat{p} = 0 \quad , \tag{220}$$

$$\frac{\mathcal{D}\hat{p}}{\mathcal{D}t} + \gamma \overline{p} \hat{d} = 0 \quad . \tag{221}$$

Operating $\mathcal{D}/\mathcal{D}t$ on eq. (220) while considering the wave number relations (202) and introducing (221) gives:

$$\frac{\mathcal{D}^2\hat{u}_2}{\mathcal{D}t^2} + \frac{k_1}{k_2} S \frac{\mathcal{D}\hat{u}_2}{\mathcal{D}t} = i k_2 \overline{c}^2 \hat{d} \quad . \tag{222}$$

This second-order hyperbolic equation for the transformed velocity fluctuation in the direction of mean shear contains the dilatation as 'forcing term'. It provides a direct link between compressibility effects (through $\hat{d}$) and the u_2-fluctuations. A second equation is available in the form of the wave equation for $\hat{d}$:

$$\frac{\mathcal{D}^2\hat{d}}{\mathcal{D}t^2} + k^2 \overline{c}^2 \hat{d} = -4 k_1 k_2 S \frac{\hat{p}}{\overline{\rho}} = -4 i k_1 S \frac{\mathcal{D}\hat{u}_2}{\mathcal{D}t} \quad , \tag{223}$$

where

$$\frac{\mathcal{D}^2}{\mathcal{D}t^2} = \frac{\partial^2}{\partial t^2} - 2 k_1 S \frac{\partial^2}{\partial t \partial k_2} + (k_1 S)^2 \frac{\partial^2}{\partial k_2^2} \quad . \tag{224}$$

Equations (222) and (223) have to be solved for suitable initial conditions. From these equations it can be concluded that intrinsic effects of

[4]The combination of linear solutions with statistical averaging is frequently referred to as rapid-distortion theory (RDT).

compressibility in the form of dilatation fluctuations at low turbulent Mach number (the acoustic time scale is small with respect to the turbulent time scale) should scale with the u_2-fluctuations. In some sense this result supports the definition of an integral length scale based on the transverse two-point correlation of u_2-fluctuations to be used in the definition of M_g, see eq. (130).

3.2.2. *Some findings based on DNS of homogeneous shear turbulence*
The extensive work of Blaisdell et al. (1991) is full of useful information. We concentrate on a few findings and conclusions only.

Independence of initial conditions:

The authors have performed five direct simulations with initial turbulent Mach numbers of 0.5, but different rms-values of density- and temperature fluctuations and varying fractions of compressible kinetic energy, χ. Fig. 5 shows the time evolution of χ_ϵ, the dilatational fraction of the dissipation rate. Depending on initial conditions this quantity goes through different transient phases, but finally settles down and becomes independent of its initial value. Other measures of compressibility such as χ and $\overline{\rho'^2}$ show a similar behaviour. This independence from the initial conditions is due to the coupling between vorticity and dilatation fluctuations and means that algebraic turbulence models for explicit compressibility terms may be able to capture compressibility effects.

Test of models for explicit compressibility terms:

Models for ϵ_d proposed by Sarkar et al. (1991) and Zeman (1990) and discussed in section 3.1.3 have been examined by Blaisdell et al. (1991, 1993). The results of eleven DNS with different initial turbulent Mach numbers and rms-fluctuations are displayed in figure 6 and compared with Sarkar's and Zeman's models. Depending on χ_0 the simulations have different initial values of ϵ_d/ϵ_s and progress according to the arrows. Only the final values should be compared with the model results. The solid/dashed curves represent the results of Sarkar resp. Zeman. Obviously, Sarkar's model provides proper prediction, at least up to M_t around 0.3, whereas Zeman's model predicts a much faster increase of ϵ_d/ϵ_s with M_t [5] and does not match so well the results of the simulations.

A model for the pressure-dilatation correlation proposed by Zeman (1991), relates $\overline{p'd'}$ to $\overline{p'^2}$ via the relation

[5]Blaisdell et al. use an rms Mach number instead of M_t which takes fluctuations in the sound speed into account. Both quantities do not differ noticeably.

$$\overline{p' \frac{\partial u_i'}{\partial x_i}} = -\frac{1}{2\gamma \bar{p}} \frac{d\overline{p'^2}}{dt} \tag{225}$$

which can be derived from the linear equation (193) (cf. also the discussion in section 2.4.1). The validity of this relation has been checked by Blaisdell et al. (1991, 1993) using a highly resolved DNS (sha 192) with 192^3 grid points for an initial M_t of 0.4 and vanishing initial values of ρ_{rms}, T_{rms}, χ. Figure 7 presents the time evolutions of $\overline{p'd'}$ and of the rhs of eq. (225). The model (discussed below) assumes the time variation of $\overline{p'^2}$ to scale with M_t^4 at low M_t and with M_t^2 at higher M_t. The DNS data follow an M_t^2 scaling much earlier than Zeman's model, cf. figure 8. This means that the model constants or the fitting function should be modified.

'Mean' polytropic coefficient:

In turbulence modelling one has usually to assume some correlation among fluctuations of thermodynamic variables. In his one-equation model Rubesin (1976) has used the following relation

$$\frac{p'}{\bar{\rho}} = n\frac{\rho'}{\bar{\rho}} = \frac{n}{n-1}\frac{T''}{\tilde{T}}. \tag{226}$$

The polytropic coefficient n is γ in isentropic flow, $n = 1$ in isothermal and $n = 0$ in isobaric flow. In turbulent flow, a local quantity n is not well defined. Blaisdell et al. (1991) therefore define an average polytropic coefficient

$$n = \left(\frac{\overline{p'^2}/\bar{p}^2}{\overline{\rho'^2}/\bar{\rho}^2} \right)^{1/2} \tag{227}$$

and demonstrate for homogeneous shear turbulence its independence on initial conditions after some transient behaviour and that it tends to a value slightly less than γ. This means that density, temperature and pressure fluctuations follow nearly isentropic processes. Figure 9 shows results for n according to (227) for seven different DNS of sheared turbulence.

This behaviour is in complete contrast to what is found in supersonic channel flow (see Huang et al. (1995)) where n obviously follows an isobaric process. An explanation for this behaviour is not easily found. It is however interesting to note that density-temperature correlations in the core region of the channel indicate that the flow there shows a tendency towards isentropic behaviour.

Structure of solenoidal and dilatational velocity fields:

Based on a Helmholtz decomposition of the fluctuating velocity vector Blaisdell et al. (1991) have investigated the different structure of the solenoidal and dilatational velocity fields. The Reynolds stresses $R_{ij} = \overline{\rho u_i' u_j'}$ are written as the sum of solenoidal, dilatational and cross terms

$$R_{ij} = R_{ij}^s + R_{ij}^d + R_{ij}^c \quad , \tag{228}$$

where

$$R_{ij}^s = \overline{\rho u_i^{s\prime} u_j^{s\prime}} \tag{229}$$

$$R_{ij}^d = \overline{\rho u_i^{d\prime} u_j^{d\prime}} \tag{230}$$

$$R_{ij}^c = \overline{\rho u_i^{s\prime} u_j^{d\prime}} + \overline{\rho u_j^{s\prime} u_i^{d\prime}} \tag{231}$$

The anisotropy tensors of the 's' and 'd' components are:

$$b_{ij}^s = R_{ij}^s / R_{kk}^s - \delta_{ij}/3 \quad , \quad b_{ij}^d = R_{ij}^d / R_{kk}^d - \delta_{ij}/3 \quad . \tag{232}$$

Each of them possesses three scalar invariants. The first, being the trace, is zero. The other two are (omitting the superscripts):

$$II = -\frac{1}{2} b_{ij} b_{ji} \quad , \quad III = \frac{1}{3} b_{ij} b_{jk} b_{ki} \quad .$$

They must lie within the regions bordered by

$$\begin{aligned} II &= -\frac{3}{2^{2/3}} (-III)^{2/3} \quad , \\ II &= -3III - \frac{1}{9} \quad , \\ II &= -\frac{3}{2^{2/3}} (III)^{2/3} \end{aligned} \tag{233}$$

in the (III, II) plane and form an invariant map first introduced by Lumley (1978). This map is presented in figure 10 for Blaisdell et al's DNS sha192. One notices that b_{ij}^d lies very close to the curve which corresponds to axisymmetric expansion and thus indicates that $u_i^{d\prime}$ tends to be planar in contrast to $u_i^{s\prime}$. A velocity field associated with sound waves can indeed be planar.

TKE growth rate and Reynolds stress anisotropy:

DNS data of Blaisdell et al. (1991, 1993) and Sarkar et al. (1991) for compressible homogeneous shear flow had indicated an exponential growth of TKE at a rate considerably below that for incompressible turbulence, cf. figure 11. This stabilizing effect of compressibility was, until recently, attributed to the presence of explicit compressibility terms like the compressible dissipation rate ϵ_d and the pressure-dilatation correlation $\overline{p'd'}$ in the K-equation (116). Indeed ϵ_d acts as a sink and $\overline{p'd'}$ is predominantly negative. It was Sarkar (1995) who provided new insight into the stabilizing effect of compressibility. His findings were later confirmed by Simone et al. (1997) and for mixing layers by Vreman et al. (1996). Sarkar (1995) performed two DNS series A, B of homogeneous shear flow in which he varied the initial values M_{go} and M_{to} individually from run to run in order to demonstrate for large nondimensional times St that

- the reduction in the growth rate of TKE as M_{go}, respectively M_{to}, increaseses, is primarily due to the reduced level of turbulence production, while the response of explicit dilatational terms is much less pronounced
- the stabilizing effect of compressibility is substantially larger in the DNS series A than in series B. In series A, M_{go} is increased via the shear rate S while $\overline{c}_o$ and M_{to} are kept constant. In series B, on the other hand, M_{to} was increased and M_{go} was kept constant.

The different behaviour is a consequence of the fact that M_{go} and M_{to} are two independent parameters since their ratio Sl_o/u_o can be varied via l_o, u_o. We recall that the nondimensionalized TKE equation (123) had already indicated the relevance of M_{go} with respect to the production term. The DNS parameters of Sarkar's series A are given in Table 5.

TABLE 5. Parameters of Sarkar's (1995) series A simulations.

Case	M_{go}	M_{to}	$Re_{\lambda o}$	Pr_o	$(SK/\epsilon)_o$
A1	0.22	0.40	14	0.7	1.8
A2	0.44	0.40	14	0.7	3.6
A3	0.66	0.40	14	0.7	5.4
A4	1.32	0.40	14	0.7	10.8

$Re_{\lambda o}$ is the Reynolds number based on the velocity scale u_o and on Taylor's microscale $\lambda_o = u_o/\overline{(\omega_i'\omega_i')_o}^{1/2}$. Sarkar (1995) writes the K-equation (116) as an evolution equation for the growth rate $\Lambda = (1/SK)\, dK/dt$, viz:

$$\Lambda = -2b_{12}\left(1 - \frac{\epsilon_s}{P}\right) - \frac{\epsilon_d - \overline{p'd'}/\overline{\rho}}{SK} = -2b_{12}\left(1 - X_\epsilon\right) \quad , \tag{234}$$

where $b_{12} = \widetilde{u_1'u_2'}/\left(2K\right)$ is the Reynolds shear stress anisotropy (cf. eq. (232)) and P the production term. The quantity

$$X_\epsilon = \left(\epsilon_s + \epsilon_d - \overline{p'd'}/\overline{\rho}\right)/P \tag{235}$$

combines all terms other than the production term. Figure 12 contains the time evolutions of Λ and $-2b_{12}$. We note that these quantities attain asymptotic values at large St which decrease as M_{go} increases. The non-dimensional production term, $P/\left(SK\right) = -2b_{12}$, is strongly inhibited when the gradient Mach number is increased. Figure 13 shows the evolution of ϵ_s in two different non-dimensionalizations, the evolutions of the explicit compressibility terms and of X_ϵ. One recognizes that the long-time behaviour ($St = 20$) of all these terms is much less affected by the gradient Mach number than the turbulent production ($-2b_{12}$). The effect of M_{go} on the dilatational terms is small, but non-negligible. It is against intuition that the sum $\left(-\overline{p'd'}/\overline{\rho} + \epsilon_d\right)$ is decreasing instead of increasing with M_{go}. From X_ϵ at ($St = 20$) Sarkar (1995) concludes that the large reduction in the value of Λ is almost wholly due to the large reduction in the magnitude of the Reynolds shear stress anisotropy b_{12}. He further comments, based on a Helmholtz decomposition of the velocity field, that the solenoidal part of b_{12} is responsible for the reduced production rate. The effect of compressibility on the b_{11} and b_{22} components of the anisotropy tensor is presented in figure 14. There is a systematic increase in the magnitude of these anisotropies from case A1 to case A4 and it may be concluded that the pressure-strain correlation tensor in the homogeneous shear flow is significantly changed due to compressibility.

Pressure strain correlation tensor:

The trace of the pressure strain correlation tensor is the pressure-dilatation correlation $\overline{p'd'}$. Sarkar (1992) showed that this correlation, obtained from spatial averaging of instantaneous turbulence fields, oscillates in time in the case of homogeneous shear flow. For low to moderate initial turbulent Mach numbers the oscillations take place at fast (acoustic) time scales, but do not contribute in a time-integrated sense to the evolution of K. By decomposing the fluctuating pressure into incompressible and compressible parts,

$$p' = p^{I'} + p^{C'} \quad , \tag{236}$$

Sarkar (1992) was able to attribute the oscillations in $\overline{p'd'}$ to the compressible component $\overline{p^{C'}d'}$ which does not need modelling due to its negligible integrated effect. The model he derived for $\overline{p^{I'}d'}$ will be discussed below. Figure 15 illustrates the time evolution of $\overline{p'd'}$ and of its compressible and incompressible contributions for a flow with the parameters: $M_{to} = 0.4$, $(2SK/\epsilon)_o = 13.6$, $Re_{to} = 441$, $\rho_{rms,o} = 0$, $\chi_o = 0$. $p_{rms,o}$ was obtained from a Poisson equation.

The motivation for the decomposition (236) was derived from the Poisson equation for p'. In incompressible turbulence such a Poisson equation forms the basis for the derivation of pressure-strain models. Sarkar's analysis starts from the following equation for the instantaneous pressure:

$$\frac{\partial^2 p}{\partial x_i \partial x_i} = -\frac{\partial^2}{\partial x_i \partial x_j}\left(\rho u_i u_j\right) + \frac{\partial^2 \rho}{\partial t^2} + \frac{\partial^2 \tau_{ij}}{\partial x_i \partial x_j} \quad , \tag{237}$$

which is the divergence of the momentum equation (2) combined with the continuity equation (1). Splitting each quantity into a mean and a fluctuation,

$$u_i = \overline{u}_i + u_i' \quad , \quad p = \overline{p} + p' \quad , \quad \rho = \overline{\rho} + \rho' \quad , \quad \tau_{ij} = \overline{\tau}_{ij} + \tau_{ij}' \quad , \tag{238}$$

substituting these into (237), and subtracting the mean of this relation gives after some algebra:

$$\begin{aligned} p'_{,jj} = \; & - \; 2\overline{u}_{i,j}\left(\overline{\rho}u_j'\right)_{,i} - 2\overline{u}_{i,i}\left(\overline{\rho}u_j'\right)_{,j} - 2\overline{u}_{i,ij}\left(\overline{\rho}u_j'\right) - \left(\overline{\rho}u_i'u_j'\right)_{,ij} \\ & - \; \rho'\left(\overline{u}_{i,i}\right)^2 - \rho'\overline{u}_{i,j}\overline{u}_{j,i} - 2\overline{u}_{i,j}\left(\rho'u_j'\right)_{,i} - 2\overline{u}_{i,i}\left(\rho'u_j'\right)_{,j} \\ & - \; 2\overline{u}_{i,ij}\left(\rho'u_j'\right) - \left(\rho'u_i'u_j'\right)_{,ij} + \frac{D^2\rho'}{Dt^2} + \tau'_{ij,ij} \quad . \end{aligned} \tag{239}$$

For convenience, commas are used to denote spatial derivatives. The first four terms on the right-hand side of this equation depend explicitly on $\overline{\rho}$, terms five to ten depend on ρ' and its gradients. Term eleven contains unsteadiness and mean convection of ρ' and the last term describes explicit viscous effects. Now, the first four terms are similar to the source terms for incompressible constant density flow. All remaining terms vanish in that

case. Therefore, the fluctuating 'incompressible' pressure is associated with the first four source terms and satisfies the Poisson equation:

$$p^{I'}_{,jj} = -2\overline{u}_{i,j}\left(\overline{\rho}u'_j\right)_{,i} - 2\overline{u}_{i,i}\left(\overline{\rho}u'_j\right)_{,j} - 2\overline{u}_{i,ij}\left(\overline{\rho}u'_j\right) - \left(\overline{\rho}u'_iu'_j\right)_{,ij} \quad . \quad (240)$$

Evaluating this equation, Sarkar obtains $p^{I'}$. Since the DNS provides p', the compressible part is the difference of p' and $p^{I'}$. That way the incompressible and compressible contributions to $\overline{p'd'}$ were obtained.
The split pressure fields $p^{I'}$, $p^{C'}$ were later used by Blaisdell and Sarkar (1993) to decompose the pressure strain terms. They discuss the deviatoric part of the pressure strain tensor

$$\begin{aligned} \overline{p's^{*\prime}_{ij}} &= \overline{p'\left(s'_{ij} - \frac{1}{3}s'_{kk}\delta_{ij}\right)} \qquad {}^{6}) \qquad (241) \\ &= \overline{p^{I'}\left(s'_{ij} - \frac{1}{3}s'_{kk}\delta_{ij}\right)} + \overline{p^{C'}\left(s'_{ij} - \frac{1}{3}s'_{kk}\delta_{ij}\right)} \quad , \end{aligned}$$

based on DNS data for the flow parameters listed above, which correspond to a high M_{to} / low M_{go} case. Figure 16 contains the time evolutions of the four relevant pressure strain components, each of them split as indicated in equation (241). The discontinuities in the curves are due to the remeshing process in the numerical simulations. The following observations were made:

- The normal components of the three pressure strain tensors $\overline{p's^{*\prime}_{ij}}$, $\overline{p^{I'}s^{*\prime}_{ij}}$ and $\overline{p^{C'}s^{*\prime}_{ij}}$ behave in a way similar to $\overline{p'd'}$, $\overline{p^{I'}d'}$ and $\overline{p^{C'}d'}$. The compressible parts are oscillatory and have much smaller magnitudes than the incompressible parts, consequently their contributions to the time evolutions of the Reynolds stresses are smaller.
- While all the 1-1 components are negative, all the 2-2 and 3-3 components are positive. The compressible 2-2 component is the weakest among these normal components.
- The compressible part of the off-diagonal (1-2) component is, however, not small and thus contributes significantly to the time evolution of $\overline{\rho u'_1u'_2}$. Its magnitude reaches 75 % of that of the incompressible part. Therefore, $\overline{p^{C'}s'_{12}}$ needs modelling. Its positive sign indicates a reduction of the magnitude of $\overline{\rho u'_1u'_2}$ (cf. eq. (122)).

[6] The star ($*$) replaces the (D) used in equation (8) to denote the deviatoric deformation tensor.

From correlation coefficients of the decomposed pressure fluctuations Blaisdell and Sarkar (1993) conclude that the two pressure fields $p^{I'}$ and $p^{C'}$ are not statistically independent, which makes a proper independent modelling of $\overline{p^{I'} s_{ij}^{*\prime}}$ and $\overline{p^{C'} s_{ij}^{*\prime}}$ difficult. Splitting the incompressible field $p^{I'}$ into rapid and slow parts

$$p^{I'} = p^{R'} + p^{s'} \quad , \tag{242}$$

moreover shows that the compressible pressure $p^{C'}$ is more closely associated with the rapid incompressible pressure $p^{R'}$ than with its slow part $p^{s'}$.

The role of linear processes in explaining structural changes due to intrinsic compressibility:

One of several important issues of the work by Simone et al. (1997) is that linear rapid-distortion theory (RDT) is capable of predicting the TKE growth rate and the Reynolds shear stress anisotropy in surprisingly close agreement with DNS data. The authors solve the rapid distortion equations (207) to (210) numerically and perform direct simulations for a turbulent Mach number of 0.25 and various gradient Mach numbers. In order to allow for comparison, they select two flow cases which are close to Sarkar's cases A3 and A4 (See table 5). Their distortion Mach number (M_d) definition uses the large-eddy lengthscale $(2K)^{3/2}/\epsilon$ instead of an integral lengthscale based on a two-point velocity correlation. Otherwise it coincides with the definition of M_g. Therefore, their values for M_{do} are by a factor of more than 6 larger than Sarkar's values for M_{go}. All the computations (RDT and DNS) start from initial conditions which correspond to a good approximation to isotropic turbulence in acoustic equilibrium.
The following findings may be listed:

- For small non-dimensional times ($St < 4$) compressibility acts destabilizing. Only at later times ($St > 4$) Sarkar's stabilizing effect of $M_{go}(M_{do})$ is observed. This 'crossover' behaviour which appears only in sheared (not in compressed) homogeneous turbulence is explained based on a semi-analytical analysis. The growth rate Λ, defined in equation (234) is used to show these effects.
- The destabilizing/stabilizing effect of M_{do} on the growth rate is nearly completely due to the behaviour of b_{12}, the non-dimensional production term.
- A Helmholtz decomposition of the velocity field shows that the dilatational part of the shear stress anisotropy, b_{12}^d is practically independent of M_{do}, while the solenoidal part b_{12}^s is dramatically decreased (with

growing M_{do}) over the entire range of St. The source for these structural changes of the solenoidal velocity fluctuations is the feedback of the dilatational disturbances upon the solenoidal field (cf. eqs. (208), (209)).

Figure 17 shows the time evolution of the TKE growth rate as obtained from DNS data (top) and RDT (bottom). The solid lines indicate the pressure-released limit which was discussed at the end of section 3.2.1 (eqs. (214)-(217)) and is given by

$$\Lambda^{pr} = \frac{2St}{3 + (St)^2} \quad . \tag{243}$$

This result follows from eq. (216) for initially isotropic turbulence with the normalized TKE, $K(0) = 1$. It represents an upper bound, found for initial $M_{do} \gg 1$. All curves exhibit the 'crossover' feature which is due to the coupling of solenoidal and dilatational velocity fields.
The DNS and RDT histories of b_{12} on top and bottom of figure 18 not only confirm Sarkar's (1995) observation that the non-dimensional production term in eq. (234) is primarily responsible for the exponential growth rate behaviour, but demonstrate that it can be extended to the regime of destabilization ($St < 4$). The bottom figure presenting RDT results contains two solid curves. The upper represents the pressure-released limit and the lower the RDT result for incompressible flow. Both form upper and lower bounds for the regime in which an increase in $M_{do}(M_{go})$ acts destabilizing and the agreement between DNS and RDT is striking.
Histories of the solenoidal and dilatational contributions to the Reynolds shear stress anisotropy, b_{ij}^s and b_{ij}^d, are shown in figures 19 and 20. While the solenoidal component is dramatically decreased with increasing M_{do} over the entire range of St, the dilatational part is essentially unaffected by compressibility. The structural changes are therefore almost exclusively felt in the solenoidal field. RDT predicts almost independence of b_{ij}^d on M_d. The large-St limits of both terms are certainly not properly captured by the RDT, because it does not treat nonlinear effects.
Summarizing, the overall good agreement between DNS and RDT has to be emphasized; which means that much of the structural effect of compressibility can be fairly well reproduced by solving linear equations. This remarkable result should be used for the development of improved turbulence models.

Dissipation rate tensor:

The work of Blaisdell et al. (1991) also provides information concerning the dissipation rate anisotropy. Unfortunately, only one flow case is considered, so that the Mach number dependence of ϵ_{ij} and of its solenoidal and dilatational components ϵ^s_{ij}, ϵ^d_{ij} (cf. eqs. (81), (82)) can only be grasped from comparison with the incompressible case. A few observations pertinent to Blaisdell et al.'s run sha92 are:

- In the transport equations for the four Reynolds stresses (119 - 122) only ϵ^d_{22} is relevant and comparable in size to ϵ^s_{22}. All other components of ϵ^d_{ij} are negligibly small. ϵ^s_{12} becomes small as the simulation progresses (in agreement with the incompressible case).
- The solenoidal dissipation rate anisotropy tensor, $d^s_{ij} = \epsilon^s_{ij}/\epsilon^s_{kk} - \delta_{ij}/3$ is highly aligned with the Reynolds stress anisotropy tensor, b_{ij}. The same is true for incompressible turbulence. The dilatational tensor, d^d_{ij}, is not aligned with b_{ij}.
- However, d^d_{ij} tends to be aligned with b^d_{ij}. A physically interesting result, but difficult to use for modelling of ϵ^d_{ij}.

These results show that the dilatational dissipation rate tensor is strongly anisotropic. So, besides altering the structure of the Reynolds stress anisotropy directly (via inviscid mode coupling) and of the pressure strain correlation tensor, intrinsic compressibility could lead to further modification of the Reynolds stress tensor via structural changes of the dissipation rate tensor.

3.2.3. *Pressure-dilatation models*
Zeman's model and extensions:

Zeman's (1991) model is based on the argument that for low turbulent Mach number homogeneous isotropic and sheared turbulence the pressure-dilatation correlation and the time derivative of the pressure variance are closely connected. The corresponding relation had already been given in eq. (225) and figure 7 had shown the excellent agreement between this relation and DNS data. Introducing relation (225) into the K-equation for homogeneous isotropic turbulence and neglecting viscosity fluctuations gives:

$$\frac{d}{dt}\left[\frac{1}{2}\left(\overline{\rho u_i'' u_i''} + \frac{1}{\gamma\overline{p}}\quad\overline{p'^2}\right)\right] = -\overline{\rho}\,(\epsilon_s + \epsilon_d) \quad . \tag{244}$$

The term in the square brackets is the total energy of turbulence. In a state of acoustic non-equilibrium kinetic and potential energies are exchanged. Assuming the rhs of eq. (244) to be closed, a model is needed for

the pressure variance. Zeman postulates that $\overline{p'^2}$ relaxes to an equilibrium value on an acoustic time scale τ_a:

$$\frac{d\overline{p'^2}}{dt} = -\frac{\overline{p'^2} - p_e^2}{\tau_a} \quad , \tag{245}$$

where $\tau_a = 0.13\,(2K/\epsilon_s)\,M_t$.

The equilibrium value p_e^2 is related to K and M_t via the empirical model:

$$\frac{p_e^2}{2\overline{\rho}^2 K \overline{c}^2} = \frac{1}{\gamma^2 M_t^2}\frac{p_e^2}{\overline{p}^2} = \frac{\alpha M_t^2 + \beta M_t^4}{1 + \alpha M_t^2 + \beta M_t^4} = f\left(M_t^2\right) \tag{246}$$

This model combines two assumptions: (1) the equilibrium ratio of compressible to solenoidal kinetic energy is $\overline{u_i^{d\prime} u_i^{d\prime}}/\overline{u_i^{s\prime} u_i^{s\prime}} = \alpha M_t^2 + \beta M_t^4$, and (2) in a state of acoustic equilibrium, the compressible potential and kinetic energies are equal, i.e.

$$p_e^2 \approx \overline{\rho}^2 \overline{c}^2 \overline{u_i^{d\prime} u_i^{d\prime}} \quad , \tag{247}$$

(cf eq. (167)). The model (246) allows for a M_t^4 behaviour for small M_t in agreement with the acoustic analysis of Sarkar et al. (1991b) and a M_t^2 variation at higher Mach numbers. The complete model reads:

$$\overline{p'd'} = -\frac{1}{2\overline{\rho}^2\overline{c}^2}\frac{\overline{p'^2} - \gamma^2\overline{p}^2 M_t^2 \cdot f\left(M_t^2\right)}{\tau_a} \quad , \tag{248}$$

where $\tau_a = 0.13\,(2K/\epsilon_s)\,M_t$ and $f\left(M_t^2\right)$ is defined in eq. (246). The constants α, β were originally given as $\alpha = 1$, $\beta = 2$. Later Durbin and Zeman (1992) extended the model to account for one-dimensional compression using RDT:

$$\overline{p'd'} = -\frac{1}{\overline{\rho}^2\overline{c}^2}\left(\frac{1}{2}\frac{d\overline{p'^2}}{dt} + \frac{\gamma - 1}{2}\overline{p'^2}\frac{\partial \tilde{u}_i}{\partial x_i}\right) \quad . \tag{249}$$

The first term on the rhs is a slow relaxation term (see (245)) and the second a rapid compression term. The coefficient in front of the rapid term was slightly modified by Zeman and Coleman (1993). In an attempt to provide a pressure-dilatation model for boundary layers in quasi-equilibrium, Zeman (1993) analyzed the pressure variance equation in more detail and obtained:

$$\overline{p'd'} = 2f_\rho\left(M_t\right)\overline{c}^2\widetilde{u_i''u_j''}\frac{K}{\epsilon}\frac{1}{\overline{\rho}}\frac{\partial\overline{\rho}}{\partial x_i}\frac{\partial\overline{\rho}}{\partial x_j} \quad , \tag{250}$$

where

$$f_\rho\left(M_t\right) = 0.02\left(1 - exp\left(-M_t^2/0.2\right)\right). \tag{251}$$

Aupoix et al's model:

Instead of using linear acoustics and scaling relations, Aupoix, Blaisdell, Reynolds and Zeman (1990) derive a transport equation for $\overline{p'd'}$ assuming that the fluid behaves as a perfect gas, and model it. For homogeneous turbulence the model reads:

$$\frac{d\overline{p'd'}}{dt} = -c_1\overline{\rho}\frac{M_t^2}{\tau}\frac{dK}{dt} - c_2\frac{1}{\tau}\overline{p'd'} \quad , \tag{252}$$

with

$$\tau = K^{3/2}/\left(\epsilon\overline{c}\right) \quad , \quad c_1 = 0.25 \quad , \quad c_2 = 0.2 \quad . \tag{253}$$

Comparison of model predictions with DNS data for homogeneous isotropic and sheared turbulence shows that the model works well for sheared flows. Isotropic flows with various initial acoustics allowed for fair predictions only due to the sensitivity of these flows to initial conditions.

Sarkar's model:

Sarkar (1992) derived a model for homogeneous flows based on a Poisson equation for the pressure fluctuations, a decomposition into incompressible and compressible pressure fields and the fact that the time-integrated contribution of the latter is negligible. Homogeneous flows have no density gradients. Equation (240), therefore, simplifies to:

$$p^{I'}_{,jj} = -2\overline{\rho}\,\overline{u}_{i,j}u'_{j,i} - 2\overline{\rho}\,\overline{u}_{i,i}u'_{j,j} - \overline{\rho}\Big(u'_iu'_j\Big)_{,ij} \quad . \tag{254}$$

As is done in incompressible modelling, the first two rhs terms define a rapid and the last term, a slow part, cf. the defining equation (242). The rapid pressure fluctuation satisfies the Poisson equation:

$$p^{R'}_{,jj} = -2\overline{\rho}\,\overline{u}_{i,j}u'_{j,i} - 2\overline{\rho}\,\overline{u}_{i,i}u'_{j,j} \tag{255}$$

and the slow fluctuation obeys

$$p^{s\prime}_{,jj} = -\overline{\rho}\Big(u_i' u_j'\Big)_{,ij} \quad . \tag{256}$$

Homogeneous flow is periodic in all spatial directions and thus allows to solve eqs. (255) and (256) exactly by Fourier transforms

$$k^2 \hat{p}^R = 2i\,\overline{\rho}\,k_i \overline{u}_{i,j} \hat{u}_j + 2i\,\overline{\rho}\,k_j \overline{u}_{i,i} \hat{u}_j \quad , \tag{257}$$

$$k^2 \hat{p}^s = -\overline{\rho} k_i k_j \widehat{u_i u_j} \quad . \tag{258}$$

Multiplying these relations by the complex conjugate (denoted by $*$) of the Fourier transformed dilatation fluctuation, $\hat{d}^* = -ik_m \hat{u}_m^*$, and integrating over all wavenumbers, gives:

$$\overline{p^{R\prime} d'} = 2\overline{\rho}\,\overline{u}_{i,j} \int \frac{k_i k_m}{k^2} E_{jm} d\vec{k} + 2\overline{\rho}\,\overline{u}_{i,i} \int \frac{k_j k_m}{k^2} E_{jm} d\vec{k} \quad , \tag{259}$$

$$\overline{p^{s\prime} d'} = \overline{\rho} \int \frac{k_i k_j k_m}{k^2} \left(i\widehat{u_i u_j} \hat{u}_m^* - i\widehat{u_i u_j^*} \hat{u}_m \right) d\vec{k} \quad , \tag{260}$$

where

$$E_{jm} = \left(\hat{u}_j \hat{u}_m^* + \hat{u}_m \hat{u}_j^* \right)/2 \tag{261}$$

denotes the spectrum of the Reynolds stress tensor $\overline{u_j' u_m'}$.

Sarkar (1992) has evaluated the integrals in the above equations using scaling arguments, truncated Taylor-series expansions and an order of magnitude analysis to obtain:

$$\overline{p' d'} \approx \overline{p^{I\prime} d'} = 2\alpha_2 M_t \overline{\rho}\,\overline{u}_{i,j} b_{ij} K + \alpha_3 \overline{\rho} \epsilon_s M_t^2 + \frac{16}{3} \alpha_4 M_t^2 \overline{\rho}\,\overline{u}_{i,i} K \quad , \tag{262}$$

where b_{ij} is the Reynolds stress anisotropy tensor. The model coefficients are $\alpha_2 = 0.15$, $\alpha_3 = 0.2$. The last coefficient has not yet been calibrated for flows with homogeneous compression. The second term on the rhs of (262) accounts for the slow pressure part. Sarkar shows that the

model provides good agreement with DNS data of homogeneous shear turbulence when used in SOC predictions with the SSG pressure-strain model and his ϵ_d-model. However, Sarkar also mentions that eq. (262) forms a reasonable approximation for weakly inhomogeneous flows without walls. In wall-bounded flows he expects $\overline{p'd'}$ to be smaller because the rms rapid pressure is a smaller fraction of $2\overline{\rho}K$ and the wall normal velocity fluctuation is damped.

El Baz and Launder's model:

Although this model is not derived from observations related to DNS of homogeneous shear flow, it is included in this subsection for later reference. The model is empirical and was designed in order to account for compressibility effects in mixing layers. An attempt was made to treat the influence of dilatational terms on the pressure-strain correlation within a Reynolds stress modelling framework. Only the rapid part of this correlation was modified with respect to the model for incompressible flow. The trace of this term (denoted by ϕ_{kk2}) vanishes in incompressible flows. In compressible flows it is generally nonzero and provides a finite pressure-dilatation correlation which is of the form (see El Baz and Launder (1993)):

$$\overline{p'd'} = 3\overline{\rho}{M_t}^2 \left(\frac{4}{3} K \frac{\partial \widetilde{u_i}}{\partial x_i} + \widetilde{u_i''u_j''} \frac{\partial \widetilde{u_i}}{\partial x_j} \right). \tag{263}$$

Applications of the model to predict simple-stream and two-stream mixing layers with sub- and supersonic convective Mach numbers provided broadly satisfactory agreement with available experiments.

Ristorcelli's model:

Ristorcelli (1997) has conducted a small M_t singular perturbation expansion of the compressible Navier-Stokes equations about a mean state corresponding to homogeneous turbulence without mean dilatation. The first order expansion of the continuity equation provides a diagnostic relation for the dilatation fluctuation of the form:

$$-\gamma d' = \frac{\partial p_1'}{\partial t} + {v_j}' \frac{\partial p_1'}{\partial x_j} \tag{264}$$

where ${v_j}'$ and ${p_1}'$ denote the incompressible velocity and pressure fluctuations. Ristorcelli calls ${p_1}'$ the 'pseudo-pressure' in order to distinguish it from the pressure associated with the acoustic problem. Multiplying (264) by ${p_1}'$, averaging and applying the homogeneity condition leads to:

$$-2\gamma\overline{p_1' d'} = \frac{d\overline{{p_1'}^2}}{dt} \quad . \tag{265}$$

This relation is similar to that used by Zeman (1991) with the difference that the 'pressure-dilatation' formed with the incompressible part of p' (cf. also Sarkar (1992)) now equals the time rate of change of the variance of the incompressible pressure. The advantage is that a model results which is consistent with the low ${M_t}^2$ asymptotics. While Zeman's model indicates $\overline{p'^2} \to 0$ as ${M_t}^2 \to 0$, Ristorcelli's model guarantees that $\overline{p_1'^2}$ is a function of K in the incompressible limit.

Without going into details of the model derivation it may be said that Ristorcelli (1997) uses the theory of incompressible homogeneous isotropic turbulence to obtain an exact expression for the time rate of change of $\overline{{p_1}'^2}$. In the case of homogeneous sheared turbulence, scaling assumptions lead to:

$$\overline{p'd'} = -\chi_{pd} M_t^2 \epsilon_s \left(\frac{-\widetilde{u_i'' u_j''}}{\epsilon_s} \frac{\partial \widetilde{u}_i}{\partial x_j} - 1 \right). \tag{266}$$

The model coefficient χ_{pd} depends on Kolmogorov's scaling parameter α and the relative strain rate $(\widetilde{s_{ij}}\widetilde{s_{ij}})^{\frac{1}{2}} K/\epsilon_s$. The result (266) is similar to that of Aupoix et al. (1990) and of Sarkar (1992). All three models allow for a change in sign from isotropic to sheared turbulence. This change in sign depends on M_t for Sarkar's model. In the case of Aupoix et al.'s and Ristorcelli's models it simply depends on whether the K-production exceeds dissipation. For more details of a model comparison we refer to Ristorcelli (1998).

References

1. Abid, R., Morrison, J. H., Gatski, T. B., Speziale, C. G. 1996 'Prediction of aerodynamic flows with a new explicit algebraic stress model'. AIAA J., 34, No. 12, pp. 2632-2635.
2. Abid, R., Rumsey, C., Gatski, T. B. 1995 'Prediction of non-equilibrium turbulent flows with explicit algebraic stress models'. AIAA J., 33, No. 11, pp. 2026-2031.
3. Adams, N. A. 1998 'Direct numerical simulation of turbulent compression ramp flow'. Theoret. Comput. Fluid Dynamics 12, pp. 109-129.
4. Adams, N. A. 1999 'Direct numerical simulation of shock-turbulence interaction in boundary layers'. Inaugural dissertation. ETH Zürich.
5. Aupoix, B., Blaisdell, G. A., Reynolds, W. C., Zeman, O. 1990 'Modelling the turbulent kinetic energy equation for compressible, homogeneous turbulence'. Proceedings of the Summer Program, Center for Turbulence Research, Stanford.
6. Batchelor, G.K. 1967 'An Introduction to Fluid Dynamics'. Cambridge University Press, U.K.
7. Batten, P., Loyau, H., Leschziner, M. A. (Eds.) 1997, ERCOFTAC Workshop on Shock/Boundary-Layer Interaction', March 25-26, 1997, UMIST, Manchester, UK. Proceedings available on the WEB site - http://sgp.me.umist.ac.uk/ercoftac97.
8. Baz, A.M. El, Launder, B.E. 1993 'Second-moment modelling of compressible mixing layers'. – In: Engineering Turbulence Modelling and Experiments 2 (ed. W. Rodi & F. Martelli). Elsevier, Amsterdam, pp. 63-72.
9. Bertoglio, J.P., Bataille, F., Marion, J.D. 1998 'Two-point closures for weakly compressible turbulence'. Phys. Fluids, under revision.
10. Bertolotti, F.P. 1997 'The influence of rotational and vibrational energy relaxation on the instability of boundary layers in supersonic flows. Report ISRN DLR-FB-97-18, DLR Göttingen.
11. Blaisdell, G.A., Mansour, N.N., Reynolds, W.C. 1991 'Numerical simulations of compressible homogeneous turbulence'. Report No. TF-50, Dept. of Mechanical Engineering, Stanford University, Stanford, California.
12. Blaisdell, G.A., Mansour, N.N., Reynolds, W.C. 1993 'Compressibility effects on the growth and structure of homogeneous turbulent shear flow.' J. Fluid Mech. 256, pp. 443-485.
13. Blaisdell, G. A., Sarkar, S. 1993 'Investigation of the pressure-strain correlation in compressible homogeneous turbulent shear flow. ASME FED-vol. 151, Transitional and Turbulent Compressible Flows, pp. 133-138.
14. Bradshaw, P. 1977 'Compressible turbulent shear layers.' Ann. Rev. Fluid Mech. 9, pp. 33-54.
15. Cambon, C. 1982 'Etude spectrale d'un champ turbulent incompressible, soumis à des effets couplés de deformation et de rotation, imposés extérieurement. Thèse d'Etat Es Sciences, Universitxié Claude Bernard de Lyon.
16. Cambon, C. 1990 'Single and double point modelling of homogeneous turbulence. CTR Annual Research Briefs, Stanford University/NASA Ames.
17. Cambon, C., Coleman, G.N., Mansour, N.N. 1993 'Rapid distortion analysis and direct simulation of compressible homogeneous turbulence at finite Mach number.' J. Fluid Mech. 257, pp. 641-665.
18. Cebeci, T., Smith, A. M. O. 1974 'Analysis of turbulent boundary layers'. Academic Press, New York, London.
19. Coleman, G.N., Kim, J., Moser, R.D. 1995 'A numerical study of turbulent supersonic isothermal - wall channel flow.' J. Fluid Mech. 305, pp. 159-183.
20. Craya, A. 1958 'Contribution à l'analyse de la turbulence associée à des vitesses moyennes.' P.S.T. Ministère de l'Air, No. 345.
21. Durbin, P.A. 1991 'Turbulence closure modeling near rigid boundaries'. Theoret. Comp. Fluid Dyn. 3, pp. 1-13.
22. Durbin, P.A., Zeman, O. 1992 'Rapid distortion theory for homogeneous com-

pressed turbulence with application to modelling.' J. Fluid Mech. 242, pp. 349-370.
23. Dussauge, J. P., Fernholz, H., Finley, P. J., Smith, R. W., Smits, A. J., Spina, E. F. 1996 'Turbulent boundary layers in subsonic and supersonic flow'. AGARDOGRAPH 335, AGARD-AG-335.
24. Fauchet, G. 1998 'Modélisation en deux points de la turbulence isotrope compressible et validation à l'aide de simulations numériques'. Thèse de doctorat. Univ. Claude Bernard-Lyon I, France.
25. Fauchet, G., Shao, L., Wunenberger, R., Bertoglio, J.P. 1997 'An improved two-point closure for weakly compressible turbulence and comparisons with large-eddy simulation.' Proc. 11th Symp. Turbulent Shear Flows, Grenoble, France, Sept. 8-10, 1997, Vol. 3, pp. 32-13 to 32-18.
26. Fernholz, H.H., Finley, P. J. 1980 'A critical commentary on mean flow data for two-dimensional compressible turbulent boundary layers. AGARD-AG-253.
27. Freund, J.B., Moin, P., Lele, S.K. 1997 'Compressibility effects in a turbulent annular mixing layer. Report No. TF-72, Dept. Mech. Engg. Stanford Univ., Stanford Calif. 94305.
28. Friedrich, R., Bertolotti, F.P. 1997 'Compressibility effects due to turbulent fluctuations'. Appl. Sci. Res. 57, pp. 165-194.
29. Fu, S., Launder, B.E. and Tselepidakis, D.P. 1987 'Accommodating the effects of high strain rates in modeling the pressure-strain correlation'. UMIST Technical Report TFD/87/5.
30. Gatski, T. B. 1996 'Turbulent flows: model equations and solution methodology'. Handbook of Computational Fluid Mechanics, Edited by R. Peyret, Academic Press, London. Chapter 6, pp. 339-416.
31. Gatski, T.B. 1997 'Modelling compressibility effects on turbulence'.-In: New Tools in Turbulence Modelling, O. Métais & J. Ferziger (Eds), Les Editions de Physique, France and Springer, Berlin, New York.
32. Gatski, T. B., Speziale, C. G. 1993 'On explicit algebraic stress models for complex turbulent flows'. J. Fluid Mech., 254, pp. 59-78.
33. Gaviglio, J. 1987 'Reynolds analogies and experimental study of heat transfer in the supersonic boundary layer'. Int J. Heat Mass Transfer, 30, pp. 911-926.
34. Herring, J.R. 1974 'Approach of axisymmetric turbulence to isotropy.' Phys. Fluids 17, pp. 859.
35. Huang, P.G., Coakley, T. J. 1993 'Modeling hypersonic boundary layer flows with second-moment closure'. - In: Near-Wall Turbulent Flows, edited by R. M. C. So, C. G. Speziale and B. E. Launder, Elsevier, Amsterdam, pp. 199-208.
36. Huang, P.G., Coleman, G.N. 1994 'Van Driest transformation and compressible wall-bounded flows.' AIAA J. 32, pp. 2110-2113.
37. Huang, P.G., Coleman, G.N., Bradshaw, P. 1995 'Compressible turbulent channel flows - DNS results and modelling'. J. Fluid Mech. 305, pp. 185-218.
38. Jacquin, L., Cambon, C., Blin, E. 1993 'Turbulence amplification by a shock wave and rapid distortion theory.' Phys. Fluids A10, pp. 2539-2550.
39. Jones, W. P., Launder, B. E. 1972 'The prediction of laminarization with a two-equation model of turbulence. Int. J. Heat Mass Transfer, 15, pp. 301-314.
40. Kavasznay, L.S.G. 1953 'Turbulence in supersonic flows'. J. Aeronaut. Sci. 20, pp. 657-682.
41. Kim, J., Moin, P., Moser, R. 1987 'Turbulence statistics in fully developed channel flow at low Reynolds number'. J. Fluid Mech. 177, pp. 133-166.
42. Knight, D. D. 1997 'Numerical simulation of compressible turbulent flows using the Reynolds-averaged Navier-Stokes equations'. –In: AGARD FDP Special Course on Turbulence in Compressible Flows, AGARD-R-819, pp. 5-1 to 5-52.
43. Launder, B. E. 1987 'An introduction to single-point closure methodology'. VKI Course, Brussels, Belgium.
44. Launder, B. E., Reece, G. J., Rodi, W. 1975 'Progress in the development of a Reynolds stress turbulence closure'. J. Fluid Mech. 68, pp. 537-566.

45. Launder, B.E., Sharma, B.I. 1974 'Application of energy-dissipation model of turbulence to the calculation of flow near a spinning disc'. Letters in Heat and Mass Transfer, 1, pp. 131-138.
46. Lele, S.K. 1994 'Compressibility effects on turbulence'. Ann. Rev. Fluid Mech., 26, pp. 211 -254.
47. Lesieur, M. 1997 'Turbulence in Fluids'. Third revised and enlarged edition. Kluwer Academic Publishers, Dordrecht.
48. Lumley, J.L. 1978 'Computational modeling of turbulent flows'. Advances in Applied Mechanics, 18, pp. 123-173.
49. Mahesh, K., Lee, S., Lele, S.K., Moin, P. 1995 'The interaction of an isotropic field of acoustic waves with a shock wave'. J. Fluid Mech. 300, pp. 383-407.
50. Menter, F. R., Rumsey, L. C. 1994 'Assessment of two-equation turbulence models for transonic flows'. AIAA Paper 94-2343, 25th AIAA Fluid Dynamics Conference, Colorado Springs, Colorado, June 20-23, 1994.
51. Morkovin, M.V. 1962 'Effects of compressibility on turbulent flows.' -In: Mécanique de la Turbulence (ed. A. Favre), Gordon and Breach, New York, pp. 367 -380.
52. Pope, S. B. 1975 'A more general effective viscosity hypothesis'. J. Fluid Mech. 72, pp. 331-340.
53. Ristorcelli, J.R. 1995 'A pseudo-sound constitutive relationship for the dilatational covariances in compressible turbulence: an analytical theory'. ICASE Rep. 95-22. NASA Langley Research Center, Hampton, VA.
54. Ristorcelli, J. R. 1997 'A pseudo-sound constitutive relationship for the dilatational covariances in compressible turbulence'. J. Fluid Mech. 347, pp. 37-70.
55. Ristorcelli, J. R. 1998 'Some results relevant to statistical closures for compressible turbulence'. ICASE Report No. 98-1, NASA Langley Research Center, Hampton, VA.
56. Ristorcelli, J.R., Blaisdell, G.A. 1996 'Consistent inital conditions for the DNS of compressible turbulence'. ICASE Report No. 96-49, NASA Langley Research Center, Hampton, VA 23681-0001.
57. Rubesin, M. W. 1976 'A one-equation model of turbulence of use with the compressible Navier-Stokes equations. NASA Tech. Mem. X-73, 128.
58. Rubesin, M.W. 1990 'Extra compressibility terms for Favre-averaged two-equation models of inhomogeneous turbulent flows. NASA CR-177556
59. Sandham, N.D., Reynolds, W.C. 1989 'A numerical investigation of the compressible mixing layer'. Rep. TF-45. Thermosciences Division, Mechanical Engineering Department, Stanford University, Stanford, California.
60. Sarkar, S. 1992 'The pressure-dilatation correlation in compressible flows.' Phys. Fluids A4, pp. 2674-2682.
61. Sarkar, S. 1995 'The stabilizing effect of compressibility in turbulent shear flow.' J. Fluid Mech. 282, pp. 163-186.
62. Sarkar, S., Erlebacher, G., Hussaini, M. Y. 1991 'Direct simulation of compressible turbulence in a shear flow.' Theor. Comput. Fluid Dyn. 2, pp. 291-305.
63. Sarkar, S., Erlebacher, G., Hussaini, M. Y., Kreiss, H. O. 1991b 'The analysis and modelling of dilatational terms in compressible turbulence'. J. Fluid Mech. 227, pp. 473-493.
64. Settles, G.S., Fitzpatrick, T.J., Bogdonoff, S.M. 1979 'Detailed study of attached and separated compression corner flow fields in high Reynolds number supersonic flow'. AIAA J. 17, pp. 579-585.
65. Shih, T.-H. 1996 'Constitutive relations and realizability of single-point turbulence closures'. - In: Turbulence and Transition Modelling. Edited by M. Hallbäck, D. S. Henningson, A. V. Johansson, P. H. Alfredsson. ERCOFTAC Series, Kluwer Academic Publishers.
66. Shih, T.H., Zhu, J., Lumley, J.L. 1992 'A realizable Reynolds stress algebraic equation model'. NASA TM 105993.
67. Simone, A. 1995 'Etude théorique et simulation numérique de la turbulence com-

pressible en présence de cisaillement ou de variation de volume à grande èchelle.' Thése. Ecole doctorale: Mècanique-Energètique. Ecole Centrale de Lyon.
68. Simone, A., Coleman, G.N., Cambon, C. 1997 'The effect of compressibility on turbulent shear flow: A rapid distortion theory and direct numerical simulation study.' J. Fluid Mech. 330, pp. 307 -338.
69. Smits, A.J., Dussauge, J.-P. 1996 'Turbulent Shear Layers in Supersonic Flow'. American Institute of Physics Press.
70. Sommer, T. P., So, R. M. C., Zhang, H. S. 1993 'Near-wall variable - Prandtl-number turbulence model for compressible flows'. AIAA J. 31, pp. 27-35.
71. Speziale, C. G. 1991 'Analytical methods for the development of Reynolds stress closures in turbulence'. Ann. Rev. Fluid Mech., Vol. 23, pp. 107-157.
72. Speziale, C. G. 1996 'Modeling of turbulent transport equations'. -In: Simulation and Modeling of Turbulent Flows, Edited by: T. B. Gatski, M. Y. Hussaini, J. L. Lumley, ICASE/LaRC Series in Computational Science and Engineering, Oxford Univ. Press, pp. 185-242.
73. Speziale, C.G., Abid, R., Mansour, N.N. 1995 'Evaluation of Reynolds stress turbulence closures in compressible homogeneous shear flow'. ZAMP, Special Issue, ed. by J. Casey & M.J. Crochet, S717-S736.
74. Speziale, C. G., Gatski, T. B., Sarkar, S. 1992 'On testing models for the pressure-strain correlation of turbulence using direct simulations'. Phys. Fluids A4, pp. 2887-2899.
75. Speziale, C. G., Sarkar, S. 1991 'Second-order closure models for supersonic turbulent flows'. AIAA Paper No. 91-0217, 29th Aerospace Sciences Meeting, Jan. 7-10, 1991, Reno, Nevada.
76. Speziale, C.G., Sarkar, S., Gatski, T.B., 1991 'Modeling the pressure-strain correlation of turbulence: A invariant dynamical systems approach'. J. Fluid Mech. 227, pp. 245-272.
77. Tennekes, H., Lumley, J.L. 1972 'A first course in turbulence'. The MIT Press. Cambridge, Massachusetts and London, England.
78. Thompson, P.A. 1988 'Compressible-Fluid Dynamics.' McGraw-Hill, New York.
79. Van Driest, E.R. 1951 'Turbulent boundary layer in compressible fluids'. J. Aero. Sci. 18, pp. 145-160 and 216.
80. Vreman, B. 1995 'Direct and large-eddy simulation of the compressible turbulent mixing layer'. Thesis, University of Twente, The Netherlands.
81. Vreman, A.W., Sandham, N.D., Luo, K.H. 1996 'Compressible mixing layer growth rate and turbulence characteristics.' J. Fluid Mech. 320, pp. 235-258.
82. Wilcox, D. C. 1988 'Reassessment of the scale-determining equation for advanced turbulence models'. AIAA J. 26, pp. 1299-1310.
83. Wilcox, D. C. 1991 'Progress in hypersonic turbulence modelling'. AIAA Paper 91-1785, Honolulu, HI.
84. Wilcox, D. C. 1993 'Turbulence Modeling for CFD'. DCW Industries Inc., 5354 Palm Drive, La Cañada, Calif.
85. Zeman, O. 1990 'Dilatation dissipation; The concept and application in modeling compressible mixing layers'. Phys. Fluids A2, pp. 178-188.
86. Zeman, O. 1991 'On the decay of compressible isotropic turbulence'. Phys. Fluids A 3, pp. 951-955.
87. Zeman, O. 1993 'New model for super/hypersonic turbulent boundary layers'. AIAA Paper No. 93-0897, January 1993.
88. Zeman, O., Coleman, G. N. 1993 'Compressible turbulence subjected to shear and rapid compression'. Turbulent Shear Flows 8, Durst et al. (Eds), Springer-Verlag, pp. 283-296.

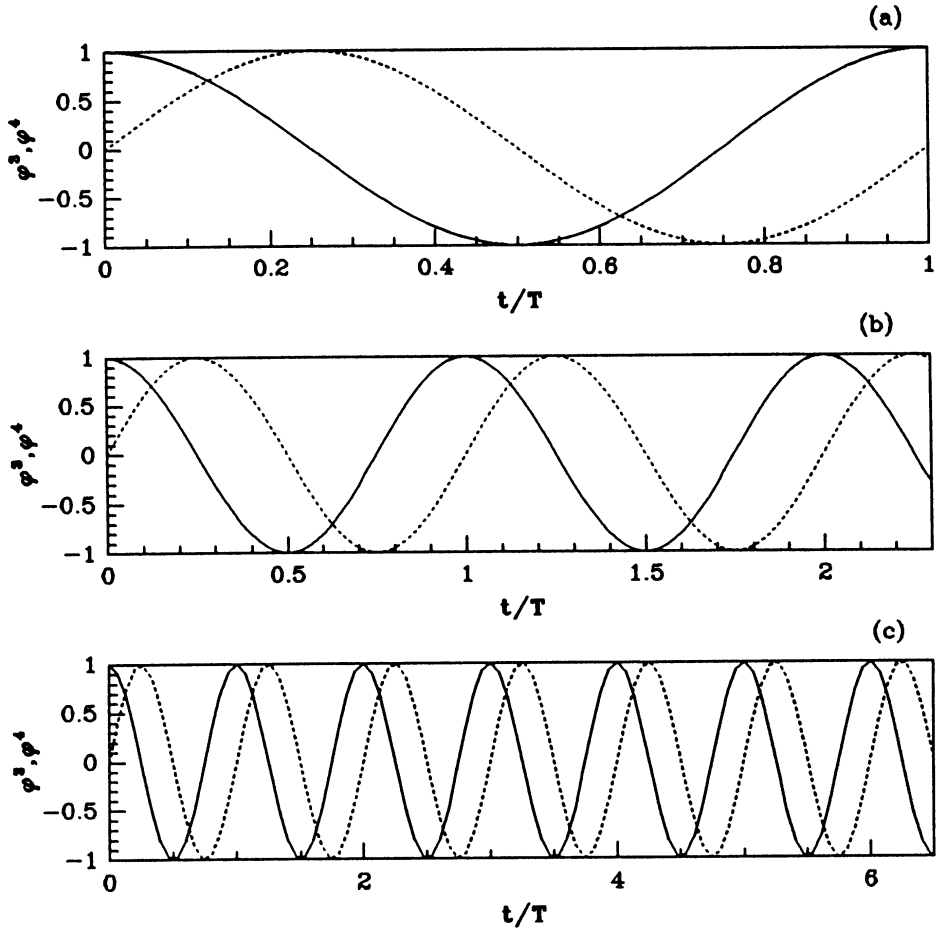

Figure 1. Time evolution of compressible modes in acoustic equilibrium (isotropic turbulence, increasing wavenumber from top to bottom). Taken from Simone (1995) by permission.

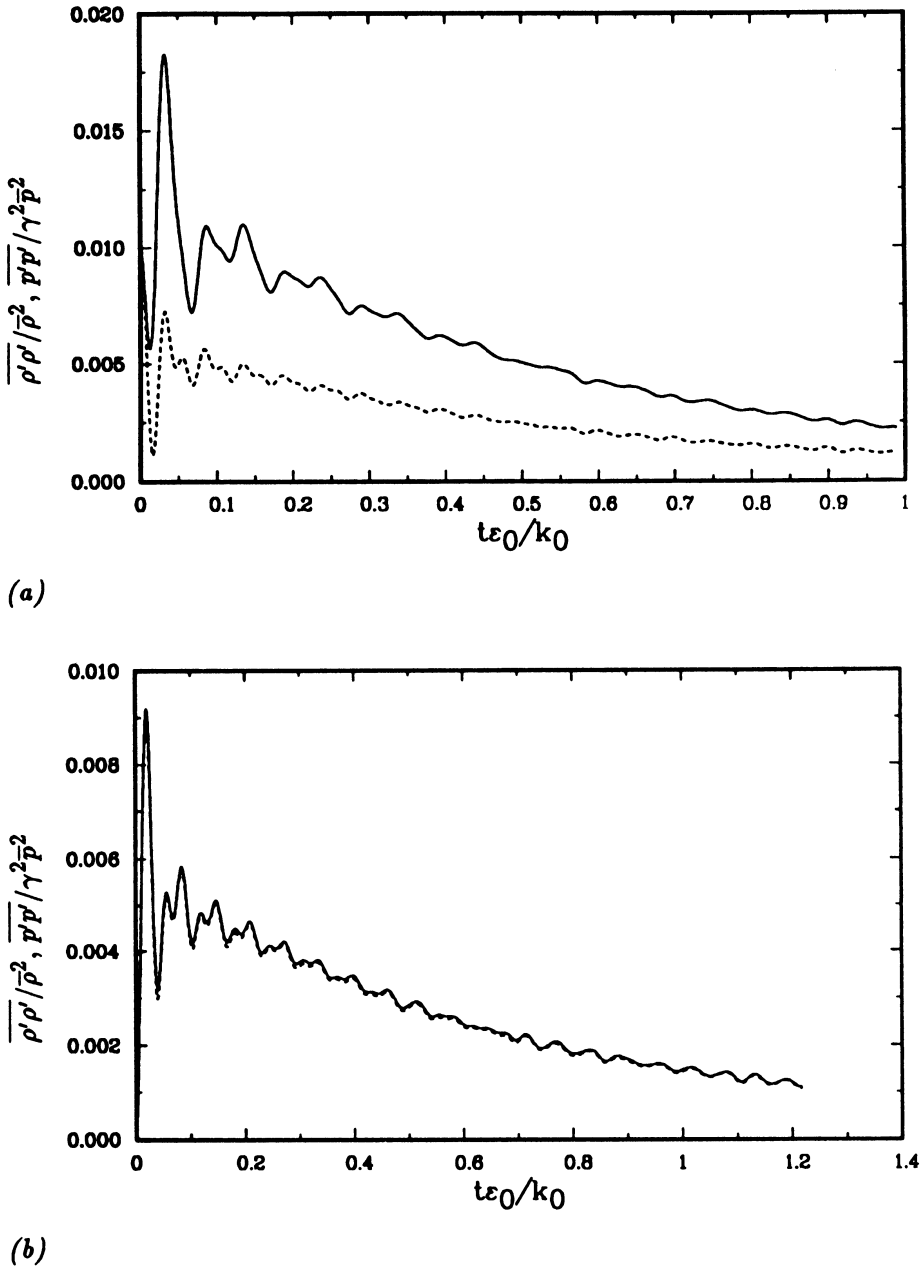

Figure 2. Evolution of normalized density and pressure variances. Blaisdell et al's (1991) DNS of isotropic turbulence. Top: $F_0 = 1/40$, large initial pressure fluctuations. Bottom: $F_0 = 40$, large initial dilatational velocity fluctuations. By permission of the authors.

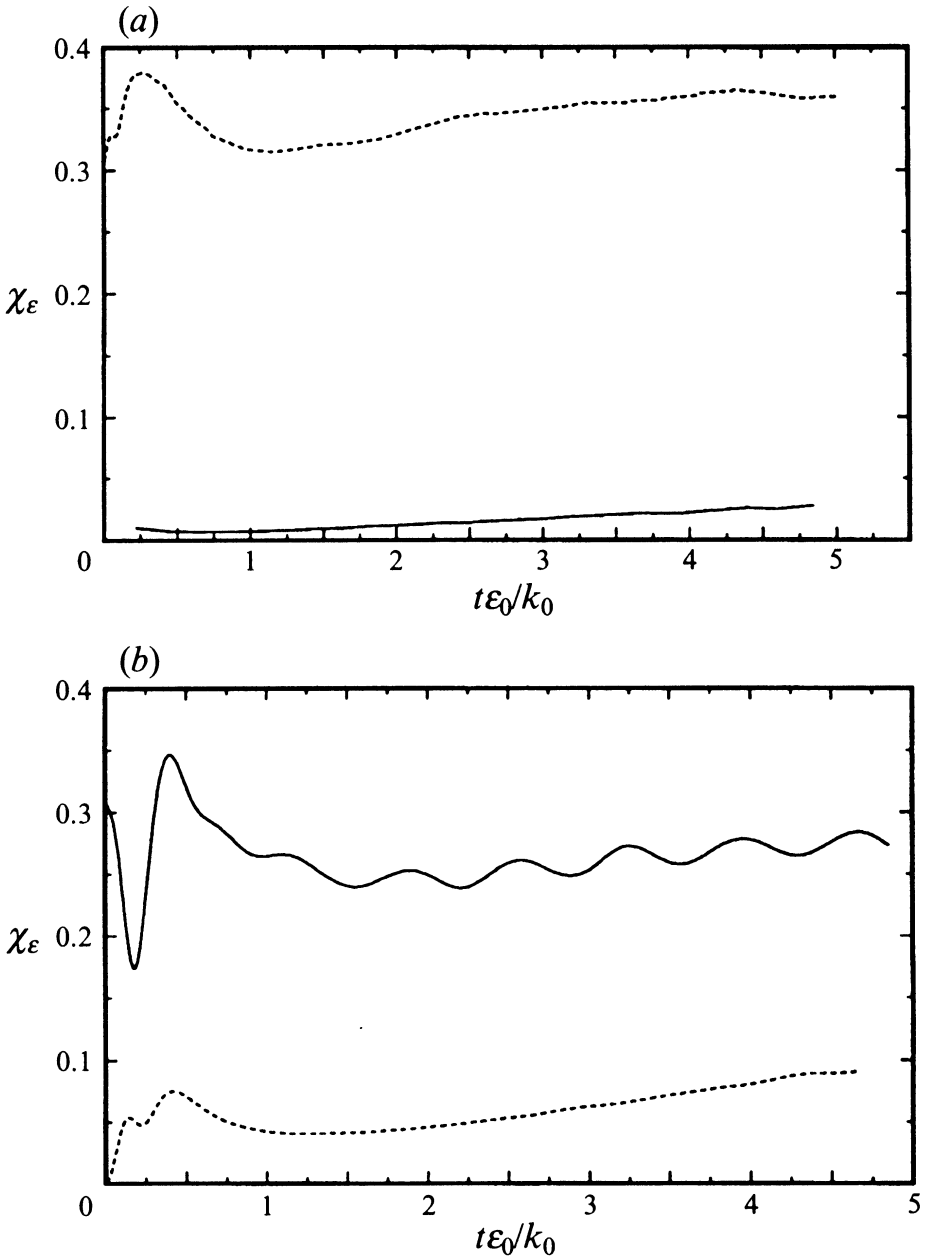

Figure 3. Influence of initial conditions on time evolution of dilatational fraction of turbulent dissipation rate. Modes are uncoupled, therefore, curves do not approach each other. Taken from Blaisdell et al. (1993) by permission.

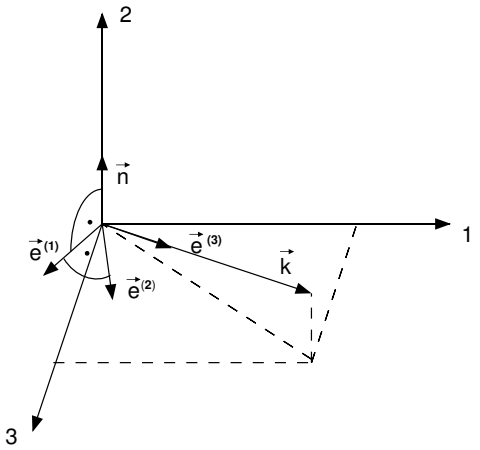

Figure 4. Craya-Herring local reference frame in wavenumber space. The polar vector $\vec{n}$ is parallel to the mean shear direction. The compressible mode is parallel to $\vec{k}$. The vorticity vector lies in the plane perpendicular to $\vec{k}$.

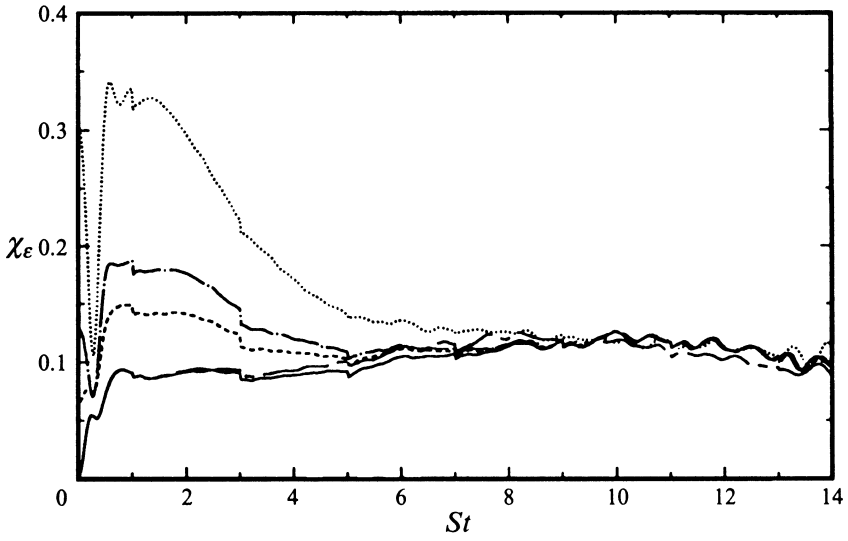

Figure 5. The dilatational fraction of the dissipation rate gets independent of initial conditions in homogeneous shear turbulence. Taken from Blaisdell et al. (1993) by permission.

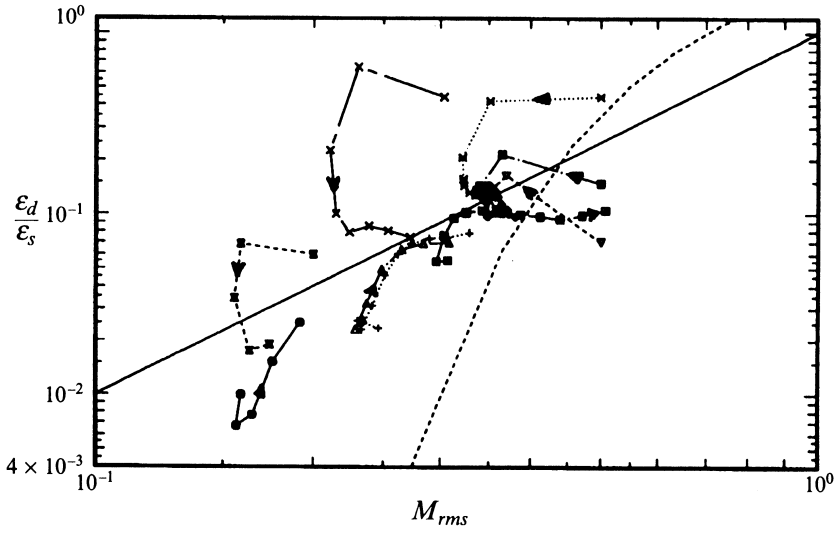

Figure 6. Comparison of Sarkar et al.'s (1991) ——— , and Zeman's (1990) model – – – – for compressible dissipation rate with DNS data of Blaisdell et al. (1991) for homogeneous shear flow. Taken from Blaisdell et al. (1991) by permission.

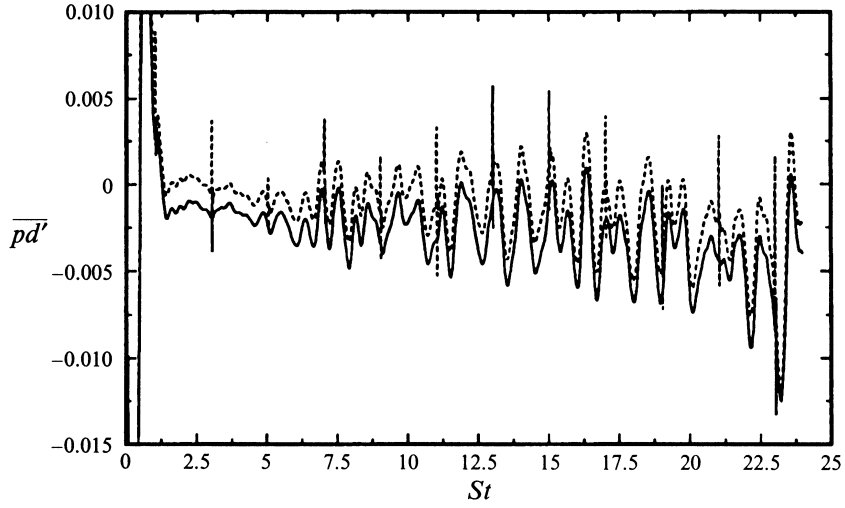

Figure 7. Time evolutions of $\overline{p'd'}$ and $d\overline{p'^2}/dt/(2\gamma\overline{p})$. Confirmation of linear theory. Taken from Blaisdell et al. (1993) by permission.

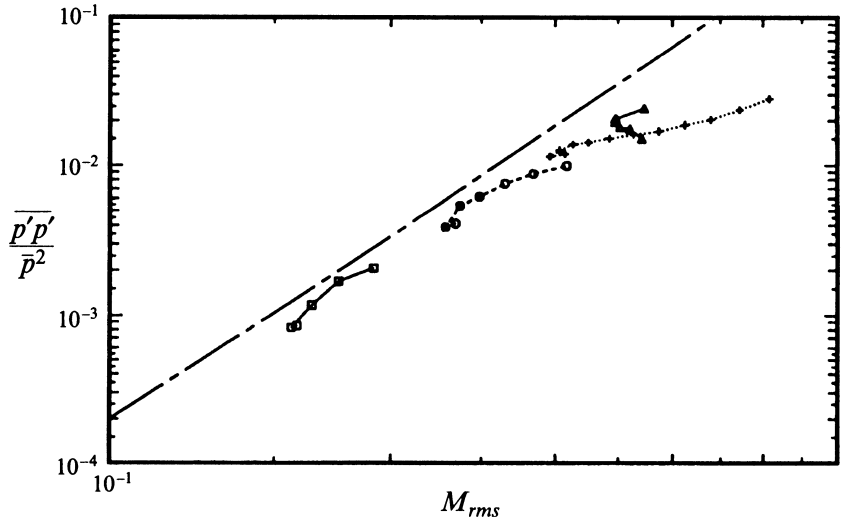

Figure 8. Test of Zeman's pressure-dilatation model. Pressure variance versus turbulent Mach number. Taken from Blaisdell et al. (1993) by permission.

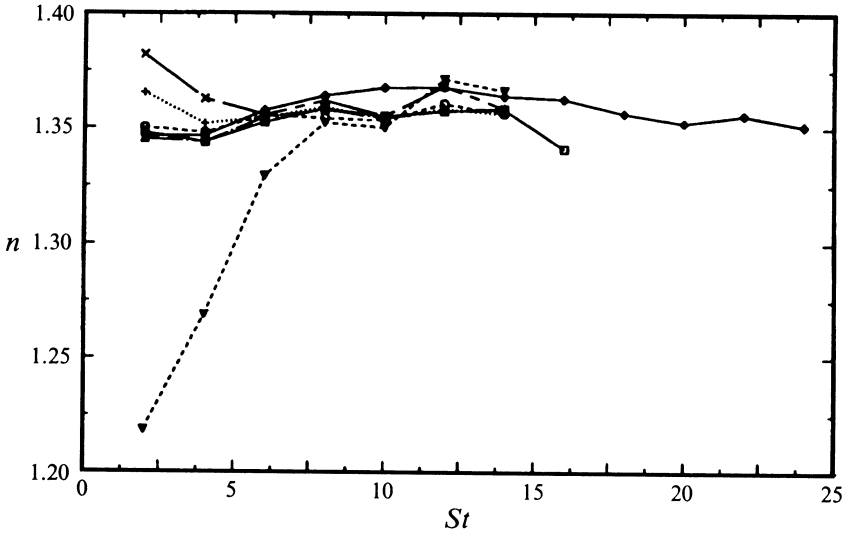

Figure 9. Development of mean polytropic coefficient. Independence of initial conditions. n close to γ. Taken from Blaisdell et al. (1993) by permission.

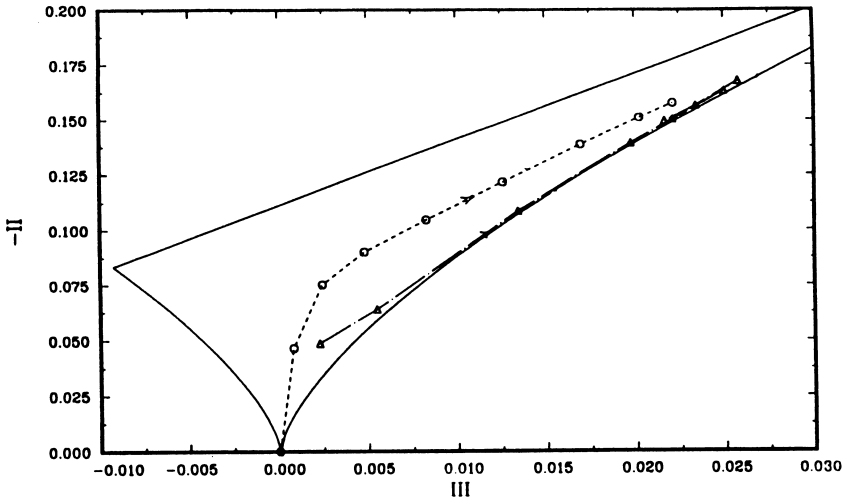

Figure 10. Solenoidal (○) and dilatational (△) Reynolds stress anisotropy tensors for Blaisdell et al.'s DNS sha192. Taken from Blaisdell et al. (1991) by permission.

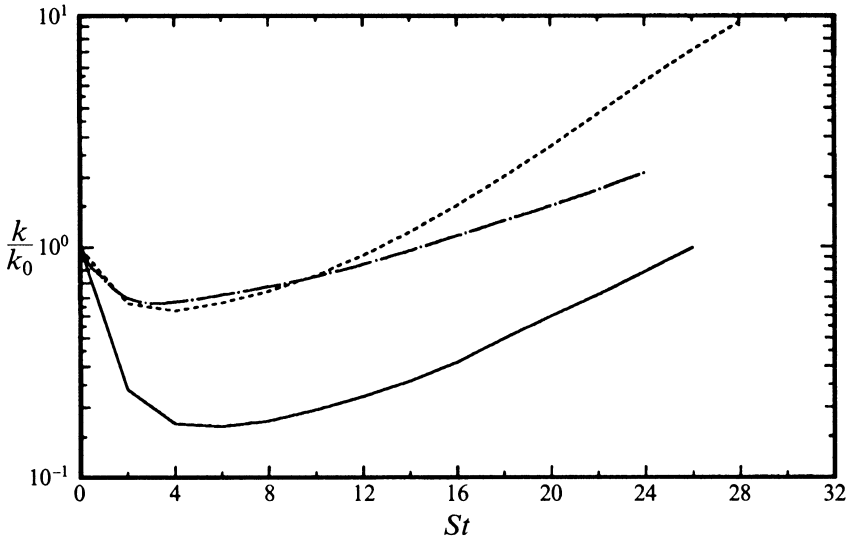

Figure 11. Comparison between compressible and incompressible time evolutions of K. ——— , – – – – incompressible homogeneous shear flow. —·—· sha192 shows reduced growth rate. Taken from Blaisdell et al. (1993) by permission.

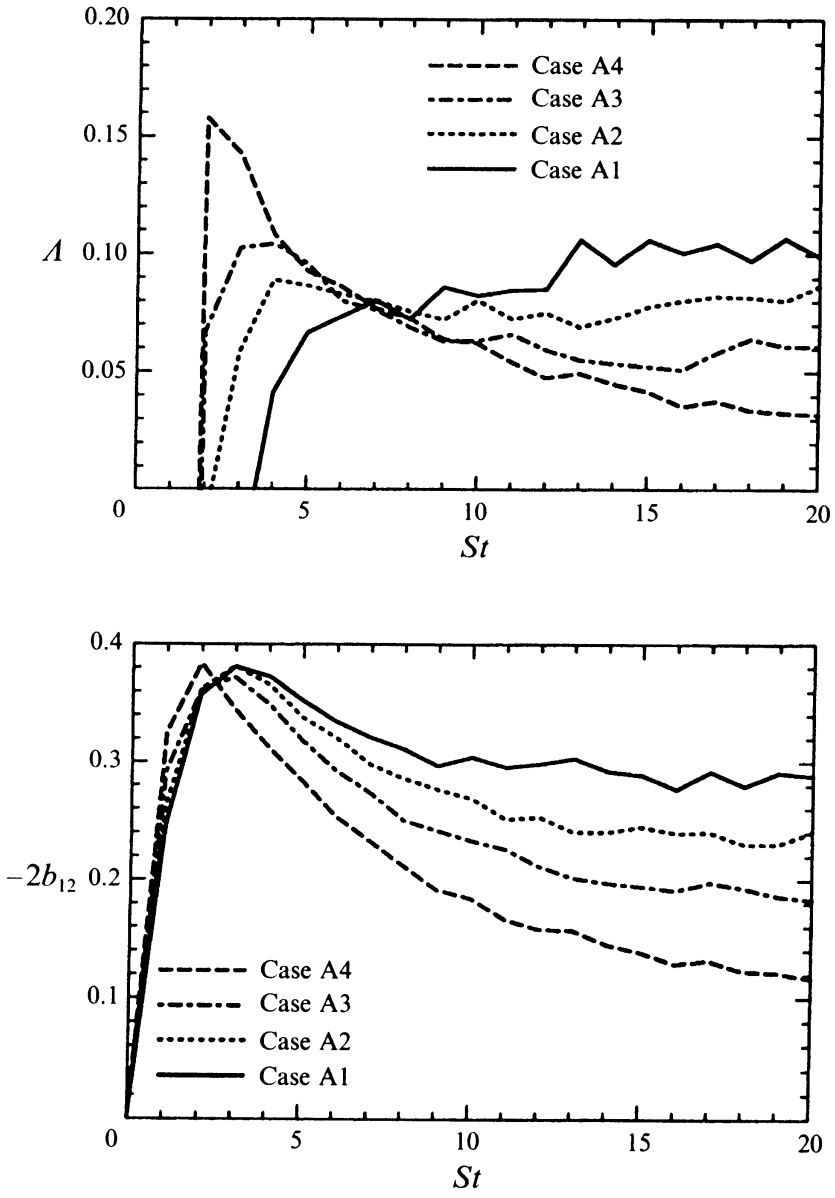

Figure 12. Growth rate reduction (top) by increased M_{g0} is primarily due to reduced non-dimensional production (bottom). Taken from Sarkar (1995) by permission.

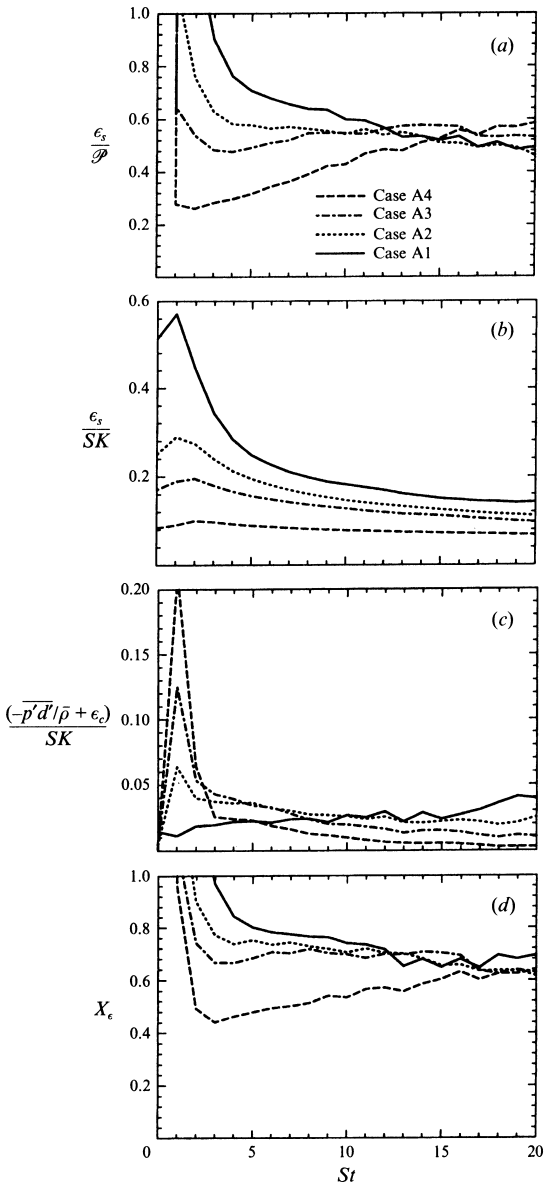

Figure 13. Evolution of ϵ_s, of explicit compressibility terms and of the sum of all terms (except b_{12}). The effect of M_{g0} is for all terms lower than for b_{12}. Taken from Sarkar (1995) by permission.

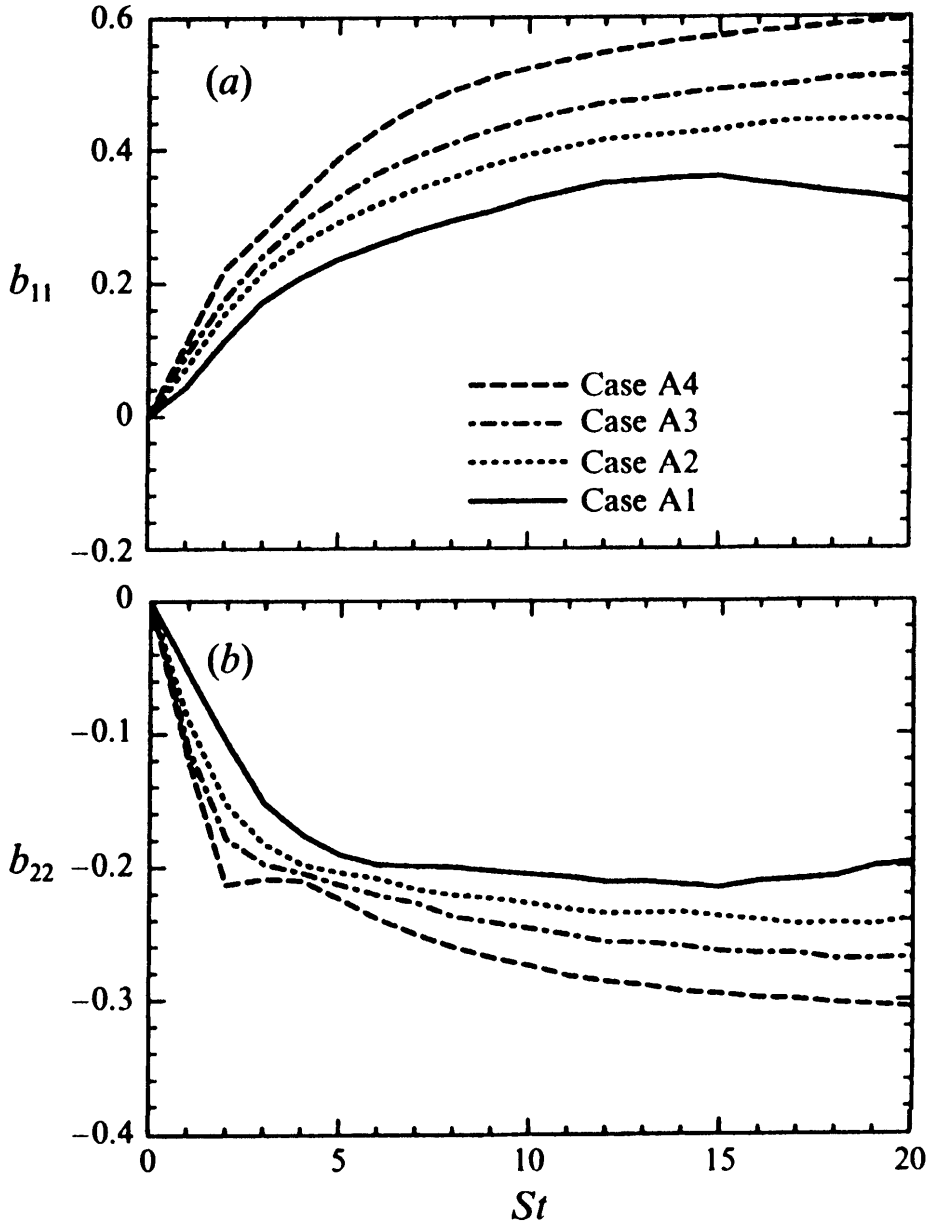

Figure 14. Effect of M_{g0} on streamwise and transverse Reynolds stress anisotropies. Taken from Sarkar (1995) by permission.

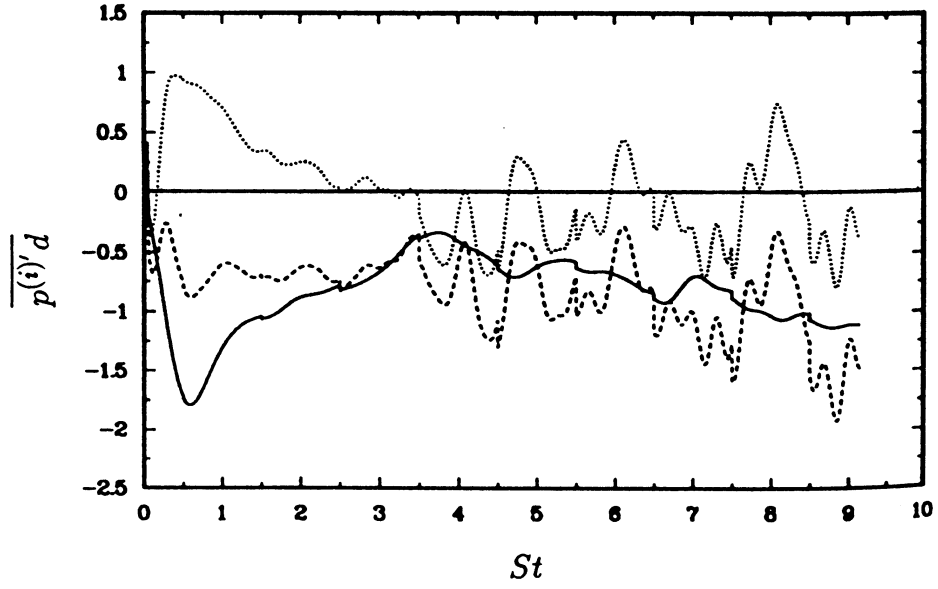

Figure 15. Time evolution of $\overline{p'd'}$ (– – – –) and its compressible (· · · · · ·) and incompressible (———) contributions. Taken from Blaisdell and Sarkar (1993) by permission.

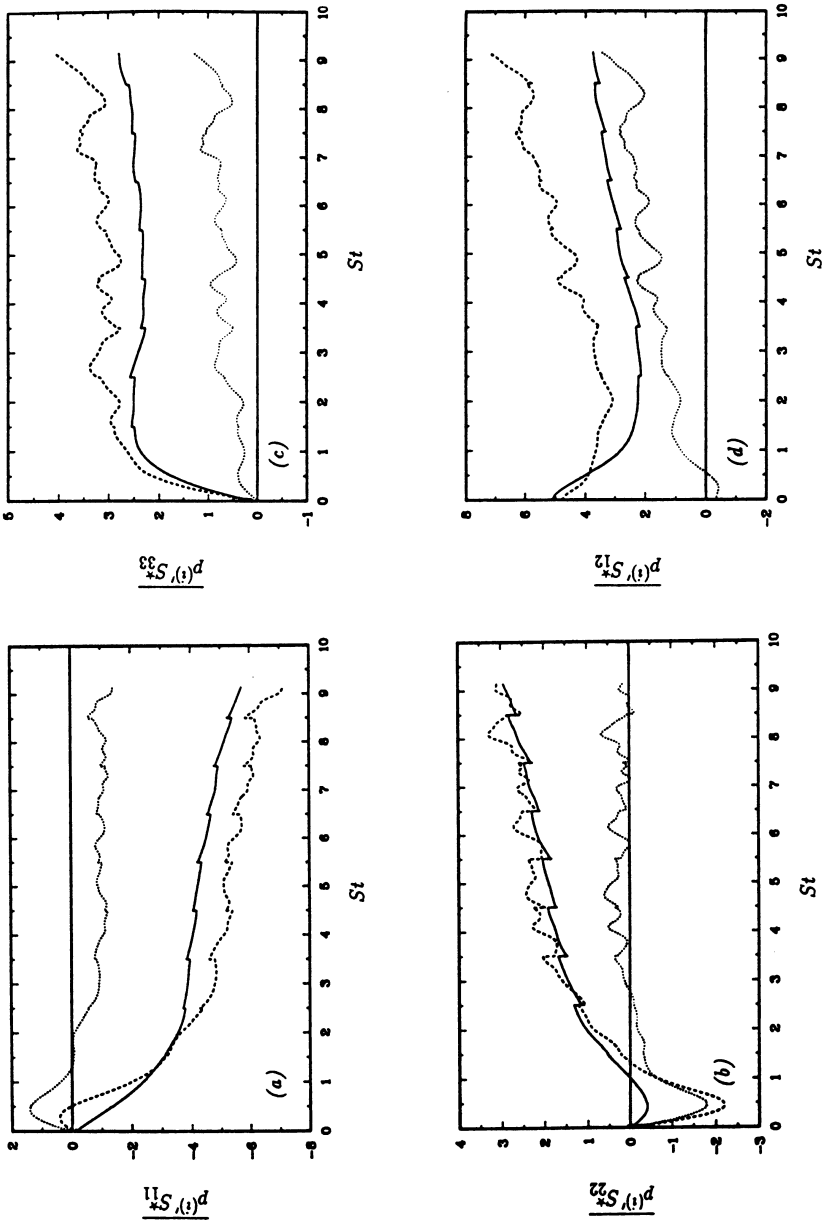

Figure 16. Time evolutions of the four deviatoric pressure-strain correlations, split as in fig. 1b. Taken from Blaisdell and Sarkar (1993) by permission.

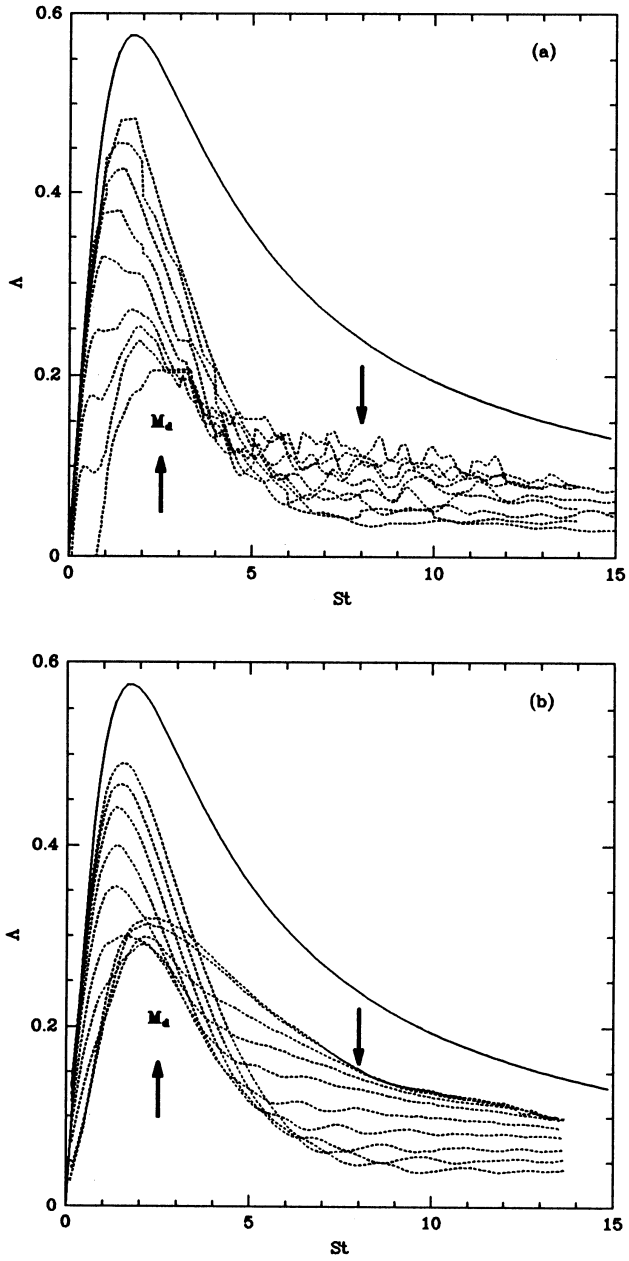

Figure 17. Comparison between DNS (top) and RDT (bottom) for TKE growth rate. Solid line: pressure-released limit. Destabilization for $St < 4$ and stabilization at later times. Taken from Simone et al. (1997) by permission.

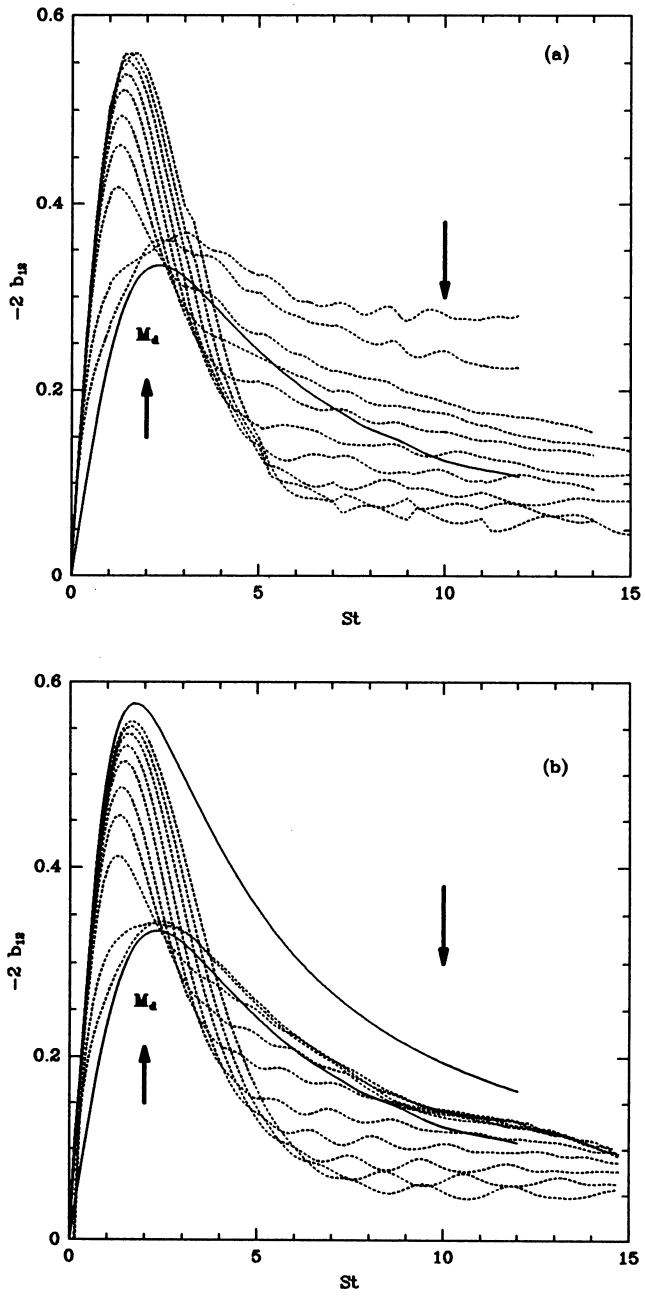

Figure 18. Comparison between DNS (top) and RDT (bottom) for b_{12}. Incompressible and pressure-released limits (higher curve). Taken from Simone et al. (1997) by permission.

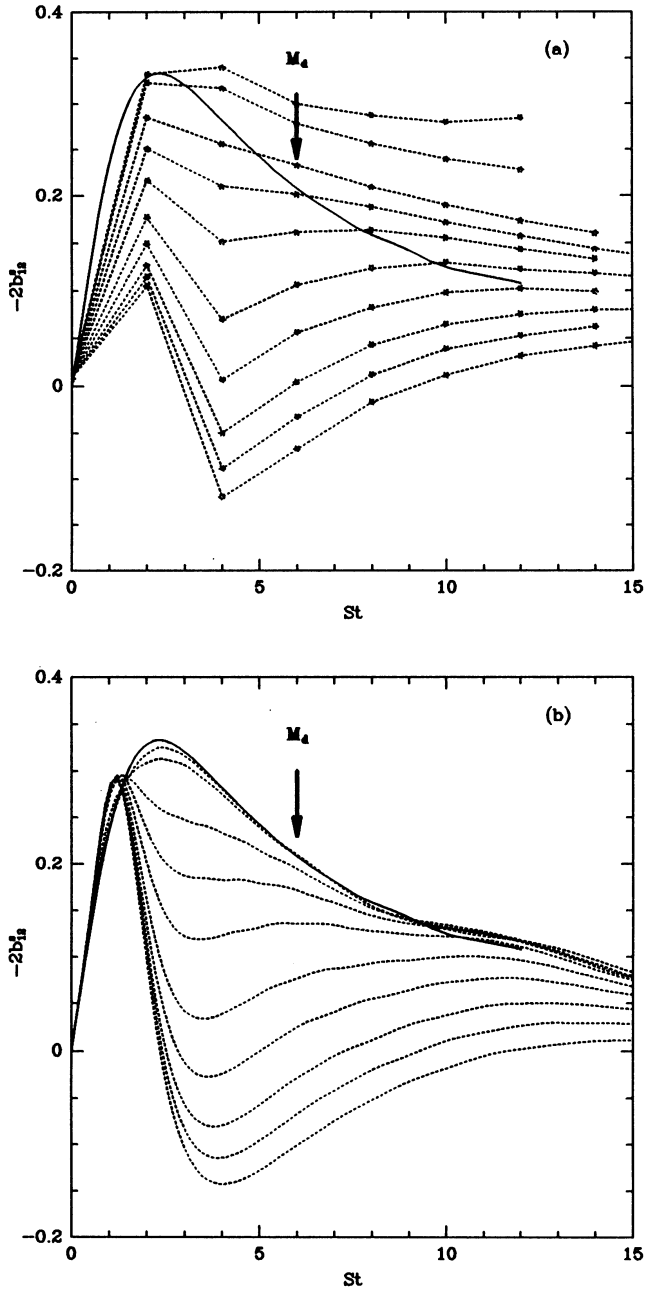

Figure 19. Behaviour of solenoidal b_{12}-component. Top: DNS, bottom: RDT. This component is strongly affected by M_d. Taken from Simone et al. (1997) by permission.

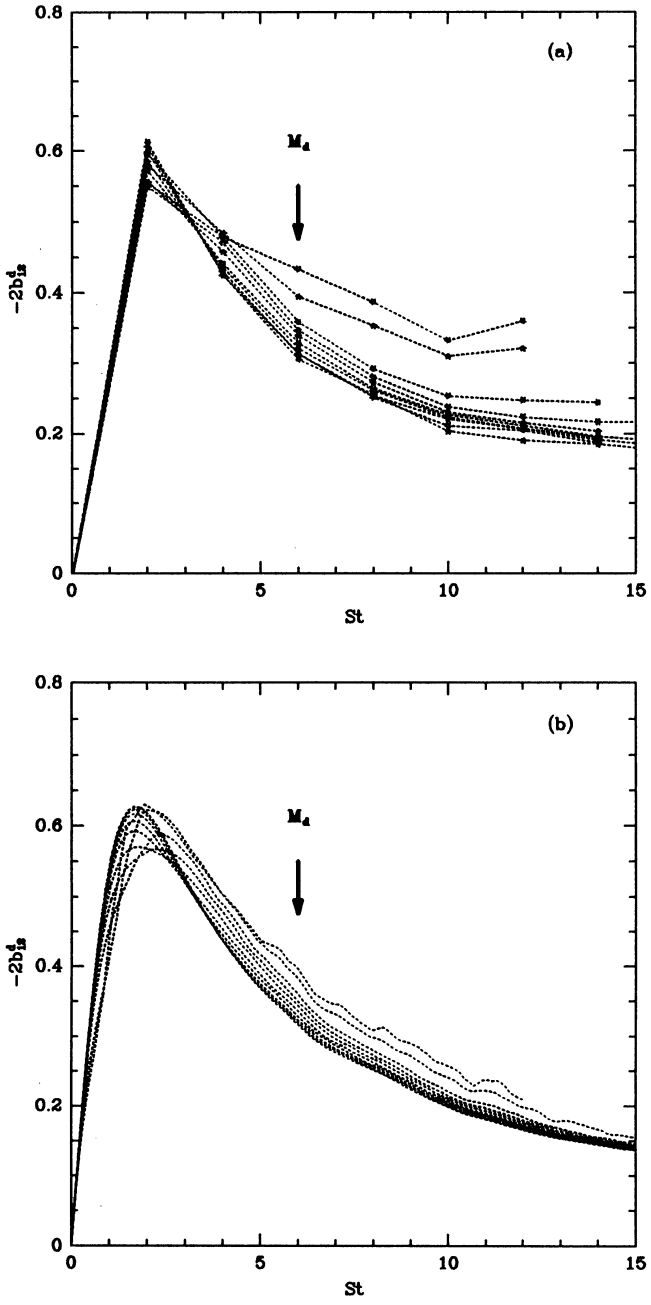

Figure 20. Behaviour of dilatational b_{12}-component. Top: DNS, bottom: RDT. It is essentially unaffected. Taken from Simone et al. (1997) by permission.

Table of Contents